Investigating the spread of MtrCAB mediated EET in Bacteria and the mechanisms of extracellular electron transfer in the heterotrophic facultative anaerobes, *Aeromonas hydrophila* and *Vibrio natriegens*

A DISSERTATION SUBMITTED TO THE FACULTY OF
THE UNIVERSITY OF MINNESOTA
BY

Bridget Eryn Conley

IN PARTIAL FULFILLMENT OF THE REQUIREMENTS
FOR THE DEGREE OF DOCTOR OF PHILOSOPHY

Advisor: Jeffrey A. Gralnick

October 2021

Acknowledgements

Jeff Gralnick is the beam of support on which this thesis was written. His continued encouragement and support for both my professional and personal wellness has made me a better person. It is a kindness that can never be repaid but instead must be passed on, thank you.

Thank you to all the lab members before me who laid the groundwork, but only to those that kept good notebooks. A special thank you to Missy Weldy, Rebecca Maysonet, Sol Choi, Ruth Lee, Drs. Eric Kees, Ben Bonis, Chi Ho Chan, Rebecca Calvo, and Fernanda Jimenez for always being kind and supportive. Thank you, Izzy Baker, for your patience, support and keeping me company on zoom during lock-down. A big hug and thank you to Dr. Komal Joshi for being my friend and source of joy, I look forward to many more shenanigans together. Thank you, Adam Chop, for teaching me how to play and keeping me company during late-night timepoints.

Thank you to all the people who made Gortner Labs a community, the administrative and custodial staff in addition to the many scientists who would brighten my day.

Thank you to my committee for being helpful and patient as I fumbled, healed old wounds, and discovered what motivates me.

Thank you to all those who lifted me up along the way, I will try my best to share it with others.

Dedication

This thesis is dedicated to Kevin Conley, world’s best dad.

Abstract

While many metabolisms make use of soluble, cell-permeable substrates like oxygen or hydrogen, there are other energy-yielding sources, like iron or manganese, that cannot be brought into the cell. Some bacteria and archaea have evolved the means to directly "plug in" to these valuable energy sources in a process known as extracellular electron transfer (EET), making them powerful agents of biogeochemical change and promising vehicles for bioremediation and alternative energy. The diversity and distribution of EET is poorly understood and the molecular mechanism has primarily been studied in two model systems, *Shewanella oneidensis* and *Geobacter sulfurreducens*. The following thesis presents evidence for the mechanism of EET in *Aeromonas hydrophila* and *Vibrio natriegens*, which enhances survival in fermentative conditions for *V. natriegens*. The genes encoding *mtrCAB* are present in a broad diversity of bacteria found in a wide range of environments, emphasizing the ubiquity and potential impact of EET in our biosphere.

List of Tables

List of Figures

Chapter 1- Living on the Edge- of the oxic/anoxic interface: Energy management in representative heterotrophic facultative anaerobes, *Shewanella*, *Aeromonas* and *Vibrio* and the role of MtrCAB-mediated extracellular electron transfer

1.1 Energy, progress, and my contribution

Every cell requires energy to power essential processes. The various ways nature has devised ways to gather energy from the environment is truly breathtaking. Even if the conditions are harsh, life finds a way. Energy comes in various forms and biology will use any energy source that can be converted and harvested. Driven by evolution, life creates molecular machines, ie. enzymes, to translate one type of energy into another. Energy conversions allows cells to harvest light energy from the sun or chemical energy from a hydrothermal vent. Biology is a great problem solver; we should take better notes. The greater our understanding of energy transfer in nature, the better we can engineer our own systems mimicking nature's time-tested efficiency.

Efforts to harness energy from nature, led to the field of electromicrobiology. Electromicrobiology examines the ability of a microorganism to manipulate electrons into and/or out of the cell from the extracellular environment, an ability termed extracellular electron transfer (EET). If we understood how to manipulate electrons in biological materials, then we can design better devices. Initial descriptions of electromicrobiology in the late 1980s examined mineral oxide reduction in two Proteobacteria, *Shewanella* (1) and *Geobacter* (2), but experimental focus shifted to the reduction of electrodes with the goal of sustainably fueling low-power devices. One application of electromicrobiology became building bioelectrical systems with organisms capable of making electricity or other energetically valuable products (3). The field has since expanded with numerous reports of enrichments and isolates of Bacteria, Archaea and Eukaryotes capable of EET (4); however, the biological significance of some of these reports remains an open question due to their experimental methods and controls.

Distinguishing between biological and abiotic reduction/oxidation of electrodes or minerals requires proper experimental controls. Additional redox active compounds in the medium such as yeast extract (5), components of lysed cells, and oxygen contamination can all contribute to high "background noise" that makes interpretation of results difficult without the proper controls (3, 6). When biologists expand into electrochemistry or mineralogy, sometimes they have trouble understanding the

machinery or technique. When engineers or chemists expand into biology, sometimes they have trouble understanding the physiologically relevant conditions. People aren't perfect and sometimes they need help, especially in a cross-disciplinary field such as electromicrobiology. It doesn't make them a bad scientist; it makes them human. If we work together, we can help each other better understand the world around us.

My efforts have focused on investigating and describing the mechanisms of EET in representative γ-Proteobacteria, *Aeromonas hydrophila* ATCC 7966 and *Vibrio natriegens* ATCC 14048. Through a lens of genetics and ecology, the evolutionary history of EET in Proteobacteria is examined. Finally, lingering mysteries of how EET in *Aeromonas* and *Vibrio* species differ from the more thoroughly characterized *Shewanella* are discussed.

1.2 Mechanisms of extracellular electron transfer- The *Shewanella* system

While EET is a shared trait in phylogenetically and ecologically diverse microorganisms, the mechanisms and physiological function of EET in these microorganisms is not shared. *Geobacter sulfurreducens* (2), *Shewanella oneidensis* (1), *Listeria monocytogenes* (7), *Mariprofundus ferroxidans* (8), *Thermincola ferriacetica* (9) are 5 examples EET-capable microorganisms that all live in drastically different conditions and utilize unique mechanisms to perform EET.

Aeromonas and *Vibrio* spp. have been reported to perform EET using various experimental approaches to examine EET activity, but methods matter. The devil is in the details i.e., the methods section. In experimental systems, the external electron acceptor provided may be an electrode, insoluble mineral oxide or chelated metal ion. Variables between lab-made extracellular electron acceptors can alter physiologically relevant conditions such as diffusion (10, 11), pH (12, 13), biofilm formation (14, 15), oxygen contamination (16, 17), and electrochemical potential (18). Additionally, the presence or absence of soluble redox active electron shuttles can alter the EET phenotype presented (19, 20). Considering the numerous variables, experimental data with proper biological and chemical controls is required to determine if an organism is capable of EET.

Aeromonas spp. have been isolated from acetate and sugar fed anodic electroactive communities (21–27) predominantly from wastewater inoculum. Experimental validation of electrode reduction while also controlling for both biological and electrochemical effects has only been shown in *A. jandaei* SCS5 (23). *Aeromonas*

spp. isolates have also been reported to reduce mineral oxides (23, 28–30), and humic acids (29). *Vibrio* spp. have been isolated from a cathodic electroactive communities (31) and studied for mineral corrosion (32) and mineral oxide reduction (33–36). As only a few studies had addressed the underlying physiology (28, 33, 34, 37), it was unclear if EET in fermentative facultative heterotrophs such as *Aeromonas* and *Vibrio* was an abiotic accident or indirect effect (38, 39), a respiration strategy (28, 33, 37), a fermentative electron sink (34, 40), or something else entirely. The logical place to start investigating was with what was already known about *Shewanella* EET and compare that to *Aeromonas* and *Vibrio*.

EET in *Shewanella* spp. has been studied for 30 years and for a more detailed discussion of the mechanism of EET in *Shewanella*, please see recent reviews (41, 42). In short, EET in *Shewanella oneidensis* MR-1 is dependent on the transfer of electrons through *c*-type cytochromes. Cytochrome maturation occurs via a Ccm system, and assembly of the cytochrome complex which spans the outer membrane is dependent on type II secretion. Electrons from catabolism enter the quinone pool to be oxidized by CymA, the versatile quinol dehydrogenase. Tetraheme cytochromes, FccA and STC (a.k.a CctA) are abundant in the periplasm and both are capable of being oxidized by CymA and reduced by outer membrane anchored, MtrA. MtrA is the periplasmic facing cytochrome of the three-protein outer membrane cytochrome complex, MtrCAB, which facilitates electron transfer through the non-conductive lipid outer membrane. An outer membrane β-barrel protein, MtrB facilitates contact of MtrA to the extracellular cytochrome, MtrC. There are different homologs of the outer membrane cytochrome MtrC, such as OmcA, which may be used for distinct electron acceptors. In addition to cytochromes, *S. oneidensis* MR-1 excretes flavin mononucleotide (FMN), a soluble electron shuttle which diffuses into the extracellular space.

The Mtr complex has a long-established role in EET, forming the essential cytochrome-porin-cytochrome wire across the insulating outer membrane. A 2.7 Å resolution crystal structure of MtrCAB from *S. baltica* OS185 shows MtrB is tightly wound around MtrA. MtrAB together act as an insulated molecular wire transmitting electrons from the periplasm to extracellular MtrC (43). MtrCAB homologs were identified in genomes of *Aeromonas* and *Vibrio* spp. and proposed to be involved in EET (44, 45). Genetic evidence for Mtr-mediated EET in *A. hydrophila* and *V. natriegens* can be found in chapters 2 and 3, respectively. A curated search for *mtrCAB* homologs in Bacteria and discussion of their phylogeny and evolution can be found in chapter 4.

Periplasmic cytochromes are abundant in *S. oneidensis* MR-1, allowing overlapping functionality and non-specific reactions to cloud the 'true' interactions the organism evolved to function. Electrons are shepherded across the periplasm by soluble tetraheme *c*-type cytochromes, FccA and CctA although additional mediators may be yet to be described as a double deletion mutant still reduces Fe (III) citrate (46). In vitro kinetics and genetic studies show the periplasmic network has some specialization of redox partner, reviewed in (41). FccA is proposed to be the preferred periplasmic electron carrier for MtrA allowing Fe (III) citrate reduction while STC/CctA shows a preference for extracellular DMSO reductase, DmsE (47, 48). MtrAB and DmsEF share homology and likely an evolutionary history (49). It would stand to reason for the periplasmic cytochromes to evolve alongside their cognate outer membrane terminal reductases while still retaining some overlap in functionality.

In addition to the inner membrane bound fumarate reductase in relatives such as *Escherichia coli*, *A. hydrophila* and *V. natriegens*, *Shewanella* also uses the dual-purpose FccA. Decoupling the direct connection with the quinone pool, periplasmic fumarate reductase may provide an additional outlet valve for electrons without further contributing to NAD^+/NADH imbalance during acceptor limitation resulting in less oxidative stress. Strategies for surviving periods of metabolic dormancy (50, 51) by altering electron flow may differ across fast growing heterotrophs. Instead of a viable but nonculturable (VBNC) state as observed in multiple *Vibrio* spp. (52), *Shewanella* spp. may 'hold their breath' and store a capacitance in the periplasm in their redox stratified environment (41, 53). Chapter 3 contributes to the mystery of metabolic dormancy by demonstrating EET in *V. natriegens* extends survival in anaerobic conditions.

While *mtrAB* is conserved in numerous genomes, inner membrane and periplasmic electron proteins were not as well conserved outside of the *Shewanella* genera. *Aeromonas* and *Vibrio* spp. do not encode homologs of FccA or CctA. Alternatively, both *A. hydrophila* and *V. natriegens* utilize a di-heme periplasmic electron shuttle, PdsA to reduce MtrA, and subsequently reduce the extracellular acceptor (chapters 2 and 3, respectively).

The periplasm of *S. oneidensis* is unique compared to other facultative heterotrophs due to its abundance of cytochromes in addition to soluble electron carrying molecules, flavins, as reviewed in (41). In *S. oneidensis* MR-1, Flavin adenine dinucleotide (FAD) is secreted into the periplasm by the inner membrane protein, Bfe. FAD can be utilized as a cofactor for periplasmic reductases, FccA and UrdA, or cleaved

to flavin mononucleotide (FMN) and adenosine mononucleotide (AMP) via UshA (53). Outside of the periplasm, FMN can shuttle electrons between the MtrC family protein and the extracellular acceptor. The distinct nature of the relationship between FMN and MtrC as cofactor or soluble shuttle is currently being investigated, as reviewed in (41). EET mediated flavin reduction in *A. hydrophila* and *V. natriegens* remains unclear and is and is discussed in appendix I.

Inner membrane quinone oxidoreductases in EET capable *G. sulfurreducens* and *S. oneidensis* respond to changes in potential of the extracellular electron acceptor, reviewed in (54). *Shewanella* spp. funnel anaerobic electrons primarily through CymA, the menaquinone oxidoreductase. CymA belongs to a large family of inner membrane menaquinone/quinone oxidoreductases, the NapC/NirT family. *G. sulfurreducens* also utilizes a NapC/NirT family protein, ImcH, whose terminal acceptors are also high potential electron acceptors (55). Examination of inner membrane quinone oxidoreductases involved in EET could help connect redox potential of the physiologically relevant minerals microorganisms are interacting with in the environment. Efficient energy extraction seems to be a driver in evolving EET mechanisms in different environmental conditions.

Initial biochemical work on *A. hydrophila* KB1 suggested the involvement of formate-hydrogen dehydrogenase and a Q-loop bc1 complex, similar to NrfD of formate dependent nitrite reduction (37). Characterization of the dedicated quinone oxidoreductase(s) for EET in *A. hydrophila* and *V. natriegens* can be found in chapters 2 and 3, respectively. *Aeromonas* and *Vibrio* spp. seem to take a more specialized approach compared to *Shewanella* spp, dedicating a specific IM quinone oxidoreductase for EET instead of the multifaceted CymA. V. *natriegens* uses a *Vibrio*naceae specific CymA homolog, while A. *hydrophila* uses the NrfBCD homologs, NetBCD.

Responding to the redox potential of the environment, it's hypothesized *S. oneidensis* CymA can modulate its interaction with the quinone pool. Menaquinone is essential for reduction of fumarate, nitrate and extracellular acceptors (56) as MQ-7 is a required cofactor for CymA (57). Recent evidence suggests CymA may also be oxidized by ubiquinone-8 while oxidizing lactate and reducing a high potential electrode (+0.5 V vSHE) (58). In conditions with H_2 as an electron donor and a high potential (+0.5 V vSHE) electrode, a *menA* mutant creates more current than a *ubiA* mutant (59), supporting the hypothesis ubiquinone can be utilized as an electron donor for certain EET conditions. The physiological and/or ecological relevance of these high potential

conditions in *Shewanella* spp. has yet to be established; however, previous studies in other respiratory systems have shown that variations in quinone structures modulate the redox potential and direction of electron flow (60–62).

Electron flow into EET metabolism and the energy harvested in various conditions is currently being investigated through multiple avenues. Discerning 'true' interactions with respiratory enzymes can be difficult due to homology and functionally redundant pathways; however, perhaps redundancy is purposeful in *Shewanella* spp. Stratifying the versatile CymA across overlapping redox windows in the electron transport chain may allow for survival in redox stratified environments with environmental fluctuations.

Shewanella spp. live in such redox stratified environments where the electron donor is not limited (63, 64). *Shewanella, Aeromonas* and *Vibrio* genera are all aquatic with overlapping environmental niches and interact with each other. For example, an obligate co-culture of *Aeromonas veronii* and *Shewanella alga* was isolated for their ability to ferment citrate with subsequent formate oxidation and iron reduction (65). Overlapping niches between *Shewanella*, *Aeromonas* and *Vibrio* spp provides opportunity for horizontal transfer as reported previously for genes encoding antibiotic resistance (66, 67) and the MotAB flagellar stator (68). MtrCAB-mediated EET may also be transferred via HGT as there is disparate spread of homologs in both *Aeromonas* and *Vibrio* genera as discussed in chapters 2 and 3, respectively. Additionally, genomic analysis in chapter 4 discusses evidence for horizontal gene transfer of MtrCAB-mediated EET within the Proteobacteria.

Examining EET in *Shewanella* spp through understanding ecology and physiology of the organism allows scientists to understand the ecosystem more completely. Differences in EET phenotypes observed between *Shewanella*, *Aeromonas* and *Vibrio* genera could be due to a variety of reasons. Research investigating EET in *Shewanella* spp. shows electron donors (NADH, formate, H_2), regulatory regimes (CRP, ArcA, RpoE, FNR, Fur and RhyB), heme synthesis and *c*-type cytochrome maturation are all input factors influencing the EET phenotype (41). Differences among these upstream factors and energy management strategies in *Vibrio* and *Aeromonas* spp. may explain the decreased rate and extent of EET among these two genera compared to *Shewanella* spp. Further examination of these differences can help link environmental conditions such as electron donor and acceptor availability with the microorganisms that survive and thrive in those conditions.

1.3 Ecology and physiology of *Aeromonas* and *Vibrio* spp.

Understanding the environment and the role *Aeromonas* and *Vibrio* spp. play in an ecosystem provides a perspective that is essential when attempting to disentangle metabolic webs. *Aeromonas* and *Vibrio* are both γ-Proteobacteria splitting into separate orders, *Aeromonadales* and *Vibrionales*, respectively. *Aeromonadales* and *Vibrionales* are chemoorganotrophic facultative anaerobic r-strategists with overlapping aquatic niches and are considered “ubiquitous” in their environments (1, 2). On the sliding scale of salinity, *Vibrionales* predominate in higher salinities of the ocean and estuaries (70), whereas *Aeromonadales* are more abundant in lower salinities of estuaries and freshwater (69). *Aeromonadales* and *Vibrionales* both survive by consuming the organic waste of micro and macroscopic animals present in their respective environments (69, 70). The aqueous environment *Aeromonadales* and *Vibrionales* inhabit allows these bacteria to be present with animals both internally in the digestive systems and externally. Presence in the external environment on the surface of an animal, in the sediment, in the water column suspended or particle associated all contributes to their description as “ubiquitous”.

The ubiquity of microorganisms led microbial ecologists to examine microbial biogeography, the distribution of specific microorganisms in the environment (71). *Vibrionales* and *Aeromonadales* species can be free-living, while others are host-associated with the potential for pathogenesis (69, 72). Similar to their γ-Proteobacteria ‘cousins’ *Enterobacteriales*, animal waste consumption can evolve into live-tissue consumption through various avenues (73). Efforts to define microscopic niches through sequencing and culturing suggest the interactions between *Aeromonas* and *Vibrio* spp. and their host animals may be species specific (74, 75). Unfortunately, the relationship between host and species is currently ill defined with the exception of the model squid-*Vibrio* (*Euprymna scolopes* and *Vibrio fisheri*) symbiosis which reveals an intricate and complicated relationship (76). Further defining the non-pathogenic niches these microorganisms inhabit and how species with the potential to be pathogenic persist and then bloom in the environment may help inform future efforts to prevent outbreaks (77).

Respiratory flexibility in changing environments has been discussed in other microorganisms (78) and isolates of *Aeromonadales* and *Vibrionales* are a variable mixed bag of metabolisms (69, 72). Respiration of oxygen or other soluble chemicals such as fumarate, nitrate, nitrite, trimethylamine N-oxide (TMAO) (76, 79–81) has been

described in isolates as well as fermentation of various sugars (69, 72). As facultative anaerobes, oxygen is the preferred electron acceptor due to its high redox potential and subsequent high energy gain (82). However, oxygen is not always available in the environment (83). The digestive tracts of animals and sediments are both limited for oxygen (84, 85); therefore, *Aeromonadales* and *Vibrionales* have to survive anaerobic conditions.

Anaerobic respiration does not yield as much energy as aerobic respiration due to differences in redox potential, and the cell must choose how to best use its energy resources while maintaining redox homeostasis. *E. coli* has been well described to fine tune their respiration machinery to optimize energy generation with changing oxygen availability and alternative electron acceptors (86, 87) and potentially displays distinct 'aero-types' (88). Similar preferential use of low potential electron acceptors in examined representatives of *Aeromonas* and *Vibrio* spp are observed (28, 34, 89, 90). Once environmental conditions shift and oxygen becomes available again, these microorganisms grow rapidly.

Fast growth is a trait of these dynamic facultative anaerobes, with *Vibrio natriegens* holding the title of fastest growing microorganism with a doubling time of 9.8 minutes (91). *Aeromonas* and *Vibrio* are described as r-strategists, or copiotrophs (92) growing at maximal speed when nutrients are replete and entering starvation mode once resources are depleted (52). Shifts in environmental conditions changes selection pressures and alters the fitness landscape; therefore adaptive gene loss (93) can be a mechanism to evolve towards more simplistic, low dimensional, metabolic pathways in fast growing cells (94). However, without the proper genotype and subsequent phenotype, the microorganism may not survive a period of environmental disturbance. Acquisition of a metabolism specific to the microenvironment a facultative anaerobe finds itself in may be a strategy to balance stochastic environmental changes with the competitive demands of fast growth.

Metabolic flexibility has been documented to occur by horizontal gene transfer, as observed in *Vibrio campbelli* with the acquisition of a horizontally acquired light driven proton pump (95). Genomic analysis in chapter 4 supports the hypothesis that MtrCAB-mediated EET can be horizontally transferred potentially across a range of γ-proteobacteria. The modular organization of respiratory chains (82) may allow facultative anaerobes to acquire and plug-in environmentally relevant pathways via a donating genetic pool that is already present or maintained in the niche. *Vibrio* spp. have been

studied for their environmentally activated natural competence and its potential role in ecological speciation of this dynamic genera (96). Horizontal gene transfer of anaerobic metabolisms that integrate into existing respiratory strategies may allow facultative anaerobes to survive, thrive and be ubiquitous in rapidly changing environments.

1.4 Diversification of Proteobacteria in a changing redox landscape- The impacts of oxygen on microbial lineages

Like many other organisms, *Aeromonas* and *Vibrio* spp. use oxygen as their primary energy source. However, oxygen hasn't always been available on Earth. In fact, it used to be completely absent. Anaerobic respiration evolved first as oxygen concentrations increased in stages (97). The Great oxidation "event" occurred within 2300-2500 MYA and there were further increases in O_2 concentrations which affected the chemistry of the environment (98, 99). There was ample time for microorganisms to adapt to increasing oxygen concentrations while those in anaerobic environments continued to thrive.

Mtr-based EET may be somewhat similar to other phenotypes observed in Proteobacteria such as magnetotaxis (100), aerobic ammonia oxidation (101) and nitrogen fixation (102); An adaptation originating in an anaerobic or semi-aerobic world which was then modified and diversified by the versatile Proteobacteria to adapt to higher oxygen concentrations. The descendants of those ancestral metabolisms may still exist in isolated redox islands where environmental conditions resemble something more ancient. Connecting extant phenotypes with environmental conditions may help us understand how microbial lineages have adapted to previous changes in climate instability.

Connecting geological history and molecular evolution with microbial lineages is multifaceted and the field is rapidly evolving (103). Recent estimates predict 'Proteobacteria' diversified greatly between 3000-2000 MYA (104), with more deeply branching phyla, ε-Proteobacteria (105) and Δ-Proteobacteria (106), diverging first. Consistent with patterns observed in previous studies (107, 108), α, β, and then γ-proteobacteria lineages diverged between 2000-1000 MYA (104). Based on Eukaryotic fossils, α-Proteobacteria are estimated to have diverged around 1900 MYA (109) experiencing fluctuating oxygen concentrations resulting in various oxygen reductases (110). Based on the *Escherichia-Salmonella* split occurring 140 MYA (111), *Aeromonas* genera are estimated to have diverged around 250 MYA (112). *Vibrionaceae* divergence

was estimated to be 124 MYA (104) which can be further constrained by dating chitinase evolution in this family to approximately 188 MYA (113). As researchers fine tune the ecological role of Proteobacteria and their many forms, we can better calibrate their evolutionary history with their hosts.

While the details are unclear, there's substantial evidence that the genera *Aeromonas* and *Vibrio* diverged well after both the Great and Neoproterozoic oxygenation events (2.3-2.5 GYA and 540-490 MYA, respectively) when the atmosphere and ocean had been oxygenated (99). Overlapping with estimated timeline of phytoplankton diversification (114), *Vibrionaceae* and *Aeromonas* genera diverged in warm productive oceans, fueled by minerals and organic matter erosion which had recently started to accumulated on land (99).

MtrCAB-mediated EET in γ-Proteobacteria likely evolved after the GOE due to its integration into oxygen-dependent energy strategies. The plug-n-play format of anaerobic metabolism in *Aeromonas* and *Vibrio* spp. supports the idea of the ocean as a 'microbial seed bank' (71). Linking energy metabolisms with microbial-biogeography can help scientists examine the microbial conveyer belt hypothesis in attempts to understand the flow over energy and nutrients in ecosystems (50). The energy in the environment selects for the metabolism of the organism and arranges the resulting food chain.

Tying together the ecology and physiology of both *Aeromonas* and *Vibrio* genera, with the knowledge of EET in *Shewanella* spp. is the intersection of knowledge my thesis explores. Differences in inner membrane quinone oxidoreductases, periplasmic electron shuttles and MtrCAB structures can partially explain the differences in EET phenotypes observed across these genera. MtrCAB-mediated EET in strains of *Aeromonas* and *Vibrio* is likely a niche specific method to survive anaerobic conditions; however, there may be alternative uses for this metabolism that are yet to be elucidated.

Chapter 2: Divergent Nrf family proteins and MtrCAB homologs facilitate extracellular electron transfer in *Aeromonas hydrophila*

This chapter is a reprint of a published article
Conley BE, Intile PJ, Bond DR, Gralnick JA. 2018. Divergent Nrf family proteins and MtrCAB homologs facilitate extracellular electron transfer in *Aeromonas hydrophila*. Appl Environ Microbiol 84:e02134-18. https://doi.org/10.1128/AEM.02134-18.

2.1 Summary

Extracellular electron transfer (EET) is a strategy for respiration in which electrons generated from metabolism are moved outside the cell to a terminal electron acceptor, such as iron or manganese oxide. EET has been primarily studied in two model systems, *Shewanella oneidensis* and *Geobacter sulfurreducens*. Metal reduction has also been reported in numerous microorganisms including *Aeromonas* spp., which are ubiquitous γ-Proteobacteria found in aquatic ecosystems with some species capable of pathogenesis in humans and fish. Genomic comparisons of *Aeromonas* spp. revealed a potential outer membrane conduit homologous to *S. oneidensis* MtrCAB. While the ability to respire metals and mineral oxides is not widespread in the genus *Aeromonas*, 90% of the sequenced *A. hydrophila* isolates contain MtrCAB homologs. *A. hydrophila* mutants lacking *mtrA* are unable to reduce metals. Expression of *A. hydrophila mtrCAB* in a *S. oneidensis* mutant lacking homologous components restored metal reduction. Although the outer membrane conduit for metal reduction was similar, homologs of *S. oneidensis* inner membrane and periplasmic EET components, CymA, FccA or CctA, were not found in *A. hydrophila*. We characterized a cluster of genes predicted to encode components related to a formate dependent nitrite reductase (NrfBCD), here named NetBCD (for Nrf-like electron transfer) and a predicted diheme periplasmic cytochrome, (periplasmic diheme shuttle), PdsA. We present genetic evidence that proteins encoded by this cluster facilitate electron transfer from the cytoplasmic membrane across the periplasm to the MtrCAB conduit and functions independently from an authentic NrfABCD system. *A. hydrophila* mutants lacking *pdsA* and *netBCD* were unable to reduce metals while heterologous expression of these genes could restore metal reduction in a *S. oneidensis* mutant background. EET may therefore allow *A. hydrophila* and other species of *Aeromonas* to persist and thrive in iron or manganese rich oxygen-limited environments.

2.2 Introduction

Dissimilatory metal reducing bacteria (DMRB) respire oxidized metals such as Fe(III) and Mn(IV) that are insoluble at circumneutral conditions and therefore unable to diffuse across the outer membrane (115). Electron transfer to these metal oxides requires specialized respiratory pathways that facilitate electron flow from inside the cell across the cell envelope to the insoluble terminal electron acceptor, a process termed extracellular electron transfer (EET). DMRB are capable of reducing a wide variety of extracellular electron acceptors such as iron, manganese, uranium, vanadium, cobalt, technetium, chromium, selenium, and arsenic (116). There are two model DMRB in which the mechanism for EET has been studied in detail, the δ-Proteobacterium *Geobacter sulfurreducens,* and the γ-Proteobacterium *Shewanella oneidensis* (reviewed in (115–121). In both *Shewanella* spp. and *Geobacter* spp., multi-heme *c*-type cytochromes play a predominant role in facilitating EET across the cell envelope.

Shewanella uses a conserved pathway for EET consisting of six primary components, mostly comprised of cytochromes. Electrons are transferred to the periplasm by an inner membrane NapC/NirT family quinole dehydrogenase tetraheme cytochrome, CymA (122, 123). Electrons are delivered from CymA across the periplasm by two parallel pathways involving CctA (also known as STC), a tetraheme cytochrome, or FccA, a flavocytochrome *c* also required for fumarate respiration (124–126). From the periplasm, electrons enter the outer membrane conduit, MtrCAB. MtrA is a periplasmic decaheme *c*-type cytochrome that receives electrons from periplasmic electron carriers, CctA or FccA, and is anchored to the outer membrane by a tight association with the integral outer membrane protein MtrB (125, 127, 128). MtrB appears to bring MtrA in close proximity to the terminal reductase, MtrC, an extracellular lipoprotein decaheme *c*-type cytochrome (127–129). *S. oneidensis* is also able to secrete and use soluble shuttles, primarily flavin species, in the extracellular environment to move electrons to a variety of insoluble electron acceptors (130, 131). In addition to shuttling, flavin molecules interact with MtrC, where they may act as co-factors and increase the rate of electron transfer (132, 133).

Cytochromes are also required for EET in *G. sulfurreducens*, but with different pathways depending on the extracellular electron acceptor. Cytoplasmic membrane multi-heme *c*-type cytochromes, ImcH or CbcL, oxidize menaquinone depending on the redox potential of the acceptor (134–136). Electrons are likely carried across the periplasm by the triheme cytochromes, PpcA-E, to a variety of outer membrane

anchored cytochrome-β-barrel-cytochrome complexes (137–139). The extracellular electron acceptor is reduced by different cytochrome conduits depending on the electron acceptor being reduced (140, 141).

There are nearly 100 reports of phylogenetically diverse DMRB, but the mechanism of EET in the vast majority of these microorganisms remains to be characterized (142). Although there are parallels in the mechanism of EET in *S. oneidensis* and *G. sulfurreducens*, there are also significant differences. In order to understand how representative the *Shewanella* and *Geobacter* strategies are for EET, the mechanism in other DMRB must be characterized.

Aeromonas spp. have been reported to perform EET, reducing a wide range of extracellular electron acceptors including Fe(III) oxide minerals and electrodes (143–147). *Aeromonas* spp. are γ-Proteobacteria ubiquitous in aquatic systems and found in sediment, water column, intestinal tracts and gills of fish (148). *Aeromonas* spp. are facultative anaerobic chemoorganotrophs generally capable of reducing fumarate, nitrate, nitrite, sulfite, arsenate, selenate, and trimethylamine N-oxide (TMAO) (145, 149–154). Generally, *Aeromonas* spp., particularly *A. hydrophila*, *A. caviae*, and *A. veronii,* have been studied for their ability to cause disease in various hosts such as fish, frogs, domestic animals and humans (155, 156).

The mechanism for metal reduction in *Aeromonas* spp. was hypothesized to be similar to *S. oneidensis* based on genome sequence analysis (157, 158). Of the 137 *Aeromonas* spp. with at least draft quality sequenced genomes, 39% are predicted to encode MtrCAB homologs using a cutoff of 30% amino acid similarity. However, attempts to predict other components of the EET pathway were unsuccessful as no homologs predicted to encode CymA, CbcL, ImcH or the periplasmic carriers PpcA, CctA and FccA could be identified in the genomes of *Aeromonas* spp. The absence of these homologs suggested *Aeromonas* spp. may use different protein(s) to transfer electrons from the quinone pool to the MtrCAB complex. In this study, we show in *A. hydrophila* that electrons from respiration travel from the inner membrane to the periplasm via a NrfBCD-like electron transfer system that we have named NetBCD, to a predicted periplasmic diheme shuttle, PdsA, and across the outer membrane via MtrCAB.

2.3 Results

Identification of outer membrane components of the metal reduction pathway in

A. hydrophila. Multiple *Aeromonas* spp. have been reported to reduce extracellular electron acceptors, though the mechanism has not yet been investigated (143–145, 159). We identified *mtrCAB* gene clusters in 39% of the sequenced *Aeromonas* genomes and 90% of sequenced *A. hydrophila* strains with a genetic arrangement similar to that of *S. oneidensis*. Unlike many *Shewanella* species that contain *mtrCAB* genes, these *Aeromonas* genomes did not contain additional paralogs of *mtrCAB* such as *mtrDEF* or *omcA*. The MtrCAB proteins encoded by *A. hydrophila* ATCC7966 are 36%, 45%, and 67% similar to *S. oneidensis* MtrCAB, respectively. The Phyre2 predicted structure of *A. hydrophila* MtrC shows homology with 100% confidence to *S. oneidensis* MtrC, MtrF, OmcA and UndA, conserving the staggered cross arrangement of the heme binding sites (132, 160–163).

To determine if the *A. hydrophila* MtrCAB homologs have a similar function to *S. oneidensis* MtrCAB, *mtrA* was deleted and strains were examined for the ability to reduce Fe(III) and Mn(IV). Deletion of *mtrA* in *A. hydrophila* resulted in a significant decrease in the amount of soluble Fe(III) citrate, Fe(III) oxide, and Mn(IV) oxide reduced (Fig 1). When complemented *in trans* with *mtrA* under the expression of the vector *lac* promoter, reduction of Mn(IV) oxide was restored to wild-type levels (Fig 1C) while reduction of Fe(III) citrate and Fe(III) oxide reduction was partially restored (Fig 1A and 1B).

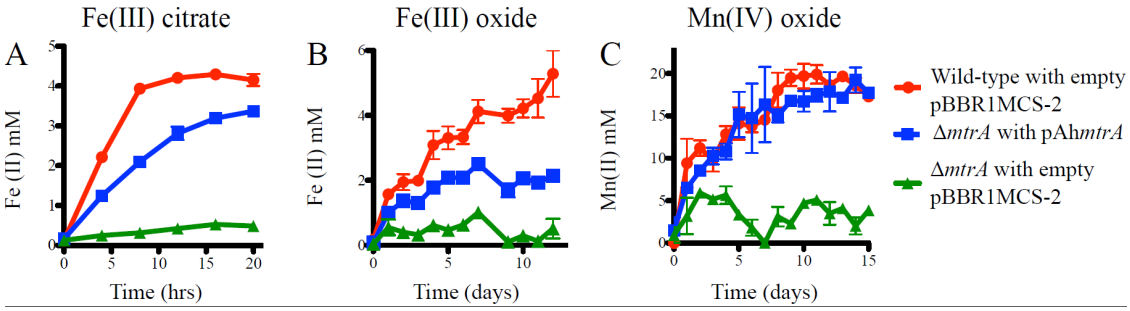

Figure 1 *A. hydrophila mtrA* is essential for metal reduction. (B) Reduction of Fe(III) oxide over time. (C) Reduction of Mn(IV) oxide over time. Wild-type with empty pBBR1MCS-2 (●), Δ*mtrA* with empty pBBR1MCS-2 (▲), Δ*mtrA* with pAh*mtrA* (■). Data representative of three independent experiments performed in triplicate displaying mean ± SEM.

We examined if *A. hydrophila* MtrCAB could restore metal reduction in a mutant strain of *S. oneidensis* lacking a range of multi-heme cytochromes, JG1453; Δ*mtrABC* / Δ*mtrDEF* / Δ*omcA* / Δ*dmsE* / ΔSO4360 / Δ*cctA* (164). *A. hydrophila mtrCAB* was

expressed using the native *lac* promoter of pBBR1MCS-2 in *S. oneidensis* strain JG1453 and reduction rates of Fe(III) citrate, Fe(III) oxide, and Mn(IV) oxide were quantified. *A. hydrophila* MtrCAB restored reduction rates of Fe(III) citrate and Mn(IV) oxide to wild-type levels in *S. oneidensis* JG1453 (Fig 2A and Fig 2C). Reduction of Fe(III) oxide was restored to wild-type levels, though the rate of reduction was slightly slower (Fig 2B). We were unable to complement *mtrA* mutants in either *S. oneidensis* or *A. hydrophila* with the *mtrA* gene from the opposite organism (Fig 3).

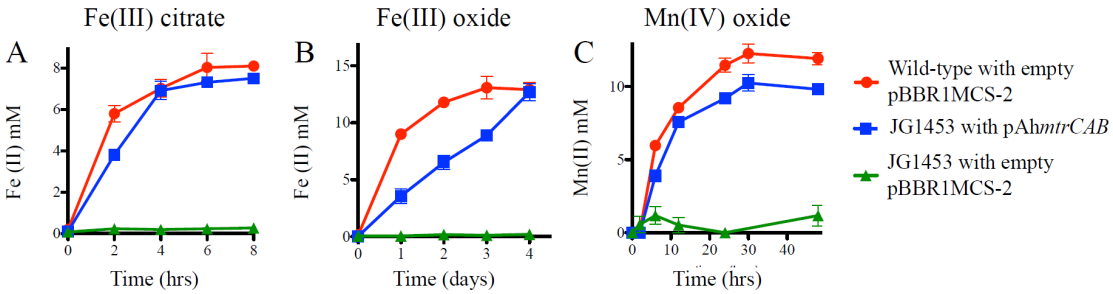

Figure 2 *A. hydrophila mtrCAB* can restore metal reduction in *S. oneidensis* mutants lacking outer membrane multi-heme cytochrome complexes (Δ*mtrABC* / Δ*mtrDEF* / Δ*omcA*/ Δ*dmsE* / ΔSO4360 / Δ*cctA*). (A) Reduction of Fe(III) citrate over time. (B) Reduction of Fe(III) oxide over time. (C) Reduction of Mn(IV) oxide over time. Wild-type with empty pBBR1MCS-2 (●), JG1453 with empty pBBR1MCS-2 (▲), JG1453 with pAh*mtrCAB* (■). Data representative of three independent experiments performed in triplicate displaying mean ± SEM.

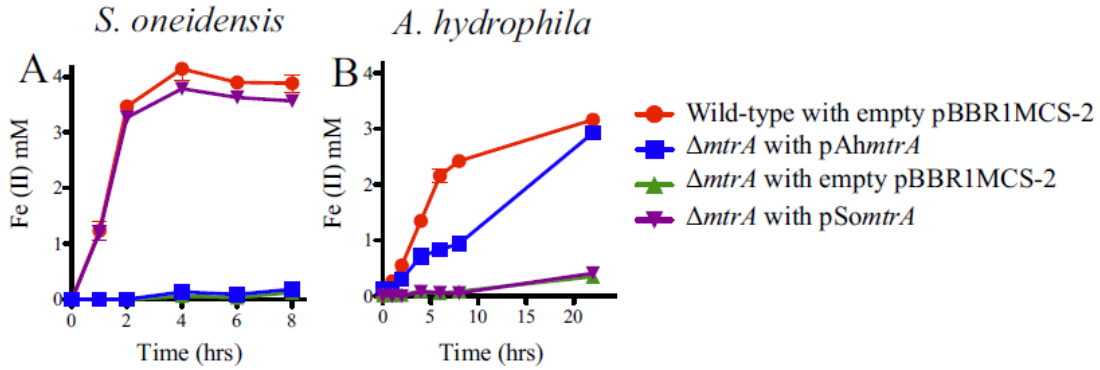

Figure 3 MtrA homologs do not function with MtrCB between *S. oneidensis* MR-1 and *A. hydrophila* ATCC7966 to reduce Fe(III) citrate. Fe(III) citrate reduction over time of (A) S. *oneidensis* and mutant strains, and (B) A. *hydrophila* and mutant strains. Wild-type (●), Δ*mtrA* with pAh*mtrA* (■), Δ*mtrA* with empty pBBR1MCS-2 (▲), Δ*mtrA* with pSo*mtrA* (▼). Data representative of two independent experiments performed in triplicate displaying mean ± SEM.

Identification of inner membrane and periplasmic components of the metal reduction pathway in *A. hydrophila*.

Considering the known role of multi-heme *c*-type cytochromes for metal reduction in *S. oneidensis* and *G. sulfurreducens,* we searched the *A. hydrophila* genome for additional genes predicted to encode multiple CXXCH heme binding motifs. We identified twelve multi-heme *c*-type cytochromes in addition to MtrA and MtrC. Predicted cytochromes identified included a peroxidase (AHA_3403), a cytochrome with 56% identity to *S. oneidensis* CytcB (AHA_0269), a predicted periplasmic diheme class I *c*-type cytochrome c_{553} (AHA_2763), and two cytochromes with unknown functions (AHA_2545 and AHA_2948). The remaining cytochromes are predicted to be involved in respiration of TMAO (*torC*, AHA_4048), nitrate (*napBC*, AHA_1589-90), oxygen (*ccoP*, AHA_2298) and nitrite (*nrfAB*, AHA_2464-65).

An additional copy of *nrfB* (AHA_2762) was located upstream and divergently transcribed from *mtrCAB* (Fig 4). In *E. coli*, the Nrf system is responsible for nitrite reduction with NrfBCD residing at the inner membrane and periplasm to transfer electrons from menaquinone to NrfA, the terminal nitrite reductase located in the periplasm (165). NrfEFG are specialized cytochrome maturation factors required for NrfA function (166). A complete *nrfABCDEFG* gene cluster (AHA_2464-2470) is present in

another location on the genome, while the gene cluster near *mtrCAB* contains only *nrfBCD,* lacking a *nrfA* paralog and the *nrfEFG* maturation genes.

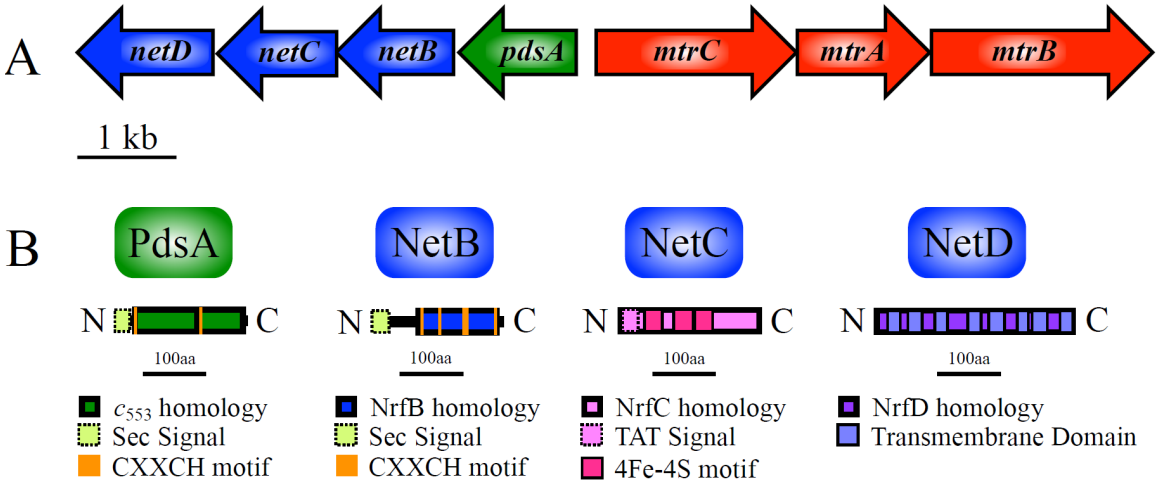

Figure 4 Key genes and proteins involved in metal reduction in *Aeromonas hydrophila* ATCC7966. (A) Blue genes, *netBCD*, encode proteins involved in menaquinone oxidation and transferring electrons from the quinone pool to the periplasm. The green gene, *pdsA*, encodes a protein involved in carrying electrons across the periplasm from the inner membrane to the outer membrane. Red genes, *mtrCAB*, encode proteins involved in transferring electrons across the outer membrane, oxidizing the periplasmic carrier and reducing the terminal electron acceptor. (B) PsdA and NetBCD with annotated domains and motifs color coded as following, secretion signals, Sec in light green and TAT in light pink, heme binding sites in orange, 4Fe-4S binding sites in pink, and transmembrane domains in lavender. Areas of homology to known proteins are also annotated in black boxes. The green protein is predicted to be soluble in the periplasm, and blue proteins are predicted to be located at and in the inner membrane.

Based on the phenotypes we describe below, we propose to rename the gene cluster upstream of *mtrCAB* as *netBCD,* for Nrf-like electron transfer (AHA_2760-62) (Fig 4A). The atypical *nrfBCD* gene cluster located upstream of *mtrCAB* also encodes a putative 22.5 kDa periplasmic diheme *c*-type cytochrome we propose to rename PdsA, periplasmic diheme shuttle (AHA_2763) (Fig 4A). PdsA is predicted to be a class I *c*-type

cytochrome c_{553} (Fig 4B), with low sequence identity, (10-35%) to other mono or diheme cytochrome c_{553} which are generally electron carriers utilized in a wide variety of metabolisms (167–170).

Further analysis of sequenced *Aeromonas* spp. genomes revealed all strains with *mtrCAB* also contain *pdsA* and *netBCD* in the same genomic architecture, except for *A. diversa* strain CECT 4254 and *A. schubertii* strains WL1483 and ATCC43700. *A. diversa* and *A. schubertii* strains are predicted to encode a diheme *c*-type cytochrome 71% and 75% similar, respectively, to *A. hydrophila* ATCC PdsA; however, instead of *netBCD* a predicted NapC/NirT family protein is encoded immediately downstream of *pdsA*. In *A. hydrophila*, NetB is 76% similar to NrfB with the N-terminal region being most divergent, while NetCD and NrfCD have a high degree of similarity (90%) (Fig 4B). Based on homology to NrfBCD, we hypothesize that NetCD oxidizes the menaquinone pool at the inner membrane and reduces NetB in the periplasm.

Deletion of *pdsA* and *netBCD* in *A. hydrophila* resulted in a significant decrease in the amount of Fe(III) citrate reduced compared to wild-type (Fig 5A). Fe(III) citrate reduction in Δ*pdsA/netBCD* was restored to wild-type levels by expressing *pdsA/netBCD* in trans under the control of a *lac* promoter (Fig 5A). Reduction of Fe(III) oxide and Mn(IV) oxide by *pdsA/netBCD* mutants and complemented strains demonstrated the same trend as Fe(III) citrate reduction (Fig 6). Deletion of *pdsA* and *netBCD* in *A. hydrophila* did not alter growth rate with nitrite as the terminal electron acceptor (Fig 7).

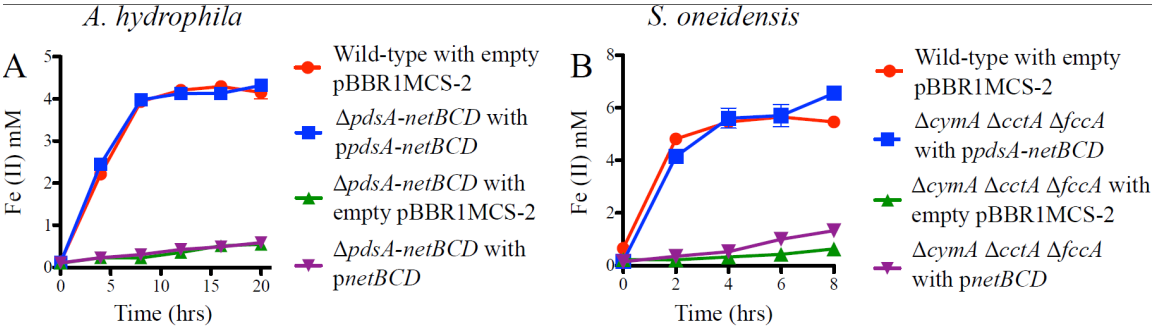

Figure 5 *pdsA* and *netBCD* are essential for Fe(III) citrate reduction in *A. hydrophila* and can complement *S. oneidensis* mutants. (A) Reduction of Fe(III) citrate by A. *hydrophila* strains over time. Wild-type with empty pBBR1MCS-2 (●), ΔpdsA/netBCD with empty pBBR1MCS-2 (▲), ΔpdsA/netBCD with ppdsA/netBCD (■), ΔpdsA/netBCD with pnetBCD (▼). (B) Reduction of Fe(III) citrate by S. *oneidensis* strains over time. Wild-type (●), ΔcymA/cctA/fccA with empty pBBR1MCS-2 (▲), ΔcymA/cctA/fccA with ppdsA/netBCD (■),

ΔcymA/cctA/fccA with pnetBCD (▼). Data representative of two independent experiments performed in triplicate displaying mean ± SEM.

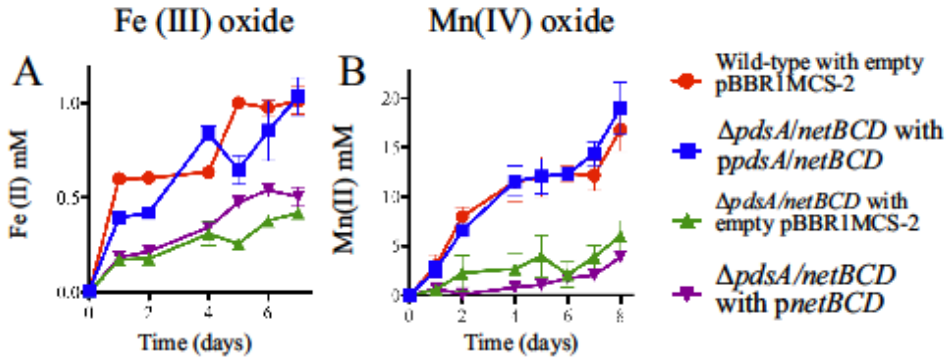

Figure 6 *pdsA* and *netBCD* are essential for Fe(III) oxide and Mn(IV) oxide reduction in *A. hydrophila*. (A) Reduction of Fe(III) oxide by *A. hydrophila* strains over time. Wild-type with empty pBBR1MCS-2 (●), Δ*pdsA/netBCD* with empty pBBR1MCS-2 (▲), Δ*pdsA/netBCD* with p*pdsA/netBCD* (■), Δ*pdsA/netBCD* with p*netBCD* (▼). (B). Reduction of Mn(IV) oxide by *A. hydrophila* strains over time. Wild-type with empty pBBR1MCS-2 (●), Δ*pdsA/netBCD* with empty pBBR1MCS-2 (▲), Δ*pdsA/netBCD* with p*pdsA/netBCD* (■), Δ*pdsA/netBCD* with p*netBCD* (▼). Data representative of two independent experiments performed in triplicate displaying mean ± SEM.

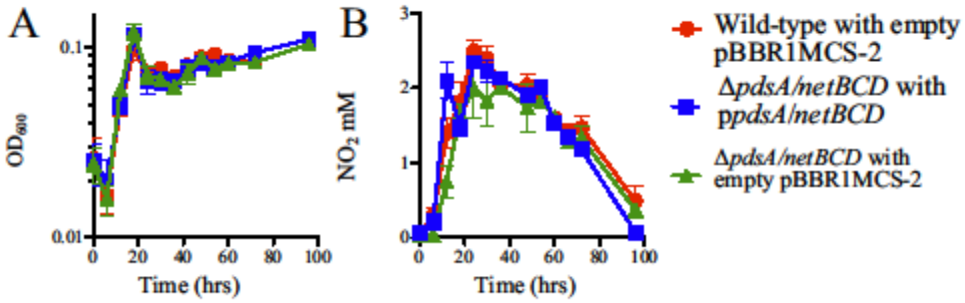

Figure 7 *pdsA* and *netBCD* are not essential for nitrate and nitrite reduction in *A. hydrophila*. (A) Growth respiring nitrate by *A. hydrophila* strains over time. (B) Nitrite consumption and production during growth respiring nitrate by *A. hydrophila* strains over time. Wild-type with empty pBBR1MCS-2 (●), Δ*pdsA/netBCD* with empty pBBR1MCS-2 (▲), Δ*pdsA/netBCD* with p*pdsA/netBCD* (■). Data representative of two independent experiments performed in triplicate displaying mean ± SEM.

To further examine the function of PdsA and NetBCD in metal reduction, we heterologously expressed *pdsA* and *netBCD* in pBBR1MCS-2 under the control of the vector *lac* promoter in a strain of *S. oneidensis* missing the inner membrane (CymA) and periplasmic cytochromes (CctA and FccA) required for EET. Expression of *pdsA/netBCD* in the *S. oneidensis* Δ*cymA/cctA/fccA* mutant restored Fe(III) citrate reduction to wild-type levels (Fig 5B). In *S. oneidensis*, CymA is also essential for nitrate, nitrite, dimethyl sulfoxide (DMSO), and fumarate reduction (171, 172). Expression of *pdsA/netBCD* in a *S. oneidensis* Δ*cymA* strain partially complemented growth in DMSO, fumarate, and nitrate but with lower final cell yield and longer lag time (Fig 8A-C); however, reduction of nitrite was not restored in these strains (Fig 8D). A negative control strain carrying only the empty vector control was unable to restore growth in fumarate, DMSO, nitrate and nitrite (Fig 8).

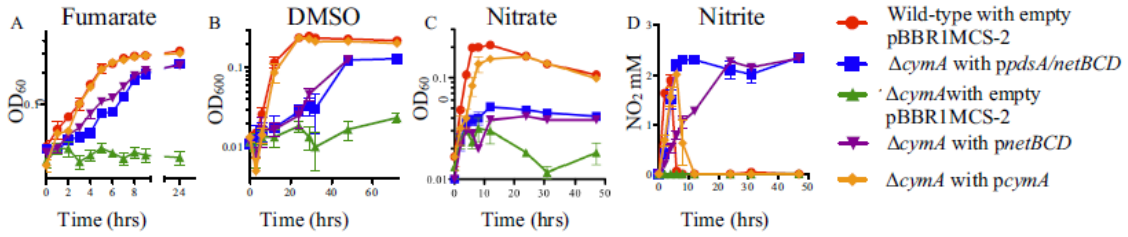

Figure 8 *pdsA* and *netBCD* can complement fumarate, DMSO, and nitrate but not nitrite reduction in *S. oneidensis*. (A) Growth respiring fumarate (B) DMSO and (C) nitrate by *S. oneidensis* strains over time. (D) Nitrite production and consumption during growth respiring nitrate by *S. oneidensis* strains over time. Wild-type with empty pBBR1MCS-2 (●), Δ*cymA* with empty pBBR1MCS-2 (▲), Δ*cymA* with p*pdsA/netBCD* (■), Δ*cymA* with p*netBCD* (▼) Δ*cymA* with p*cymA* (◆). Data representative of two independent experiments performed in triplicate displaying mean ± SEM.

In *S. oneidensis*, periplasmic tetraheme cytochromes FccA and CctA carry electrons across the periplasm from CymA to MtrA (124–126). *A. hydrophila* also requires a strategy to move electrons across the periplasm. Due to the genomic context and predicted cellular localization, we hypothesized PdsA is the periplasmic electron carrier for EET in *A. hydrophila*. We examined a series of mutants complemented with and without *pdsA* for the ability to restore Fe(III) citrate reduction in both *A. hydrophila*

and *S. oneidensis*. *A. hydrophila* Δ*pdsA/netBCD* complemented only with *netBCD* is unable to reduce Fe(III) citrate (Fig 8A). Expression of *netBCD* alone in a *S. oneidensis* Δ*cymA*/*cctA*/*fccA* mutant strain was also unable to restore Fe(III) citrate reduction (Fig 5B). Fe(III) citrate reduction was rescued in both cases when *pdsA* and *netBCD* were expressed together on a plasmid. Growth on fumarate, DMSO and nitrate in *S. oneidensis* Δ*cymA* was complemented by expressing *netBCD* with or without *pdsA* under the same promoter (Fig 8A and B). It should be noted that the native periplasmic electron carriers (FccA and CctA) were present in this genetic background. The addition of *pdsA* resulted in an increased rate of nitrite production when grown on nitrate compared to strains not expressing *pdsA* (Fig 8D). These phenotypes are consistent with our hypothesis that the diheme *c*-type cytochrome PdsA traffics electrons between NetBCD and MtrCAB.

A phylogenetic analysis was performed to better understand how NrfBCD and NetBCD are related. NetB and NrfB were selected because of greater differences in amino acid similarity compared to NrfCD and NetCD. *A. diversa* and *A. schubertii* were excluded from analysis because they do not encode a NetB homolog. NetB and NrfB from *Aeromonas* spp. clustered separately from each other (Fig 9). NrfB from other γ-Proteobacteria, orders *Vibrio*nales, Pasteurellales and Enterobacteriales representatives, clustered separately from *Aeromonas* spp. NrfB and NetB.

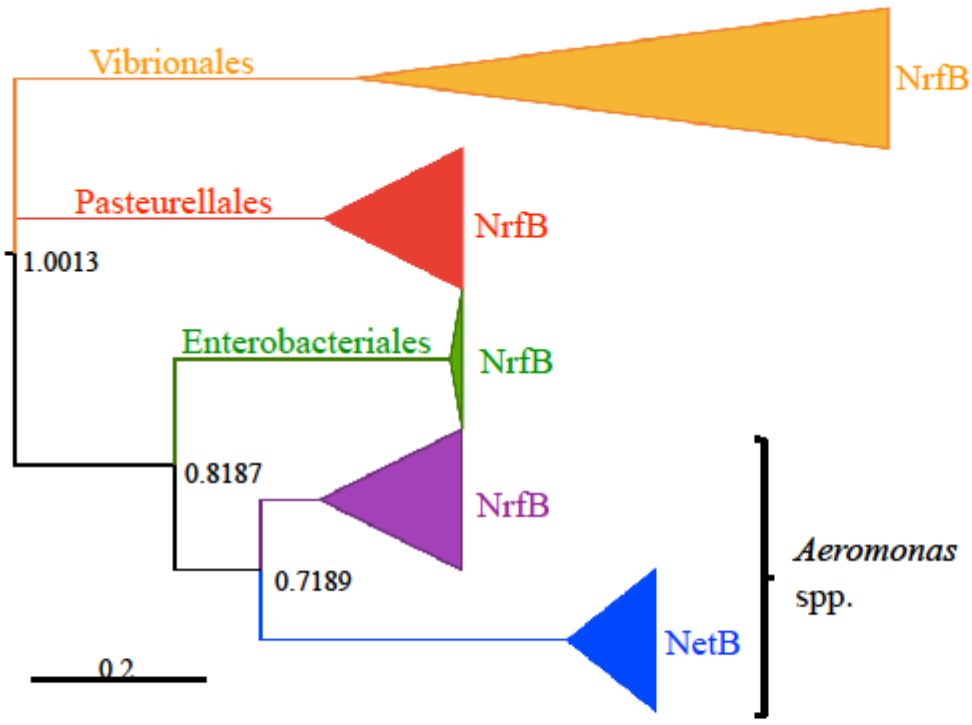

Figure 9 Molecular phylogenetic analysis of NrfB, and NetB. NrfB from selected *Vibrio*nales, Pasteurellales, and Eneterobacteriales representative strains are shown in yellow, red and green, respectively. NrfB from selected *Aeromonas* spp. are shown in blue, NetB from selected *Aeromonas* spp. are shown in purple. Amino acid sequences were aligned with ClustalW, and evolutionary relationships were inferred using maximum likelihood method with 1000 bootstrap replicates based on the JTT matrix-based model. The tree is drawn to scale with the scale bar representing substitutions per site.

2.4 Discussion

Metal reducing bacteria have been isolated from a wide range of environments and are phylogenetically diverse, yet our understanding of EET mechanisms in microorganisms beyond *Shewanella* and *Geobacter* is limited. Here we present a working model of EET in *A. hydrophila* consistent with our findings (Fig 10). NetCD oxidizes the menaquinone pool and reduces the periplasmic cytochrome NetB. PdsA receives electrons from NetB, which can move across the periplasm to reduce MtrA. MtrC oxidizes MtrA and reduces an extracellular electron acceptor while in a conduit

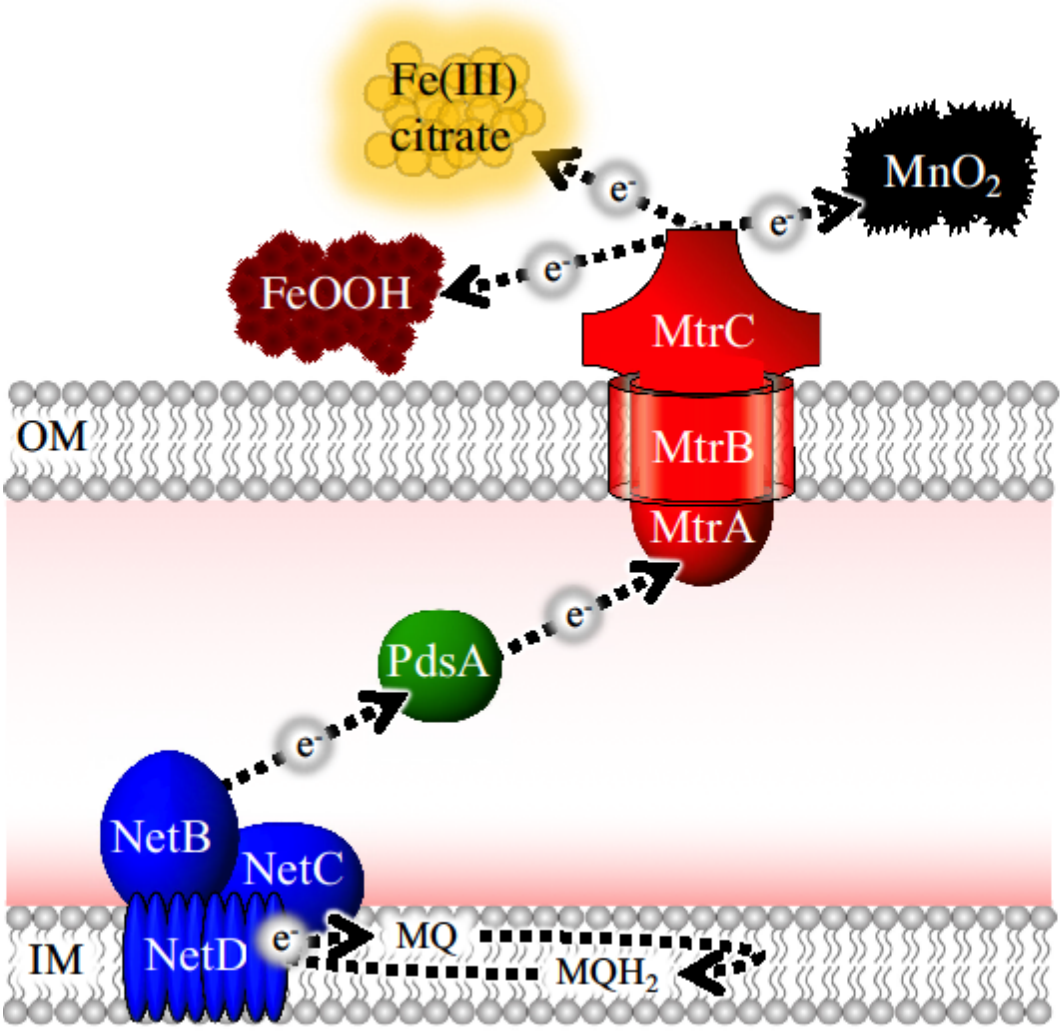

Figure 10 Model for the mechanism of extracellular electron transfer in *A. hydrophila*. NetBCD, a NrfBCD-like complex, oxidizes the menaquinone pool and transfers electrons to PdsA, a predicted periplasmic diheme. Electrons are then transferred across the periplasm to MtrABC which moves electrons across the outer membrane to the extracellular acceptor.

Multiple *Aeromonas* sp. have been reported to reduce extracellular electron acceptors (143–147, 159). Initial examinations of *Aeromonas* spp. genomes revealed homologs to *Shewanella* spp. *mtrCAB*-like gene clusters which were targeted for mutagenesis in *A. hydrophila*. Deletion of the *mtrA* homolog in *A. hydrophila* resulted in a significant decrease in the reduction of Fe(III) citrate, Fe(III) oxide and Mn(IV) oxide, and

could be restored with complementation (Fig 1). Reduction of Fe(III) oxide was only partially restored in *A. hydrophila ΔmtrA* expressing *mtrA* on a plasmid possibly due to differences in expression or production of MtrA versus the natively encoded MtrC or MtrB. Because MtrCAB proteins form a complex together, differences in expression or production levels could result in the observed partial complementation. Additionally, Fe(III) oxide is reduced slower than the higher potential Mn(IV) oxide and Fe(III) citrate which may allow the observation of partial complementation. Reduction of Fe(III) citate, Fe(III) oxide and Mn(IV) oxide could be restored by *A. hydrophila mtrCAB* expression in a *S. oneidensis* mutant missing all homologs of this conduit system (Fig 2). *Shewanella* spp. reduce soluble shuttles via the Mtr pathway to help facilitate extracellular electron transfer. We are currently exploring the possible role of soluble shuttles in *Aeromonas* EET. Gene deletions and heterologous expression experiments strongly suggest that *A. hydrophila* uses a strategy similar to *Shewanella* to move electrons across the outer membrane for EET. However, the mechanism to deliver electrons to MtrA from the cytoplasmic membrane and across the periplasm of *A. hydrophila* was less clear.

CymA from *S. oneidensis* and ImcH from *G. sulfurreducens* both belong to the NapC/NirT family of quinol dehydrogenases, multi-heme *c*-type cytochromes generally responsible for oxidizing menaquinone and reducing an acceptor cytochrome in the periplasm (122, 123, 134). The only NapC/NirT family protein predicted to be encoded in the genome of *A. hydrophila* is a NapC homolog (AHA_1590) which is likely involved in nitrate reduction and is encoded in the *napFDAGBC* gene cluster. By searching the genome for predicted multi-heme cytochromes, we identified a cluster of genes upstream and divergently transcribed from *mtrCAB* previously annotated as being involved in nitrite reduction (*nrfBCD*). In *E. coli*, NrfBCD forms a complex to transfer electrons from menaquinone to the periplasmic terminal nitrite reductase, NrfA (165, 173). NrfD contains eight transmembrane domains and forms a complex with NrfC which is predicted to contain four [4Fe-4S] cluster cofactors (174). The NrfCD complex oxidizes menaquinone and reduces NrfB, a periplasmic pentaheme *c*-type cytochrome (174). Electrons are passed from NrfB to NrfA, which facilitates reduction of NO_2^- to NH_3 (175). Due to the genomic context, predicted function and evidence we present here, we hypothesize *A. hydrophila* uses a NrfBCD-like complex to oxidize menaquinone and reduce a periplasmic acceptor, which we have renamed Nrf-like electron transfer NetBCD based on its role in EET. A periplasmic diheme *c*-type cytochrome encoded directly upstream of *netBCD* works to shuttle electrons between NetB and MtrA across

the periplasm as shown in Figure 7. We propose to rename this locus *pdsA* for periplasmic diheme shuttle. The N-terminal domain of NetB that diverges in sequence similarity with NrfB (Fig 4B) may be responsible for interacting with PdsA.

Fe (III) citrate reduction by *A. hydrophila* was significantly impaired when *pdsA/netBCD* was deleted and this gene cluster restored Fe(III) citrate reduction when expressed in a strain of *S. oneidensis* missing inner membrane and periplasmic proteins involved in metal reduction (Fig 5). Complementation required PdsA in both *A. hydrophila* and *S. oneidensis* mutants (Fig 5), consistent with a role for this putative diheme cytochrome as a periplasmic electron carrier. The use of a diheme cytochrome as a periplasmic shuttle is mechanistically unique among described DMRB to date. *S. oneidensis* uses two tetraheme cytochromes, CctA and FccA to transfer electrons from CymA to MtrA (124–126) while *G. sulfurreducens* is hypothesized to use triheme cytochromes, PpcA-E to transfer electrons across the periplasm (137, 138). The diheme cytochrome MacA from *G. sulfurreducens* was originally proposed to be involved in metal reduction; however, biochemical characterization shows MacA is a diheme peroxidase of the CcpA family (176, 177). In contrast, PdsA is annotated as cytochrome c_{553}, class I *c*-type family of cytochromes and does not share homology to diheme peroxidases. Cytochromes c_{553} are generally small soluble electron carriers, and have been reported to be involved in multiple metabolisms. In the sulfate reducing δ-Proteobacterium, *Desulfovibrio vulgaris*, cytochrome c_{553} is a periplasmic monoheme electron carrier oxidizing formate dehydrogenase and reducing cytochrome *c* oxidase (167). In multiple Cyanobacteria species, cytochrome $c_{553,}$ also known as cytochrome c_6, is a monoheme electron carrier oxidizing cytochrome b_6f complex and reducing photosystem I (168). In the purple sulfur γ-Proteobacterium, *Allochromatium vinosum*, cytochrome c_{553} (TsdA) is a periplasmic diheme protein that oxidizes thiosulfate and reduces multiple electron carriers (169). TsdA has been reported to be widespread in Proteobacteria with homologs present in α, β, δ, ε and γ-Proteobacteria (170). The role of electron shuttling for cytochrome c_{553} in other organisms is consistent with our observations in *A. hydrophila*.

CymA in *S. oneidensis* is required for a variety of respiratory pathways including fumarate, DMSO, nitrate and nitrite. An *S. oneidensis* mutant lacking *cymA* was able to respire fumarate, DMSO and nitrate when expressing *netBCD* but with longer lag times and a lower final cell density (Fig 8A-C). Nitrate reduction as measured by nitrite production was faster in *S. oneidensis* Δ*cymA* expressing *pdsA*

and *netBCD* compared to *S. oneidensis* Δ*cymA* expressing only *netBCD* (Fig 8D). The periplasmic shuttles, *fccA* and *cctA* are still encoded in the Δ*cymA* background, and might contribute to electron transfer from NetBCD to nitrate reductase, NapC. The presence of PdsA, an additional periplasmic electron shuttle, in *S. oneidensis* lacking *cymA* increases the transfer of electrons to NapC compared to a strain not producing PdsA. Additionally, interactions between CctA or FccA with NetB may be less efficient than PdsA interacting with NetB which could result in an increased rate of nitrite production. Reduction of nitrite was not complemented by expression of *netBCD* (Fig 8D), suggesting that NetB may be unable to directly interact with NrfA. These data suggest NetBCD is capable of reducing alternative terminal reductases when expressed in *S. oneidensis.* In *A. hydrophila,* however, there are dedicated menaquinone/quinone oxidases involved in the reduction of fumarate, nitrate and nitrite. We hypothesize in *Aeromonas* spp. NetBCD is specifically used in extracellular electron transfer unlike the versatile CymA of *Shewanella* spp..

Not all sequenced *Aeromonas* spp. are predicted to encode EET machinery. Strains predicted to encode EET machinery, indicating the presence of homologs to *mtrCAB*, *pdsA* and *netBCD*. The majority (> 60%) of *A. bestiarum, A. pisciola, A. popoffii, A. hydrophila, A. dhakensis, A. diversa,* and *A. schubertii* contain *mtrCAB, pdsA* and *netBCD*. *A. diversa* and *A. schubertii* are atypical in this group as they encode a NapC/NirT family protein ~ 45% similar to CymA from *S. oneidensis* in place of *netBCD*. All *Aeromonas* spp. that contain *mtrCAB* also have *pdsA,* regardless of the inner membrane component. Of the *Aeromonas* spp. with at least draft quality sequenced genomes, 61% do not encode MtrCAB or PdsA and NetBCD. In some genera of *Aeromonas* spp., *A. salmonicida, A. veronii, A. jandaei,* and *A. enteropelogenes,* only a few strains are predicted to encode MtrCAB and PdsA and NetBCD representing the minority of their species (<35% of strains encoding MtrCAB) in the genus. The variability between species to encode metal reduction in *Aeromonas* spp. may suggest metal reduction traits can be transferred by horizontal gene transfer or may become lost in a genus as strains diversify.

Phylogenetic analyses show NetB clusters with other putative NetB in *Aeromonas* spp., while NrfB from *Vibrio*nales, Pasteurellales, and Eneterobacteriales representatives cluster separately from *Aeromonas* spp. NrfB and NetB (Fig 9). The N-terminus of all encoded *Aeromonas* spp. NetB contains 70 amino acids that do not share homology to NrfB. The unique N-terminus sequence of NetB could have evolved to allow

electron transfer to PdsA and/or prevent electron transfer to NrfA, which may explain why NetBCD could not complement nitrite reduction when expressed heterologously in *S. oneidensis* Δ*cymA* (Fig 8D). NetB is phylogenetically distinct from NrfB, consistent with these proteins diverging from a common ancestor to facilitate electron transfer via different pathways beyond the cytoplasmic membrane.

For metal reduction in γ-Proteobacteria, the outer membrane conduit structure appears to be more conserved than the inner membrane and periplasmic components. The diversity of inner membrane proteins involved in the metal reduction pathway could be due to the fact that proton motive force (PMF) is only generated at the inner membrane and not the outer membrane. The generation of PMF, use of different quinones, and potential dependence of the electron acceptor may have spurred greater innovation of proteins in the inner membrane. Attempts to find other genera predicted to encode NetBCB by homology searches were not successful. To the best of our knowledge, the use of NetBCD for metal reduction is unique to *Aeromonas* spp.

2.5 Materials and Methods

Bacterial strains and growth conditions. Stains used in this study are listed in Table 1. *A. hydrophila* ATCC7966 was obtained from the American Type Culture Collection (Manassas, VA). *S. oneidensis* strain MR-1 was originally isolated from Lake Oneida in New York State (178). All chemicals were obtained from Sigma-Aldrich (St. Louis, MO). Strains were grown aerobically in Lysogeny Broth (LB) during routine manipulation and strain construction. Media was supplemented with 50 μg/mL (*S. oneidensis* and *Escherichia coli*) or 75 μg/mL (*A. hydrophila*) kanamycin, 100 μg/ml gentamycin, and 250 μM 2,6-diaminopimelic acid (DAP) as necessary. The strains used for cloning, derivative strains of *S. oneidensis* and *A. hydrophila*, and the plasmids used in this study are found in Table 1. The minimal medium used for experiments was *Shewanella* basal medium (SBM) containing (per L) 0.225 g K_2HPO_4, 0.225 g KH_2PO_4, 0.46 g NaCl, 0.225 g $(NH_4)SO_4$, 0.117 g $MgSO_4$•7H2O, 2.38 g HEPES, 10 ml of mineral mix (179) , 10 ml vitamin mix excluding riboflavin (180), 0.5 g Casamino Acids, and 20 mM lactate at pH 7.2. Cultures were grown at 30 °C (*S. oneidensis* and *A. hydrophila*) or 37 °C (*E. coli*) and shaken at 250 rpm when grown aerobically. Fe(III) oxide (β-FeOOH), and Mn(IV) oxide was prepared as previously described (181, 182). Electron donors and acceptors were provided in the following final concentrations: 20 mM lactate, 40 mM sodium

fumarate, 50 mM DMSO, 3 mM $NaNO_3$, 5 mM Fe (III) citrate, 20 mM Mn (IV) oxide and ~10 mM Fe(III) oxide.

Table 1. Strains and plasmids described in chapter 2

Strain or plasmid	Genotype, relevant characteristics	Source or reference
Strains		
JG274	*S. oneidensis* MR-1, wild-type	(178)
JG168	JG274 with empty pBBR1MCS-2, Km^r	(179)
JG730	JG274 Δ*mtrA*	(157)
JG1064	JG274 Δ*cymA*	(183)
JG1224	JG1064 with empty pBBR1MCS-2, Km^r	This study
JG1453	JG274 Δ*mtrABC*/Δ*mtrDEF*/ Δ*omcA*/ Δ*dmsE*/ ΔSO4360/ Δ*cctA*	(164)
JG3522	JG3423 with empty pBBR1MCS-2, Km^r	This study
JG3568	JG1453 with pAh*mtrCAB*, Km^r	This study
JG3584	JG1453 with empty pBBR1MCS-2, Km^r	This study
JG3423	*Aeromonas hydrophila* ATCC7966	ATCC
JG3626	JG3423 Δ*mtrA*	This study
JG3634	JG3626 with empty pBBR1MCS-2, Km^r	This study
JG3658	JG3626 with p*mtrA*, Km^r	This study
JG3689	JG1064 with p*netBCD*, Km^r	This study
JG3711	JG1064 with p*pdsA* and *netBCD*, Km^r	This study
JG3745	Δ*cymA*/*fccA*/*cctA*	This study
JG3746	JG3745 with p*pdsA* and *netBCD*, Km^r	This study
JG3747	JG3745 with p*NetBCD*, Km^r	This study
JG3752	JG3745 with empty pBBR1MCS-2, Km^r	This study
JG3786	JG3423 Δ*pdsA* and *netBCD*	This study
JG3788	JG3786 with p*NetBCD*, Km^r	This study
JG3790	JG3786 with empty pBBR1MCS-2, Km^r	This study
JG3793	JG3786 with p*pdsA* and *netBCD*, Km^r	This study
JG3796	JG1064 with p*cymA*, Km^r	This study
JG4008	JG730 with empty pBBR1MCS-2, Km^r	This study
JG4009	JG3626 with pSo*mtrA*, Km^r	This study

JG4015	JG730 with pSo*mtrA*, Km^r	This study
JG4016	JG730 with pAh*mtrA*, Km^r	This study
UQ950	*E. coli* DH5α λ(pir) host for cloning, F$^-$Δ(*argF-lac*)*169* ϕ80*dlacZ58*(ΔM15) *glnV44*(AS) *rfbD1 gyrA96*(NalR) *recA1 endA1 spoT1 thi-1 hsdR17 deoR* λ*pir*$^+$	(184)
WM3064	*E. coli* donor strain for conjugation, *thrB1004 pro thi rpsL hsdS lacZ*Δ M15 RP4–1360 Δ(*araBAD*)*567* Δ*dapA*1341::[*erm pir*(wt)]	(184)
Plasmids		
pSMV3	Deletion vector, Km^r, *sacB*	(184)
pBBR1MCS-2	Broad-host range cloning vector, Km^r	(185)
pEXG2	Deletion vector, Gent^r, *sacB*	(186)
p*cymA*	*cymA* in pBBR1MCS-22 with 12 bp upstream and 78 bp downstream in pBBR1MCS-2	Lab stock
pAh*mtrCAB*	*mtrCAB* (AHA_2764-66) with 75 bp upstream and 90 bp downstream in pBBR1MCS-2	This study
pAh*mtrA*	*mtrA* with 25 bp upstream and 20 bp downstream in pBBR1MCS-2	This study
pSo*mtrA*	*mtrA* with 20bp upstream and 20bp downstream in pBBR1MCS-2	This study
p*pdsA/netBCD*	*pdsA* and *netBCD* (AHA_2760-63) with 35 bp upstream and, 77 bp downstream in pBBR1MCS-2	This study
p*netBCD*	*netBCD* with 62 bp upstream and, 42 bp downstream in pBBR1MCS-2	This study
pΔAh*mtrA*	1138 bp upstream and 1102 bp downstream of *mtrA* in pEXG2	This study
pΔ*pdsA/netBCD*	1196 bp upstream and 1052 bp downstream of *pdsA* and *netBCD* in pSMV3	This study
pΔ*cymA*		(183)
pΔ*fccA*		(183)

pΔ*cctA*	951 bp upstream and 861 bp downstream *cctA* in pSMV3	(157)

Plasmid and mutant construction. Primers used to construct plasmids are listed in Table 2. Construction of in-frame deletion mutants was performed as previously described (184). For both *Shewanella* and *Aeromonas*, 1 kb fragments upstream and downstream of the targeted sequence including nine nucleotides after the start codon and nine nucleotides before the stop codon were amplified and cloned into the suicide vector pSMV3 (184) or pEXG2 (for *A. hydrophila* Δ*mtrA*) (186). Merodiploids were selected for by kanamycin or gentamycin resistance, and clones were screened by PCR. Merodiploids were resolved by sucrose counter selection mediated by *sacB* and screened by PCR. Complementation strains were constructed using pBBR1MCS-2 (185). All constructs and deletion mutants were verified with Sanger sequencing by ACGT, Inc (Wheeling, IL).

Table 2. Primers for the studies described in Chapter 2

Function and Primer	Sequence	Cut Site
Complement		
Ah*mtrCAB*_F	ACCTAGCTCGAGATACTCAAGGTTGATTTTCGATCCG	XhoI
Ah*mtrCAB*_R	TCTTACAAGCTTAGATGATGAAAGAGGGGAGCCTGG	HindIII
Ah*mtrA*_F	AATCGTCTCGAGCCCTTTGCCGTTGAAGAACACGAT	XhoI
Ah*mtrA*_R	TCAGCTAAGCTTTATTTCATGACTTCTCTCC	HindIII
So*mtrA*_F	NNNNNNAAGCTTGACAAATTGGGAAGCCTATT	HindIII
So*mtrA*_R	NNNNNNTCTAGAAATTTCATTTTCTCGTCTCC	XbaI
*pdsA/netBCD*_F	GCTTATAAGCTTGGGTTTATAGACCTTTTCTG	HindIII
*pdsA/netBCD*_R	CTATTATCTAGATTAGCAGCAATAAAAAAGGC	XbaI
*netBCD*_F	NNNNNNAAGCTTCTCCTTTTTGTTGCCAGGCG	HindIII
*netBCD*_R	TTTGTTTGCCTGCGATTTGCTCTAGANNNNNN	XbaI
*cymA*_F	NNNNNNGAATTCGGAGATAGAGTAATGAACTG	EcoRI
*cymA*_R	NNNNNNGAGCTCCTATCTAGATAGATCTGCTA	SacI

Deletion		
ΔAh*mtrA*_upF	GGACAAGCTTTGTTCAAGTTTGACGACGTG	HindIII
ΔAh*mtrA*_upR	CCAGTCTAGACGGGGTGATTCTTTTCATATCGTGTC	XbaI
ΔAh*mtrA*_downF	GTCCTCTAGACAATCACTGCGGCGCTGAGGAGAG	XbaI
ΔAh*mtrA*_down R	GTCCAGAATTCTCATCGGACTTGTCCTTGCG	EcoR1
Δ*pdsA/netBCD*_ upF	CAATTTACTAGTTGTTGATCTTGCCGTTGATG	SpeI
Δ*pdsA/netBCD*_ upR	CTATTATCTAGAGCGTTTCATTTCTTATCC	XbaI
Δ*pdsA/netBCD*_ downF	CTATTATCTAGACAGATGACGGTGATGTAGCC	XbaI
Δ*pdsA/netBCD*_ downR	GCTTATGCGGCCGCCGGTGCAACGTTTTATCACC	NotI

Metal reduction assays. Metal reduction was measured using ferrozine assays as previously described with some modifications (187). Single colonies freshly streaked from frozen stocks were inoculated into LB and grown overnight. Cells were washed once in SBM and resuspended to an OD_{600} of 1. This suspension was diluted 1:10 into 270 μL of SBM with either ~5 mM of Fe(III) citrate, ~10 mM Fe(III) oxide, or ~20 mM Mn(IV) oxide in a 96-well plate. Plates were kept in a GasPak system anaerobic petri dish holder (Becton, Dickinson and Company) that was flushed with Argon for 15 min between time points and incubated at room temperature. At each time point, samples were diluted 1:10 into 0.5 N HCl to prevent the oxidation of Fe(II) (187). Fe(II) was measured by diluting the acid-fixed sample 1:10 into a solution containing 2 g/L ferrozine buffered in 100 mM HEPES (188) and OD_{562} was quantified. Standard curves for Fe(II) were made from $FeSO_4$ dissolved in 0.5 N HCl. Biological Mn(IV) reduction was quantified indirectly via the abiotic reduction of Mn(IV) by Fe(II) which can be quantified by ferrozine. Samples from Mn(IV) reduction assays were mixed with Fe(II) and measuring the remaining Fe(II) via ferrozine which corresponds to the amount of remaining Mn(IV). Mn(IV) was diluted 1:5 into 4 mM $FeSO_4$ in 2 M HCl, and incubated in the dark overnight, and the resulting Fe(II) was measured (134). Standard curves for Mn(IV) were made by diluting 1:10 of Mn(IV) oxide in 4 mM $FeSO_4$ in 2 M HCl and

incubating in the dark overnight. Mn(IV) standards were diluted 1:5 in 0.5 M HCl, diluted 1:10 into a solution containing ferrozine and OD_{562} was quantified.

Genome Comparisons and Phylogeny. Integrated Microbial Genomes (IMG: https://img.jgi.doe.gov/cgi-bin/m/main.cgi) was used to compare both draft and finished *Aeromonas* genomes using a cut off of 30% amino acid identity. Multiple sequence alignments of NrfB and NetB amino acid sequence were generated using ClustalW (189). MEGA7 was used to generate a phylogenetic tree using the maximum likelihood method using 1000 bootstrap replications based on the JTT matrix-based model (190, 191). The analysis involved 70 amino acid sequences with a total of 143 positions in the final dataset. All positions containing gaps and missing data were eliminated. The graphical representation of the phylogenetic tree was generated using FigTree version 1.4.3 (192).

Structural Modeling. *A. hydrophila* ATCC7966 MtrC, AHA_2764, was aligned to homologs proteins using the intensive modeling mode in Phyre2 version 2.0 (160). The resulting predicted structure was visualized using PyMOL version 2.0 (www.pymol.org) and compared to published structures of *Shewanella* spp. MtrC (PDB 4LM8), MtrF (PDB 3PMQ), OmcA (PDB 4LMH) and UndA (PDB 3UFK) (132, 161–163).

2.6 Acknowledgements

We thank Tim Yahr (University of Iowa) for sharing the pEXG2 vector. This work was supported by a grant from the National Science Foundation (DEB-1542513) to JAG and DRB. BEC was partly supported by the Stanwood Johnston Fellowship from the University of Minnesota

Chapter 3: A hybrid extracellular electron transfer pathway enhances survival of *Vibrio natriegens*

This chapter is a reprint of a published article
Conley BE, Weinstock MT, Bond DR, Gralnick JA. A hybrid extracellular electron transfer pathway enhances survival of *Vibrio natriegens*. Appl Environ Microbiol 86:e01253-20 https://doi.org/10.1128/AEM.01253-20

3.1 Summary

Vibrio natriegens is the fastest growing microorganism discovered to date, making it a useful model for biotechnology and basic research. While it is recognized for its rapid aerobic metabolism, less is known about anaerobic adaptations in *V. natriegens* or how the organism survives when oxygen is limited. Here we describe and characterize extracellular electron transfer (EET) in *V. natriegens*, a metabolism that requires movement of electrons across protective cellular barriers to reach the extracellular space. *V. natriegens* performs extracellular electron transfer under fermentative conditions with gluconate, glucosamine and pyruvate. We characterized a pathway in *V. natriegens* that requires CymA, PdsA and MtrCAB for Fe(III) citrate and Fe(III) oxide reduction, which represents a hybrid of strategies previously discovered in *Shewanella* and *Aeromonas*. Expression of these *V. natriegens* genes functionally complemented *Shewanella oneidensis* mutants. Phylogenetic analysis of the inner membrane quinol dehydrogenases CymA and NapC in γ-proteobacteria suggests that CymA from *Shewanella* diverged from *Vibrionaceae* CymA and NapC. Analysis of sequenced *Vibronaceae* revealed that the genetic potential to perform EET is conserved in some members of the Harveyi and Vulnificus clades but is more variable in other clades. We provide evidence that EET enhances anaerobic survival of *V. natriegens*, which may be the primary physiological function for EET in *Vibrionaceae*.

3.2 Introduction

Vibrio natriegens (formerly *Pseudomonas natriegens*) is the fastest growing microorganism with a doubling time of 9.8 minutes in nutrient rich, aerobic conditions (193). *V. natriegens* was isolated from salt marsh sediment (194, 195) where periods of anoxia occur during flooding (196). One strategy used by *V. natriegens* and other *Vibrio*

spp. to survive in fluctuating environments (197) is adapting to changes in electron acceptor availability by respiratory flexibility (198). In the absence of oxygen, many *Vibrio* spp. are capable of reducing fumarate, nitrate, nitrite, and trimethylamine-N-oxide (TMAO), in addition to fermenting numerous compounds (199–202). In *V. cholerae*, TMAO respiration induces cholera toxin production (203), and in *V. fisheri,* the promoter controlling TMAO reductase expression is transcribed during growth in the light organ of a juvenile squid host (204). Nitrate reduction in *V. cholerae* enhances viability in a murine model of intestinal colonization (205), and in *V. vulnificus*, cells lacking the fumarate and nitrate reduction regulatory protein (FNR) are outcompeted by wild-type cells in a murine model of infection (206). These studies suggest anaerobic metabolism is an important aspect of *Vibrio* spp. physiology and pathogenesis.

Many γ-Proteobacteria related to *Vibrio* are facultative anaerobes capable of respiring a variety of electron acceptors. The family *Shewanellaceae*, specifically *Shewanella* spp., are known for their ability to respire numerous terminal electron acceptors, including acceptors that must be reduced extracellularly due to solubility or toxicity constraints (207, 208). Extracellular electron transfer (EET), especially as it applies to environmental metal reduction and renewable energy production has been best characterized in *Shewanella oneidensis* and the δ-Proteobacterium *Geobacter sulfurreducens* (115).

Originally isolated from anoxic sediments based on an ability to reduce solid manganese oxides (178), *S. oneidensis* MR-1 uses a series of multiheme *c*-type cytochromes to transfer electrons from the inner membrane quinone pool to extracellular acceptors (208). CymA is a tetraheme NapC/NirT family quinol dehydrogenase anchored in the inner membrane, and is a central hub for anaerobic respiration in *S. oneidensis* (122, 123). CymA funnels electrons to one of two periplasmic electron-carrying proteins; FccA, a tetraheme flavocytochrome also required for fumarate respiration, or CctA, (also known as STC), a small tetraheme cytochrome (124–126, 209). Electrons are carried across the periplasm to the outer membrane-anchored Mtr complex, which consists of the periplasmic facing MtrA decaheme *c*-type cytochromes and the extracellular facing lipoprotein decaheme *c*-type cytochrome MtrC, held in contact through a non-heme β-barrel protein, MtrB (127–129). FccA or CctA reduces MtrA in the periplasm, and MtrA reduces MtrC within the outer membrane complex (129, 209, 210). MtrC can then reduce extracellular acceptors via direct contact, or by reducing a soluble shuttling molecule (211). *S. oneidensis* secretes and reduces flavin

mononucleotide as an extracellular electron shuttle (130, 212). Additionally, an abiotically modified menaquinone derived compound has also been shown to function as an electron shuttle, but the biological relevance of this compound remains to be determined (213).

Extracellular electron transfer is not limited within the γ-Proteobacteria to the *Shewanellaceae*. In *Aeromonas hydrophila*, a model for EET was proposed based on genetic experiments and bioinformatic predictions (214). *A. hydrophila* uses a similar MtrCAB complex to move electrons across the outer-membrane and to extracellular electron acceptors, but MtrCAB receives electrons from a small periplasmic di-heme shuttle, PdsA. *A. hydrophila* also differs from *S. oneidensis* by using NetBCD, a relative of the NrfABCD nitrite respiration pathway, to move electrons from the menaquinone pool to PdsA in place of CymA.

Six years before the isolation and characterization of *S. oneidensis* MR-1 (178), a series of studies described the isolation and characterization of *Vibrio* spp. capable of reducing solid minerals (215–217). A glucose fermenting *Vibrio* sp. reduced multiple extracellular acceptors including Mn(IV), As(V), U(VI) and Fe(III), but reduction was not coupled to an increase in molar growth yield (215, 216). A separately isolated malate-fermenting *Vibrio* sp. reduced Fe(III) using glucose, pyruvate and malate as electron donors, but only malate supported an increase in molar growth yield in the presence of Fe(III) (217). This increase in growth yield was not due to the addition of nutritional Fe(II) nor a more favorable redox potential (217). A more recent study showed Fe(III) citrate and Mn(IV) oxide reduction by *V. parahaemolyticus* RIMD 2210633 but not *V. harveyi* BB120 which was correlated with the presence of an MtrB homolog in *V. parahaemolyticus* (218). *V. natriegens* has been shown to accelerate steel corrosion when growing as a biofilm (219–221), while a cathode oxidizing (-550 mV vs. Ag/AgCl) nitrate-reducing *Vibrio* sp. was isolated from cathodic marine sediment enrichments (222). The electrode isolate produced both anodic current (indicating electron transfer to the electrode), as well as cathodic current, suggesting EET can occur in the oxidative or reductive direction (222). Thus, the literature provides evidence that *Vibrio* spp. can perform EET, but there have been no mechanistic studies.

Previous bioinformatic analysis have identified possible *mtrCAB* (157, 158, 218, 223) and *cymA* (224) homologs encoded in *Vibrio* spp. genomes. Here, we characterize the mechanism of EET in *V. natriegens,* show that it is dependent upon these homologs, and explore potential physiological roles for this pathway. Electron donors were

examined for their ability to support EET in *V. natriegens* to gain insight into conditions where EET may benefit the cell. Our work shows that reduction of extracellular metals is dependent on a hybrid pathway using CymA, PdsA and MtrCAB, and is sufficient to rescue analogous *S. oneidensis* mutants. We propose that a function of EET for *V. natriegens* is survival rather than growth under anaerobic conditions. Additional *Vibrio* spp. predicted to perform EET, most notably the described pathogens *V. parahaemolyticus* and *V. vulnificus*, were identified by genomic comparisons. Phylogenetic analysis of the evolutionary relationship between NapC/NirT family members demonstrates CymA from *S. oneidensis* has diverged from *Vibrionaceae* CymA, and the nitrate-linked quinol dehydrogenase NapC is distinct from CymA.

3.3 Results

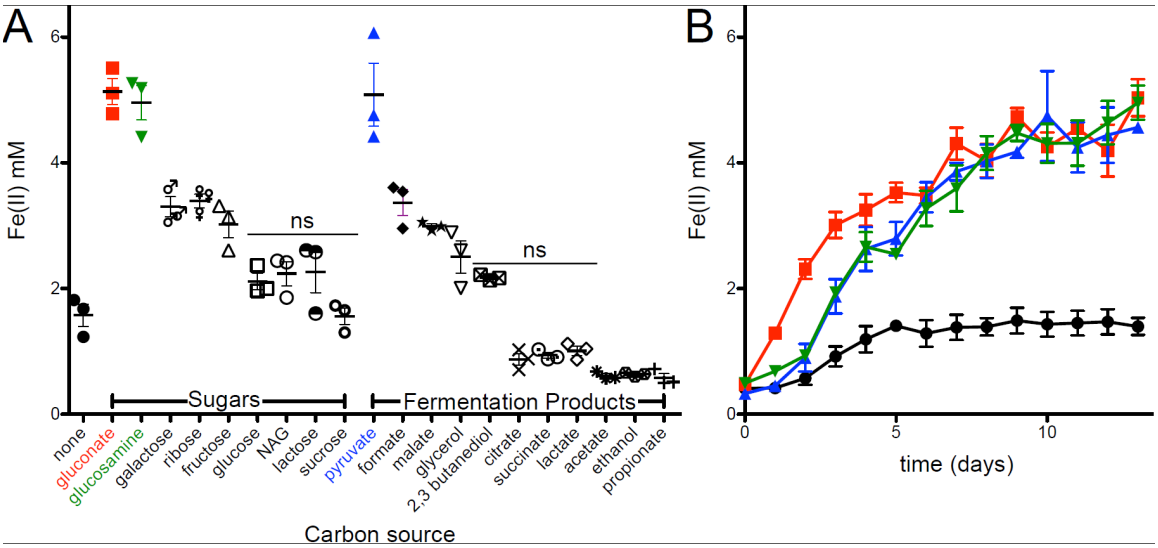

Figure 11 Fe(III) citrate reduction by *V. natriegens* using various carbon sources. (A) Maximum Fe(II) produced after 13 days of anaerobic incubation with a 10 mM concentration of the indicated carbon source. (B) Fe(II) was measured over time to assay Fe(III) citrate reduction with 10 mM gluconate (red squares), pyruvate (blue triangles), glucosamine (green inverted triangles), or no additional carbon source (black circles). Statistical significance was determined by one-way analysis of variance (ANOVA) using a P value of 0.001, followed by Dunnett's multiple-comparison test using the group with no electron donor as the control group. ns, not significant. Data are representative of two independent

experiments performed in triplicate, displaying mean ± standard error of the mean (SEM).

Electron donors supporting Fe(III) citrate reduction. Electrons donors that support EET in *V. natriegens* may provide insight into the environmental conditions in which this metabolism is used. To better understand the effects of electron donor on EET, various sugars and organic acids were examined for their ability to support Fe(III) citrate reduction in anaerobic conditions by wild-type *V. natriegens*. The maximum Fe(II) produced from the oxidation of various electron donors after 13 days of anaerobic incubation is shown in Figure 11A. Oxidation of gluconate, glucosamine, and pyruvate supported reduction of 100% of the Fe(III) citrate provided. Galactose, ribose, fructose, formate, malate, and glycerol supported the reduction of 60-70% of the Fe(III) citrate provided. Glucose, N-acetylglucosamine (NAG), lactose, sucrose, 2,3 butanediol, citrate, succinate and lactate did not support significant Fe(III) citrate reduction above the levels of a no-donor control. When no electron donor or sucrose was added, 30% of the Fe(III) citrate was reduced. Acetate, ethanol and propionate resulted in 20-10% of the total Fe(III) citrate reduced, significantly below the levels of the no donor control. The maximum Fe(II) concentrations are derived from data displayed in Figure 11B (gluconate, glucosamine and pyruvate) and Figure 12 (galactose, ribose, fructose, glucose, NAG, lactose, sucrose, formate, malate, glycerol, 2,3- butanediol, citrate, succinate, lactate, acetate, ethanol and propionate). Of the substrates examined, only fermentable electron donors supported robust Fe(III) reduction phenotypes. Fe(III) citrate reduction occurred after growth of the fermentable substrate, as evidenced by the slow Fe(II) production rates for substrates that support rapid growth such as glucose and pyruvate (Fig 11 and Fig 12). Oxidation of gluconate resulted in the fastest iron reduction rate and was therefore used as the electron donor for subsequent experiments.

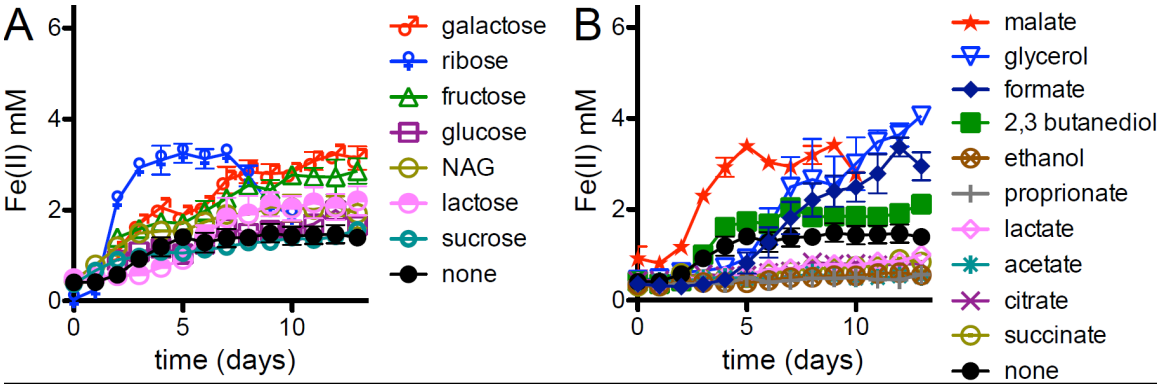

Figure 12 Fe(III) citrate reduction in *V. natriegens* using various carbon sources. Fe(II) was measured over the course of time to assay Fe(III) citrate reduction with 10 mM of indicated carbon source. Data representative of two independent experiments performed in triplicate displaying mean ± SEM.

Identification of metal reduction homologs from *Shewanella* and *Aeromonas* spp. in V. *natriegens*. Homologs of proteins previously shown to be involved in EET in *Shewanella* and *Aeromonas* were identified in *V. natriegens*. Figure 13 displays the genome organization of genes encoding the predicted EET pathway, and the percent amino acid similarity between homologs found in in *V. natriegens*, *A. hydrophila* ATCC 7966, *A. schubertii* WL 1483 and *S. oneidensis* MR-1.

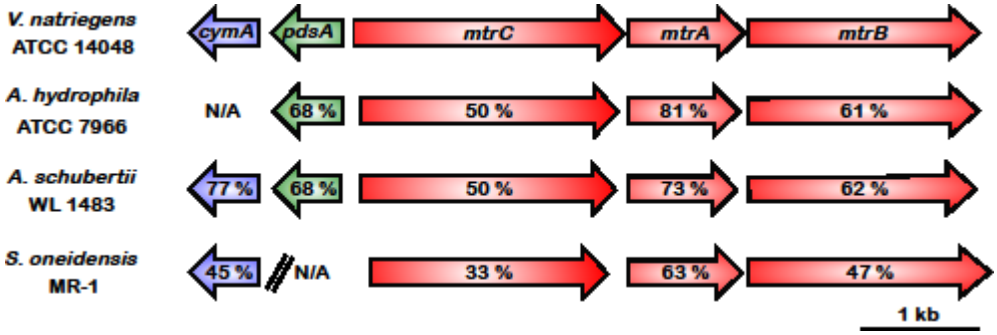

Figure 13 Comparison of metal reduction components from *V. natriegens* ATCC 14048 with those from A. *hydrophila* ATCC 7966, A. schubertii WL 1483, and S. *oneidensis* MR-1. The percent similarities between the encoded proteins are reported, except for when no homolog involved in metal reduction is encoded, which is labeled not applicable (N/A). Arrows representing genes are drawn to scale in the order they are located in the genome except where indicated by //. The color of the gene indicates where predicted proteins are localized via bioinformatic predictions or previous biochemical evidence. Red indicates outer

membrane bound, green indicates periplasm, and blue indicates inner membrane.

Previous genomic analysis identified homologs of *mtrCAB* encoded in multiple *Vibrio* strains (157, 218, 225). The genes encoding the *mtrCAB* putative outer membrane conduit in *V. natriegens* (accession numbers WP_020332994, WP_014231553, WP_020332993, respectively) were encoded in the same order as *Aeromonas* and *Shewanella mtrCAB* homologs. Within γ-Proteobacteria, MtrA is the most conserved component of the outer membrane conduit, followed by MtrB and MtrC (Figure 13). Accessory EET proteins found in *S. oneidensis*, such as MtrDEF and OmcA, were not encoded in the genome of *V. natriegens*.

The combination of inner membrane quinone oxidoreductase and periplasmic cytochromes found in *V. natriegens* differ from those *Shewanella* spp. and *A. hydrophila* (214). *V. natriegens* was predicted to encode a homolog of the *A. hydrophila* periplasmic electron shuttle, PdsA (WP_020332995), while no homologs of *Shewanella* spp. FccA or CctA were identified. *V. natriegens* was also predicted to encode a homolog of *Shewanella* spp. inner membrane cytochrome CymA (WP_020332996), while no homologs of NetB, NetC or NetD from *A. hydrophila* were identified in *V. natriegens*. In *V. natriegens*, *pdsA* and *cymA* are encoded upstream and divergently transcribed of *mtrCAB*, similar to the genomic architecture observed in *Aeromonas* spp. Homology to previously described proteins involved in EET, and conserved genomic architecture lead to the hypothesis that MtrCAB, PdsA and CymA comprise an EET pathway in *V. natriegens*, that is a hybrid of the *Shewanella* inner membrane and *Aeromonas* periplasmic strategies.

CymA, PdsA and MtrCAB are necessary for EET in V. *natriegens*. The ability of strains lacking PdsA, CymA or MtrCAB to reduce Fe(III) citrate and Fe(III) oxide when grown with gluconate was assessed to determine their role in EET. *V. natriegens* mutants grew similar to wild-type when cultured anaerobically with gluconate, suggesting observed Fe(III) reduction phenotypes were not due to a general growth defect (Figure 14). Compared to the wild-type strain carrying an empty vector (pBBR1MCS-2), replacement of *cymA* with a chloramphenicol resistance (Cm^r) cassette in *V. natriegens* also bearing an empty vector resulted in a significant decrease in the amount of soluble Fe(III) citrate reduced (Figure 15A). Fe(III) citrate reduction could be restored when complemented *in*

trans under the expression of the vector-encoded *lac* promoter driving *V. natriegens* (Vn) *cymA.* To better understand the modularity of EET in *V. natriegens*, we examined the ability of *S. oneidensis* (So) CymA and *A. hydrophila* (Ah) NetBCD to complement Fe(III) citrate reduction in the *V. natriegens cymA* mutant. Expression of Ah *netBCD* complemented Fe(III) citrate reduction to wild-type levels; whereas So *cymA* only complemented Fe(III) citrate reduction to 57% of wild-type.

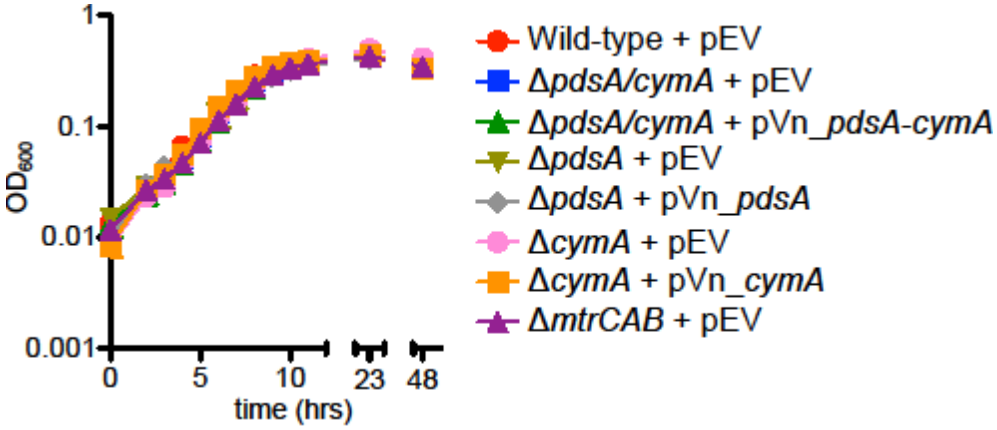

Figure 14 *V. natriegens pdsA*, *cymA*, *pdsA-cymA*, *mtrCAB* mutants do not have a defect in anaerobic gluconate growth. Data representative of two independent experiments performed in triplicate, displaying mean ± SEM.

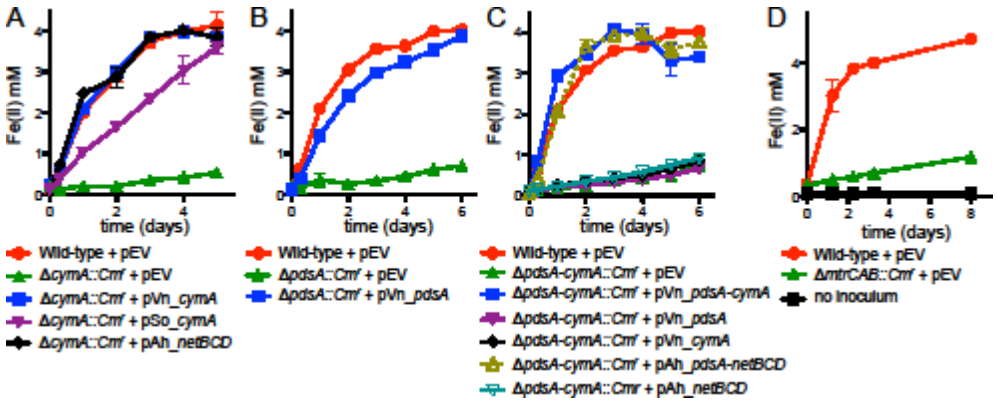

Figure 15 Fe(III) citrate reduction by wild-type and mutant *V. natriegens*. Fe(II) was measured over time to assay Fe(III) citrate reduction. (A) Wild-type V. *natriegens* (red circles) and V. *natriegens* Δ*cymA::Cm*^{r} complemented with *V. natriegens cymA* (blue squares), S. *oneidensis cymA* (purple inverted triangles), *A. hydrophila netBCD* (black diamonds), or empty vector pBBR1MCS-2 (green triangles). (B) Wild-type V. *natriegens* (red circles) and V. *natriegens* Δ*pdsA*::*Cm*^{r}

complemented with V. *natriegens pdsA* (blue squares) or empty vector (green triangles). (C) Wild-type V. *natriegens* (red circles) and V. *natriegens* Δ*pdsA cymA*::*Cm*^{r} complemented with V. *natriegens pdsA-cymA* (blue squares), V. *natriegens* pdsA (purple inverted triangles), V. *natriegens* cymA (black diamonds), A. *hydrophila pdsA-netBCD* (open gold triangles; dashed line), A. *hydrophila netBCD* (cyan inverted triangles), or empty vector pBBR1MCS-2 (green triangles). (D) Wild-type V. *natriegens* (red circles) and V. *natriegens* Δ*mtrCAB*::*Cm*^{r} (green triangles) complemented with empty vector pBBR1MCS2 compared to conditions with no inoculum (black squares). Data are representative of two independent experiments performed in triplicate, displaying mean ± SEM

V. natriegens strains lacking *pdsA* reduced significantly less Fe(III) citrate compared to wild-type controls carrying an empty vector, and could be complemented with Vn *pdsA in trans* (Figure 15B). Strains lacking both *pdsA* and *cymA* were defective in Fe(III) citrate reduction compared to wild-type and were complemented when both Vn *pdsA* and Vn *cymA* were provided *in trans* (Fig 15C). Similarly, Fe(III) citrate reduction could be restored in the *V. natriegens pdsA-cymA* mutant strain by a plasmid encoding Ah *pdsA-netBCD*, but not with Ah *netBCD* alone (Fig 15C). A *V. natriegens mtrCAB* gene replacement mutant reduced significantly less Fe(III) citrate compared to wild-type controls (Fig 15D), but attempts to complement this defect in either an insertional mutant or an in-frame deletion mutant were unsuccessful.

Fe(III) citrate is soluble, and complexation of Fe(III) with different ligands can alter the solubility, crystal structure and redox potential of Fe(III) (226). To determine if MtrCAB, PdsA, and CymA are also required for reduction of insoluble Fe(III), mutants were assessed for their ability to reduce solid Fe(III) oxides. *V. natriegens* mutants lacking *cymA*, *pdsA*, *pdsA-cymA*, or *mtrCAB* decreased significantly less Fe(III) oxide when compared to wild-type (Figure 16).

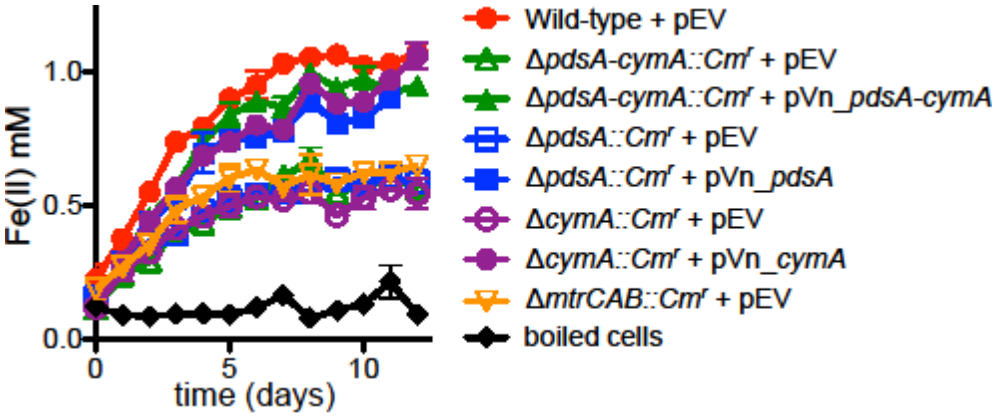

Figure 16 Fe(III) oxide reduction by wild-type and mutant *V. natriegens*. Fe(II) was measured over the course of time to assay Fe(III) oxide reduction. (A) Wild-type (red circle) and V. *natriegens* Δ*pdsA-cymA*::*Cm*^{r} completed with empty vector (empty green triangle) or *pdsA-cymA* (filled green triangle), Δ*pdsA::Cm*^{r} complemented with empty vector (empty blue square) or *pdsA* (filled blue square), Δ*cymA::Cm*^{r} complemented with empty vector(empty purple circle) or *cymA* (filled purple circle), Δ*mtrCAB::Cm*^{r} with empty vector (empty yellow triangle), and boiled cells abiotic control (black diamond). Data representative of two independent experiments performed in triplicate displaying mean ± SEM

CymA, PdsA and MtrCAB are sufficient to restore EET in S. *oneidensis* mutants.

Heterologous expression has previously been used to assay the function of putative EET associated proteins (214, 227, 228). Expression of *cymA*, *pdsA*, and *mtrCAB* from the phylogenetically related *V. natriegens* in analogous *S. oneidensis* mutants allows the assessment of how EET in these microorganisms has evolved with divergent pathways. An *S. oneidensis cymA* deletion mutant with an empty vector reduced significantly less Fe(III) citrate compared to the wild-type strain also bearing an empty vector. When expressed from the vector encoded *lac* promoter, native So *cymA*, Vn *pdsA-cymA*, or Vn *cymA* restored Fe(III) citrate reduction to wild-type levels in a *S. oneidensis cymA* deletion mutant; however, the rate of reduction was 20% slower in the strain only expressing Vn *cymA* compared to a strain expressing Vn *pdsA-cymA* (Fig 17A). Fe(III) citrate reduction in *S. oneidensis* mutants lacking CymA and two key periplasmic cytochromes, FccA and CctA, could be restored to wild-type rates and levels when Vn *pdsA-cymA* was expressed under the control of the vector encoded *lac* promoter *in trans* (Fig 17B). Expression of Vn *cymA* resulted in reduction of the Fe(III) citrate, but at a 66% slower rate compared to a strain expressing both Vn *pdsA-cymA*. The outer membrane

conduit, MtrCAB, heterologously expressed from *V. natriegens* complemented Fe(III) citrate reduction in *S. oneidensis* lacking all described outer membrane cytochromes (Δ*mtrABC*/ Δ*mtrDEF*/ Δ*omcA*/ Δ*dmsE*/ ΔSO_4360/ Δ*cctA*), albeit at a slower rate (Fig 17C).

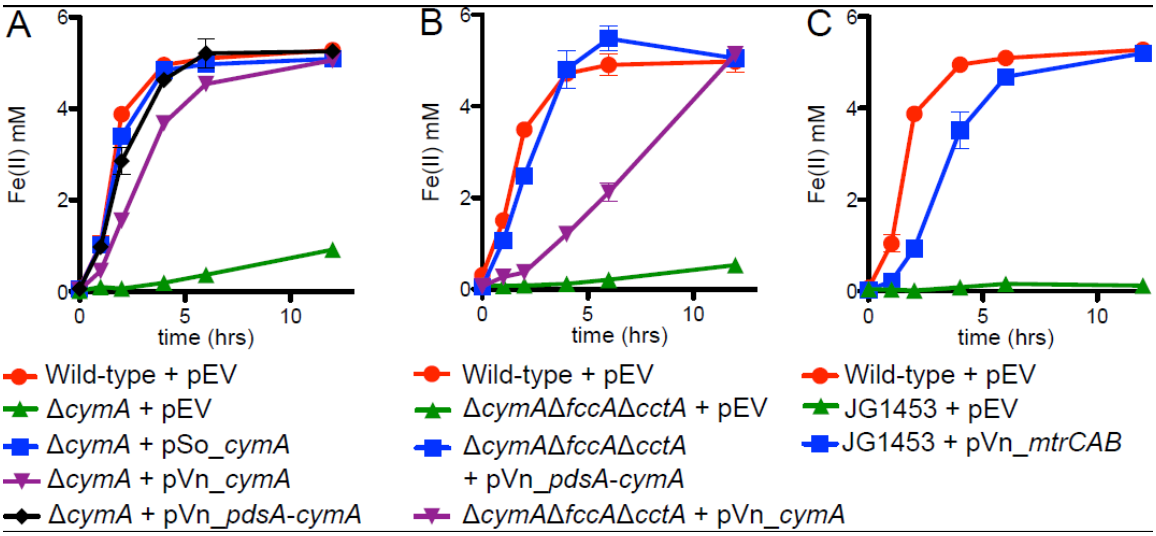

Figure 17 Metal reduction components from *V. natriegens* functionally complement Fe(III) citrate reduction in analogous *S. oneidensis* mutants. Fe(II) was measured over time to assay Fe(III) citrate reduction. (A) Wild-type S. *oneidensis* (red circles) and S. *oneidensis* Δ*cymA* mutants complemented with S. *oneidensis cymA* (blue squares), V. *natriegens cymA* (purple inverted triangles), *pdsA-cymA* (black diamonds), or empty vector pBBR1MCS-2 (green triangles). (B) Wild-type S. *oneidensis* (red circles) and S. *oneidensis* inner membrane and periplasmic cytochrome mutants (Δ*cymA* Δ*fccA* Δ*cctA*) complemented with *V. natriegens pdsA-cymA* (blue squares), *cymA* (purple inverted triangles), or empty vector pBBR1MCS-2 (green triangles). (C) Wild-type S. *oneidensis* (red circles) and S. *oneidensis* mutants lacking outer membrane multiheme cytochrome complexes (Δ*mtrABC* Δ*mtrDEF* Δ*omcA* Δ*dmsE* ΔSO_4360 Δ*cctA*) complemented with V. *natriegens mtrCAB* (blue squares) or empty vector pBBR1MCS-2 (green triangles). Data are representative of two independent experiments performed in triplicate, displaying mean ± SEM.

S. oneidensis CymA is the quinone-oxidoreductase for the reduction of fumarate, NO_3, NO_2 in addition to all extracellular acceptors (171, 172). Based on the homology

between *S. oneidensis* and *V. natriegens* CymA, we hypothesized *V. natriegens* CymA may also have the capacity to serve as the quinol dehydrogenase for fumarate, DMSO, NO_3 and NO_2 in an *S. oneidensis cymA* mutant strain. Expression of *V. natriegens pdsA-cymA* from the vector encoded *lac* promoter restored growth on fumarate and DMSO to wild-type levels, but at a slower rate compared to wild-type with an empty vector and a strain complemented with the native *S. oneidensis cymA* under the same promoter (Fig 18A and 18B). *V. natriegens* CymA restored NO_3, but not NO_2 reduction in an *S. oneidensis cymA* mutant, resulting in a decreased growth yield when grown on NO_3 compared to wild-type with empty vector and *S. oneidensis cymA* complemented strains (Fig 18C and 18D).

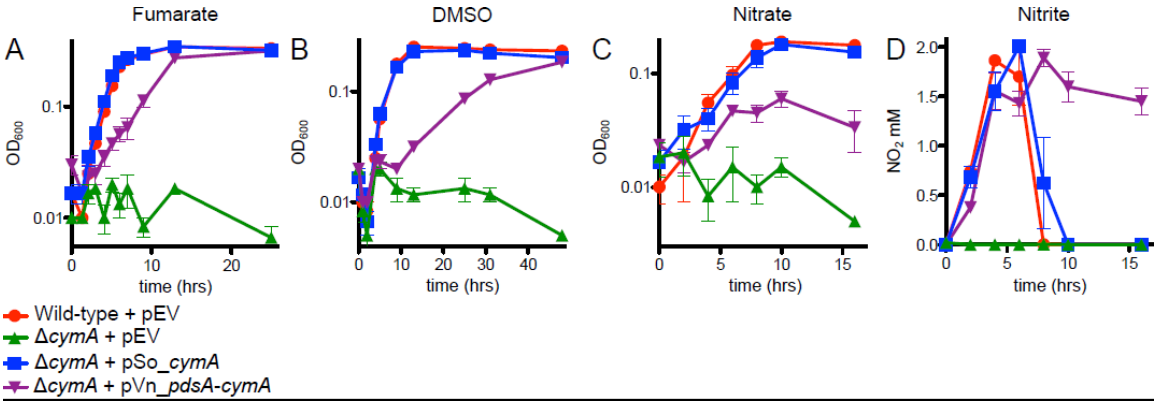

Figure 18 CymA from *V. natriegens* can complement fumarate, DMSO, nitrate, but not nitrite reduction in *S. oneidensis*. (A) Growth respiring fumarate (B) DMSO and (C) nitrate by S. *oneidensis cymA* mutant strains over time. (D) Nitrite production and consumption during growth respiring nitrate by S. *oneidensis* strains over time. Data representative of two independent experiments performed in triplicate, displaying mean ± SEM.

EET enhances anaerobic survival. In *S. oneidensis*, anaerobic growth is dependent on substrate-level phosphorylation (229) but EET is essential for the electron disposal that enables this ATP production (178). Having shown *V. natriegens* can perform EET via a mechanism related to *Shewanella* spp., we endeavored to determine if Fe(III) reduction supported a growth or survival benefit. We hypothesized the addition of an extracellular electron acceptor would allow *V. natriegens* to support moderate growth or survive longer compared to conditions without an extracellular electron acceptor. Cell growth

and death were examined by measuring CFU/mL with and without the addition of an extracellular electron acceptor in the form of Fe(III) citrate while oxidizing gluconate (Fig 19).

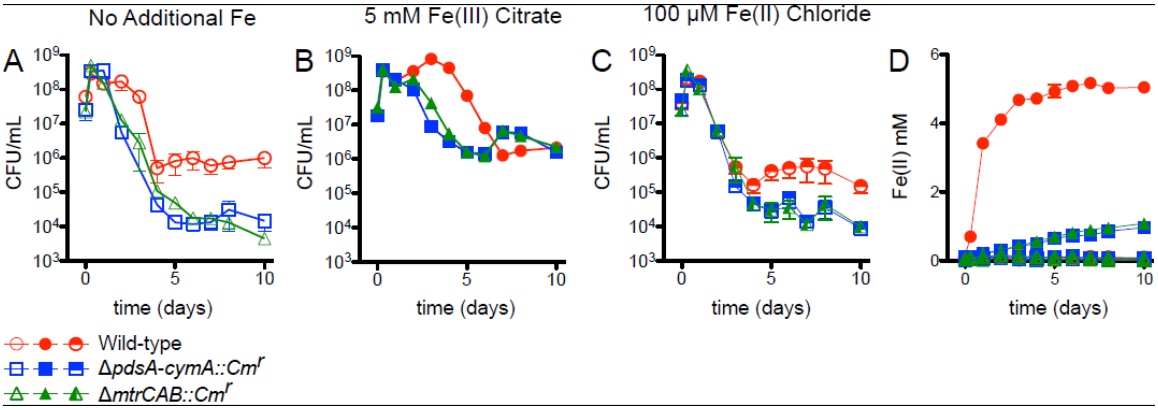

Figure 19 Survival of wild-type and mutant *V. natriegens* under conditions with and without Fe(III) citrate and nutritional Fe(II). (A) CFU/ml of wild-type (red circles) Δ*pdsA cymA::Cm*^{r} (blue squares), and Δ*mtrCAB::Cm*^{r} (green triangles) V. *natriegens* with 10 mM gluconate. (B) CFU/ml of wild-type (red circles), Δ*pdsA cymA::Cm*^{r} (blue squares), and Δ*mtrCAB::Cm*^{r} (green triangles) *V. natriegens* with 10 mM gluconate and 5 mM Fe(III) citrate. (C) CFU/ml of wild-type (red circles) Δ*pdsA cymA::Cm*^{r} (blue squares), and Δ*mtrCAB::Cm*^{r} (green triangles) *V. natriegens* with 10 mM gluconate and 100 M $FeCl_2$. (D) Fe(II) concentration measured over time to assay Fe(III) citrate reduction. Data are representative of two independent experiments performed in triplicate, displaying mean ± SEM.

Anaerobic oxidation of gluconate with or without the addition of Fe(III) citrate yielded a similar increase in CFU/mL from 2.1±0.6x10^7 to 3.5±0.1x10^8 in CFU/mL over the first 8 hours. After initial gluconate fermentation ended at day 2, cell numbers increased to 8.24±2.9x10^8 in Fe(III) citrate-supplemented cultures, whereas cell numbers decreased to 7.02±2.28x10^7 without Fe(III) citrate (Fig 19A and 19B). Wild-type *V. natriegens* cell numbers without electron acceptor continued to decrease between days 3 and 4 to 5.1±3.3x10^5 CFU/mL; whereas, in the presence of Fe(III) citrate cell number only decreased to 1.3±0.3x10^6 CFU/mL by day 7 (Fig 19A and 19B). Fe(II) concentrations were measured over the course of the experiment to monitor Fe reduction (Fig 19D). When provided with Fe(III) citrate, wild-type *V. natriegens* reduced 14±0.01% of the available Fe(III) citrate after 8 hours when cell numbers had reached its

maximum. After 3 days of incubation, 100±0.02% of the available Fe(III) was reduced, coinciding with the maximum CFU/mL and beginning of the fastest CFU/mL decrease.

Fe(III) citrate reduction results in the accumulation of Fe(II), which may provide a nutritional benefit for the cells. In order to control for this effect, we also examined the survival of *V. natriegens* with the addition of nutritional Fe(II) in the form of $FeCl_2$. However, the addition of equimolar Fe(II) in the form of 5 mM $FeCl_2$ resulted in an abiotic precipitate, likely an Fe-phosphate mineral. A concentration of 100 μM $FeCl_2$ was chosen because it did not abiotically precipitate. In wild-type *V. natriegens* with the addition of Fe(II), CFUs increased similar to conditions with and without Fe(III) citrate (Fig 19C). After four days with additional Fe(II), the cell number decreased to $1.7\pm0.7x10^5$ CFU/mL as observed in the condition without an extracellular acceptor.

Considering CymA/PdsA/MtrCAB are involved in Fe(III) citrate reduction, we hypothesized the extended survival benefit in conditions with an extracellular electron acceptor would be dependent on CymA/PdsA/MtrCAB. Initial growth was not affected in *pdsA-cymA* or *mtrCAB* mutant strains under any of the conditions examined (Figure 19ABC). When *V. natriegens* mutants with *pdsA-cymA* or *mtrCAB* deleted were grown without additional Fe, the cell number decreased earlier in the incubation to $1.4\pm0.6x10^4$ and $5.0\pm1.5x10^4$ CFU/mL respectively, compared to wild-type (Fig 19A). In the presence of Fe(III) citrate, the *pdsA-cymA* and *mtrCAB* mutants began decreasing in CFUs two days before wild-type, but reached the same cell density at the end of the experiment (Fig 19B). Increased cell numbers at day 2 by wild-type in Fe(III) citrate conditions was dependent on *pdsA-cymA* and *mtrCAB*, as all mutants did not grow further after initial gluconate fermentation (Fig 19B). Addition of Fe(II) to the *pdsA-cymA* and *mtrCAB* mutants strains resulted in approximately ten fold decrease (to $8.9\pm1.9x10^3$ and $1.0\pm0.1x10^4$ CFU/mL, respectively) in final cell number, and still showed a CFU decrease after fermentation (Fig 19C). The cell number decrease in *pdsA-cymA* and *mtrCAB* mutants suggests electron transfer to extracellular metals provides a survival benefit when alternative electron acceptors are absent.

Distribution of MtrCAB/PdsA/CymA homologs in *Vibrio*nales. Considering the survival benefit provided by EET in *V. natriegens*, the genomic potential to perform EET by other members of the order *Vibrionales* was examined. The majority of sequenced *Vibrionales* strains are not predicted to encode EET proteins. Homologs of MtrCAB/PdsA/CymA are predicted to be encoded in 31% of sequenced *Vibrionales* with complete or draft

genomes available in IMG as of January 2020. Sequenced strains of *V. diabolicus* (10/10), V. *hangzhouensis* (1/1), *V. rotiferianus* (2/11) *V. parahaemolyticus* (491/494), *V. natriegens* (6/6), and *V. vulnificus* (47/47) strains are predicted to encode MtrCAB/PdsA/CymA. Outside of the genera *Vibrio*, two *Photobacterium* spp. encode MtrCAB/PdsA/CymA, *P. gaetbulicola* (3/3) and *P. lutimaris* (2/2). In strains with complete genomes, *mtrCAB/pdsA/cymA* is contained on chromosome 1 in *V. natriegens, V. parahaemolyticus* and *V. rotiferianus*, but on chromosome 2 in *V. vulnificus*. Interestingly, *P. gaetbulicola* Gung47 harbor two copies of *mtrCAB/pdsA/cymA*, one on each chromosome.

CymA is a member of a large class of inner membrane proteins involved in respiration of multiple electron acceptors. A phylogenetic analysis was performed to better understand the relationship between quinol dehydrogenases CymA and NapC in γ-Proteobacteria (Fig 20). NrfH, the dedicated quinol dehydrogenase for nitrite reduction from *DesulfoVibrio vulgaris,* was chosen as an outgroup. *Shewanella* CymA branched separately from both CymA and NapC in *Vibrionales* and *Aeromonadales*, with posterior probability support of 1 (Figure 20). *Vibrionales* and *Aeromonadales* CymA from representative strains branched separately from NapC with posterior probability support of 1. Phylogenetic trees built using maximum likelihood and neighbor-joining methods resulted in identical branching of NrfH, CymA and NapC clades with >95% bootstrap support (data not shown).

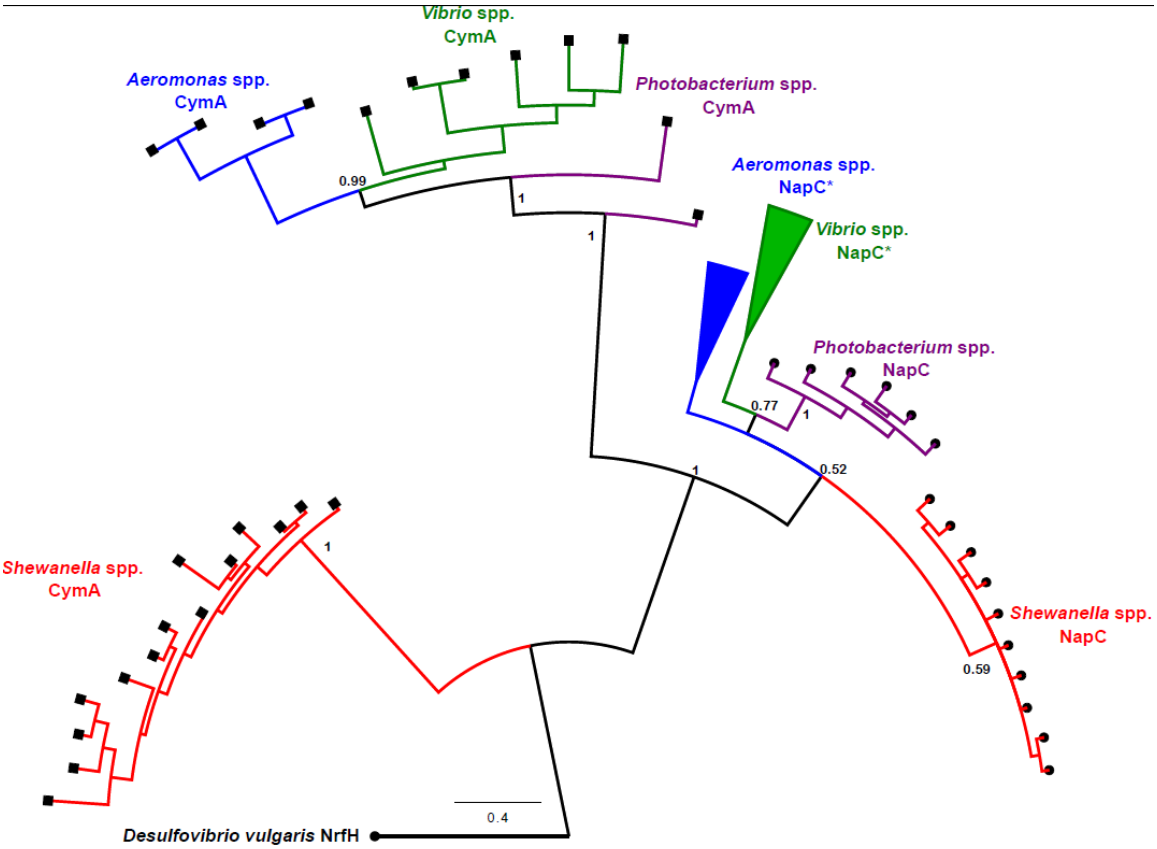

Figure 20 Molecular phylogenetic analysis of quinol dehydrogenases CymA and NapC. CymA (square nodes) and NapC (circular nodes) from selected representative strains of *Shewanella*, *Aeromonas*, *Vibrio*, and Photobacterium spp. are colored red, blue, green, and purple, respectively. * indicates a branch with the majority of nodes from the indicated genus but with some sequences from other genera. D. vulgaris NrfH was used as an outgroup and is shown in black. The sequences were aligned using ClustalO, and evolutionary relationships were inferred using Bayesian inference. The tree is drawn to scale with posterior probabilities supporting branch structure shown at relevant nodes and the scale bar representing substitutions per site.

Evidence for transfer of NapC homologs between species was suggested by our analysis. The clade containing all "*Aeromonas* spp. NapC" sequences also contained the NapC found in *Photobacterium* sp. AK15 and *P. lutimaris* CECT7642. In addition, the clade containing all "*Vibrio* spp. NapC" contained NapC from *S. benthica* KT99 and *S. marina* JCM15074, as well as some *Photobacterium* spp. (*P. profundum* SS9, *P. aquae* CGMCC, *P. aphoticum* DSM25995, *P. swingsii* CAIM1393, *P. galatheae* S2753, *P.*

halotolerans DMS19608, *P. iliopiscarium* ATCC17749, and *P. damselae* CIP102761). The posterior probability at the NapC branches was too low to infer finer phylogenetic relationships within the NapC clades.

Analysis of CymA amino acid alignments identified conserved motifs that are known to be involved in functional electron transport, heme attachment and coordination. The only available crystal structure for CymA family of proteins is NrfH from *DesulfoVibrio vulgaris* (230). Electrons flow from Heme I through IV to the periplasmic partner with the menaquinone binding site in close proximity to the high-spin heme I. Instead of the usual histidine coordination from the CXXCH motif, *D. vulgaris* NrfH Heme I is penta-co-ordinate with proximal ligation to methionine (CXXCHXM) and this residue is conserved in many NapC proteins (230). Heme I in *S. oneidensis* CymA has axial ligands of His and water (122). The exact residue of the axial His ligand in *S. oneidensis* CymA is unknown, but is postulated to be either His^{50} or His^{53} in CXXCHXXH (122). Heme I in CymA of *Vibrionales* and *Aeromonadales* does not contain the *Shewanella* CXXCHXXH, but instead encodes a conserved CXXCHXXM motif (Figure 22). CymA from all genera contain the conserved Lys^{91} and Asp^{97} (Lys^{82} and Asp^{89} of *D. vulgaris* NrfH numbering) which is predicted to play a role in quinol dehydrogenase function (Figure 21) (231). The proposed His ligands of hemes II, III and IV of *S. oneidensis* CymA are also conserved in *Vibrionales* and *Aeromonadales* CymA (122) (Figure 21). These signature residues could be used in motif-based searches to identify additional CymA homologs.

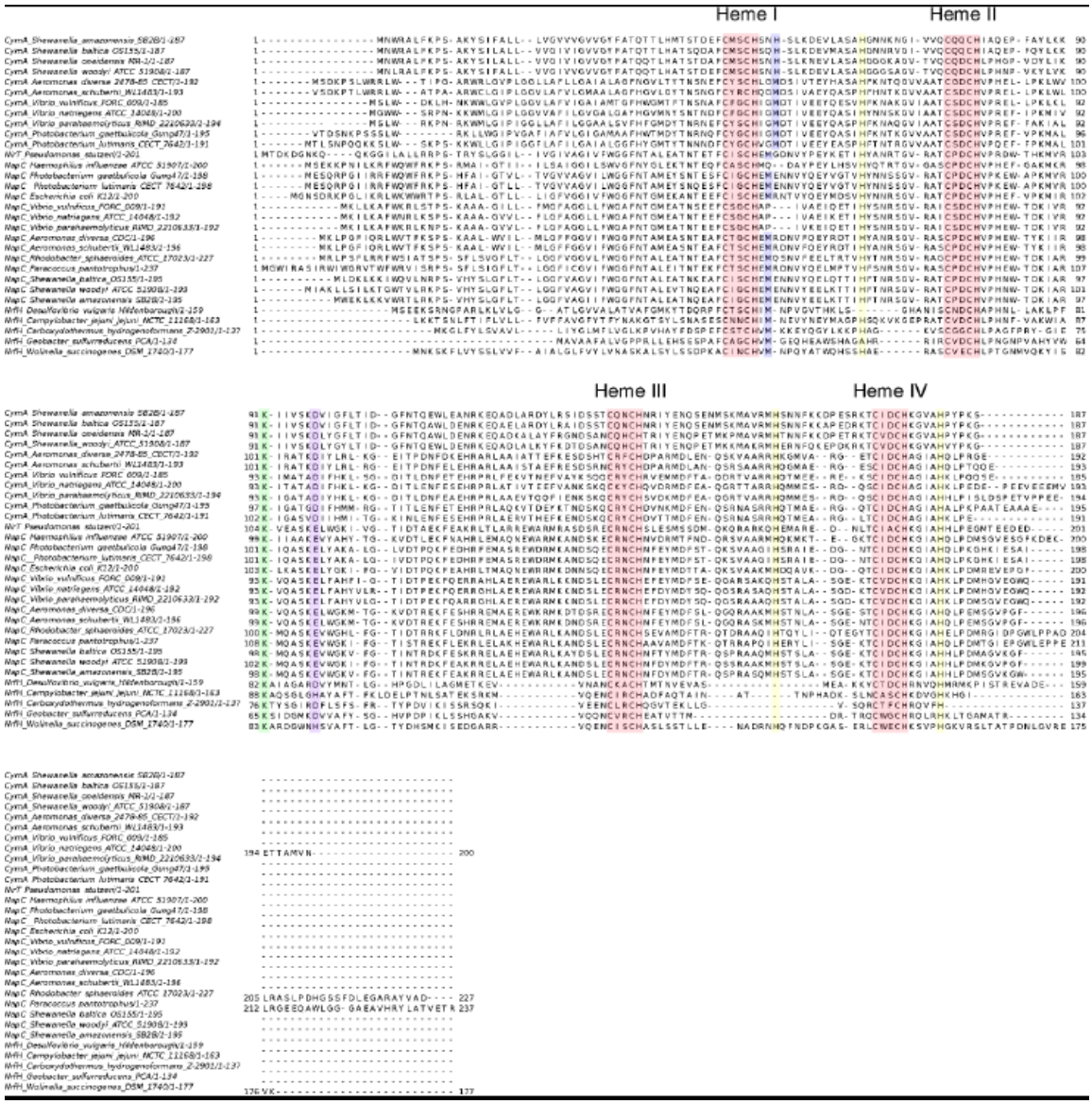

Figure 21 Amino acid alignment of quinol dehydrogenases CymA, NapC and NrfH sequences from selected microorganisms. Heme binding sites (CXXCH) motifs are highlighted in red. The predicted His coordinating residues for heme II-IV are highlighted in yellow while the heme I coordinating residues are highlighted in blue. Using S. *oneidensis* MR-1 numbering, the conserved Lys91 is highlighted in green and conserved acidic residue Asp97 is highlighted in purple (Lys82 and Asp89 of D. vulgaris NrfH numbering).

3.4 Discussion

The differences in cytochrome-based extracellular electron transfer (EET) between *Shewanella* and *Geobacter* spp., combined with recent findings that Firmicutes

such as *Listeria monocytogenes* and *Enterococcus faecalis* dispose of fermentative electrons via an extracellular flavin-based mechanism, highlights how divergent the pathway and physiological roles of EET can be in Bacteria (115, 232, 233). Even within related γ-Proteobacteria, we observe differences in mechanisms of EET between *S. oneidensis*, *A. hydrophila* and *V. natriegens* (208, 214). Variation in the mechanisms of EET demonstrates the diverse strategies microorganisms have evolved to transfer electrons into the extracellular space, potentially under different environmental pressures. Previous studies suggested *Vibrio* spp. could reduce extracellular electron acceptors (216–218). The isolates from Jones *et al*. were assigned to the genus *Vibrio* based on biochemical testing; however, it was possible the isolates were *Aeromonas* sp. due to limitations of O/129 sensitivity testing historically used to distinguish between *Vibrio* and *Aeromonas* spp (234). *Vibrio* spp. enriched on anodes and cathodes were also capable of electron transfer to and from a poised electrode (219–222). While this previous literature indicated *Vibrio* spp. could perform EET, the metabolism, molecular mechanism, phylogenetic distribution, physiology, and ecology was unexplored. Here we present a working model of EET in *V. natriegens* (Fig 22). CymA oxidizes the menaquinone pool and reduces PdsA. PdsA transits across the periplasm to reduce MtrA which is anchored in the outer membrane MtrCAB complex by MtrB. MtrC is oxidized by MtrA and reduces the extracellular acceptor.

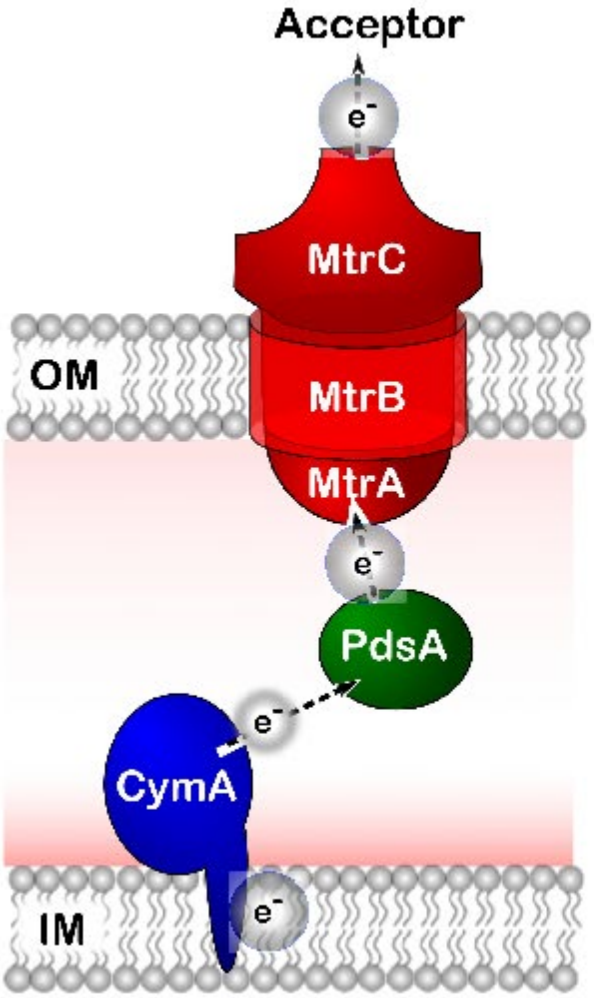

Figure 22 Proposed model for extracellular electron transfer in *V. natriegens*. The quinone pool is oxidized by CymA, which reduces PdsA. PdsA carries electrons across the periplasm to the outer membrane and reduces MtrA. The MtrCAB complex allows electron transport across the outer membrane. MtrA is oxidized by MtrC, which then reduces the extracellular acceptor.

Insights into the metabolic role of EET in *V. natriegens*

Understanding central metabolism in defined conditions can provide insights into the potential environmental conditions where microorganisms live (235–237). *V. natriegens* was capable of using all the carbon sources tested as an electron donor when respiring oxygen except for lactose and 2,3-butanediol (238, 239). Numerous electron donors supported anaerobic Fe(III) citrate reduction in wild-type *V. natriegens* to

various extents (Fig 11 and Figure 12). Of the substrates tested, only gluconate, glucosamine and pyruvate supported full reduction of all the Fe(III) citrate provided. Galactose, ribose, fructose, formate, malate and glycerol supported reduction of a portion of the Fe(III) citrate provided. Glucose, NAG, lactose, sucrose, 2,3 butanediol, citrate, succinate and lactate did not support Fe(III) citrate reduction above the levels of a no electron donor control. Acetate, ethanol and propionate did not support Fe(III) citrate reduction, and compared to the no donor control, resulted in a decreased amount of Fe(II) produced.

The extent of EET did not correspond with the redox potential of the electron donor, but it did correlate with the oxidation state of downstream metabolic substrates. While gluconate is more oxidized than glucose and its isomers, gluconate fermentation supported Fe(III) citrate reduction in *V. natriegens* to a greater extent than glucose, fructose or galactose (Fig 11A). One hypothesis for this increase in Fe(III) reduction could be that oxidized sugars decreased the demand for use of pyruvate as an electron acceptor in reductive NAD^+ regeneration pathways, allowing pyruvate to be oxidized to Acetyl-CoA and more energetically favorable fermentation products (observed in *Vibrio* spp. (217) and fermentative Gram positive bacteria (240–242)). This hypothesis is supported by the strong Fe(III) reduction observed when pyruvate alone was added as a donor. Malate, which is capable of producing pyruvate via malic enzyme, supported Fe(III) citrate reduction but to a lesser extent than pyruvate (Fig 11A and Figure 12B). Mixed acid fermentation by *V. natriegens* results in formate production (243) and in *S. oneidensis* formate oxidation drives menaquinone reduction in conditions where an extracellular acceptor is available (244, 245). The increased Fe(III) citrate reduction when formate was supplied suggests formate produced from pyruvate oxidation could be is a source of electrons for EET (Fig 11A and Fig 12). Substrate-based differences have also been observed in an EET capable *Bacillus* sp., which reduced Fe(III) when fermenting fructose but not glucose (241). A similar phenomena was previously observed in *Vibrio* spp. in which oxidation of malate or pyruvate yielded similar final amounts of Fe(II) produced from $FeCl_3$ reduction despite the additional NADH generated when converting consuming malate (217).

The Fe(III) citrate reduction observed in the no electron donor control may be due to several factors. Acquisition of Fe(III) via siderophores and subsequent reduction via siderophore related ferric reductases may have attributed to some of the reduced Fe(III) citrate (246). When grown in the presence of yeast extract and tryptone, *V.*

natriegens is capable of producing poly-β-hydroxyburyrate (PHB) storage inclusions (239). The subsequent degradation of PHB may have supported reduction of Fe(III) citrate. Fe reduction for nutritional purposes and storage of an electron donor may have contributed to the observed ~1.5 mM of Fe(III) citrate reduced in the no electron donor control condition. These result suggests in the conditions tested, there is a basal level of Fe(III) citrate reduction that occurs without the addition of an electron donor and EET occurs only with particular carbon sources.

Molecular mechanism and modularity of EET

Regardless of the electron donor, for extracellular transfer to occur electrons must traverse two lipid bilayers. Use of MtrCAB to transfer electrons across the insulating outer membrane has now been confirmed in multiple metal reducing γ-Proteobacteria, with MtrA homologs being most conserved (Fig 13) potentially due to the close interactions with MtrB required to anchor MtrA to the outer membrane for contact with MtrC (210). No additional outer membrane cytochromes (MtrF or OmcA) were predicted to be encoded in the genome of *V. natriegens*, as observed previously in *Aeromonas* spp. (214). MtrCAB from *V. natriegens* was essential for Fe(III) citrate and Fe(III) oxide reduction and could restore Fe(III) citrate reduction in an *S. oneidensis* mutant lacking outer membrane cytochromes (Fig 15D and 15C).

Although MtrA is conserved in *Shewanellaceae*, *Aeromonadaceae*, and *Vibrionaceae*, the mechanisms of menaquinone oxidation and MtrA reduction vary across these families. The quinol dehydrogenase, CymA is conserved in *Shewanellaceae*, *Vibrionaceae* and two species of deeply branching *Aeromonadaceae*, *Aeromonas schubertii* and *Aeromonas diversa* (Displayed in Fig 13). Once electrons are delivered to the periplasm, they must be carried to the outer membrane MtrCAB complex, which is common to all families. According to structural models from *S. oneidensis*, MtrA is tightly associated with MtrB, and does not protrude far enough into the periplasm to be directly reduced by the inner membrane quinol dehydrogenase (129, 209, 247), thus requiring electron shuttle(s) to move electrons across the periplasm. The periplasmic di-heme shuttle, PdsA reduces MtrA in *A. hydrophila* (214), and *Vibrionaceae* are also predicted to encode a PdsA homolog arranged in the genome in a similar manner to *Aeromonadaceae* members (Fig 13). Instead of PdsA, *S. oneidensis* uses two tetraheme cytochromes, FccA and CctA, to shuttle electrons across the periplasm.

The differences in inner membrane quinone oxidoreductases and periplasmic electron carriers may give insight into how EET evolved in γ-Proteobacteria, and how easily modules can be horizontally transferred. NetBCD from *A. hydrophila* ATCC 7966 (Ah) and CymA from *S. oneidensis* (So) MR-1 were able to restore Fe(III) citrate reduction in the *V. natriegens cymA* mutant (Fig 15A). These data indicate Ah NetBCD and So CymA can reduce Vn PdsA, but the slower rate of reduction with So CymA may be due to a decreased ability for So CymA to reduce Vn PdsA (Fig 15A). *A. hydrophila* PdsA-NetBCD could also restore Fe(III) citrate reduction in *V. natriegens* mutants lacking PdsA-CymA, but Ah NetBCD or Ah PdsA alone could not (Fig 15C), suggesting Ah PdsA can reduce Vn MtrA, and supporting their shared ancestry. The fact that complementation of *pdsA-cymA* mutants was only possible with both inner membrane and periplasmic components from other organisms highlight the requirement of a periplasmic electron shuttle to transfer electrons across the periplasm for EET in *V. natriegens,* as was previously observed in *A. hydrophila* (214).

Although FccA and CctA have been identified as the major periplasmic carriers in *S. oneidensis*, residual electron transfer via an unknown mechanism occurs in Δ*fccA*Δ*cctA* mutants (125, 209). Fe(III) citrate reduction can be restored in *S. oneidensis* Δ*cymA* and Δ*cymA*Δ*fccA*Δ*cctA* mutants with Vn PdsA-CymA and CymA alone, although Vn CymA alone resulted in a slower rate than Vn PdsA-CymA in both *S. oneidensis* mutant backgrounds (Fig 17A and 17B). These data suggest CymA from *V. natriegens* is capable of reducing *S. oneidensis* FccA and/or CctA and other unidentified periplasmic electron carriers, but reduction of the native PdsA is favored. The Fe(III) citrate reduction in *S. oneidensis* Δ*cymA*Δ*fccA*Δ*cctA* mutants complemented with *V. natriegens* CymA (Fig 17B) is in contrast with the lack of Fe(III) citrate reduction when complemented with *A. hydrophila* NetBCD (214), providing evidence that the unknown periplasmic electron carrier in *S. oneidensis* is capable of interacting with CymA, but not NetB.

Phylogenetic analysis of EET in *Vibrio*naceae, Aeromonadaceae and *Shewanella*ceae

Having established the role of CymA/PdsA/MtrCAB for Fe(III) reduction in *V. natriegens*, we searched for homologs encoded in other *Vibrionaceae* and found *cymA/pdsA/mtrCAB* gene clusters in phylogenetically separate *Vibrionales* members, similar to what we observed in *Aeromonas* spp. (214). *V. vulnificus* belongs to the Vulnificus clade, while *V. parahaemolyticus*, *V. diabolicus*, *V. rotiferianus* and *V. natriegens* belong to the Harveyi clade of *Vibrio* spp., and strains of *V. antiquarius* (EX25

and 939) and *V. alginolyticus* (TS13, FF273, V2, and E0666) have been proposed to be reclassified as *V. diabolicus* (248). All strains in the diabolicus subclade encode *mtrCAB/pdsA/cymA,* but none of *V. alginolyticus* strains in the alginolyticus subclade do so. Intriguingly *V. diabolicus* strains have been isolated from hydrothermal vent ecosystems as free living (EX25), in association with the polychaete annelid, *Alvinella pompejana* (CNCM I-1629) and from other marine sources (249, 250). Because EET is a variable trait within the *Vibrionaceae*, predicting EET ability from 16S microbial community analyses is not advisable because 16S rRNA gene based surveys are not sufficient to determine interspecies relationships within *Vibrio* spp. (238).

Members of *Shewanella*, *Aeromonas, Vibrio* and *Photobacterium spp.* share evolutionary history and overlapping environmental niches. *Shewanella* spp. are unique among this group as they use CymA as a central hub for electron flow out of the inner membrane (122); whereas other facultative anaerobes encode multiple NapC/NirT family proteins, each dedicated for a particular electron acceptor. Using NrfH from the δ-Proteobacterium *DesulfoVibrio vulgaris* as an outgroup, NapC from all microorganisms formed a coherent cluster (Fig. 20). In contrast, *Shewanella* spp. CymA diverged from *Aeromonas*, *Vibrio* and *Photobacterium* CymA, as well as all NapC sequences. As *S. oneidensis* MR-1 CymA is essential for the reduction of extracellular acceptors as well as nitrate, nitrite, DMSO, fumarate, urocanate (171, 172, 251), the evolutionary pressure to interact with a variety of periplasmic proteins may have driven this divergence. CymA from *V. natriegens* was able to restore growth in *S. oneidensis* Δ*cymA* when respiring Fe(III) citrate, DMSO, nitrate and fumarate, but not nitrite (Fig 17 and Fig 18), suggesting *V. natriegens* CymA can reduce *Shewanella* FccA, CctA and NapB, but not NrfA Similarly, *A. hydrophila* NetBCD was able to donate electrons to the periplasmic network of *S. oneidensis* for growth of fumarate, nitrate and DMSO, but not nitrite in a Δ*cymA* mutant (214).

There are currently no conserved motifs available that predict the terminal electron acceptor for a NapC/NirT family protein, but the surrounding genes contain useful context clues as terminal reductases and associated maturation factors are frequently encoded in the same region. Previous analysis reported “CymA homologs” in multiple *Vibrio* spp. (224); however, the CymA homologs identified by Zhong and Shi (2018) are predicted to contain five hemes instead of four, which is a characteristic of TorC within the superfamily of NapC/NirT cytochromes. Of the strains used in (224), our alignments suggest only two are predicted to be capable of EET, as they encode a *cymA*

homolog in a genetic cluster with *pdsA* and *mtrCAB*. The NapC/NirT family protein in (224) is also encoded upstream of a *torZ* homolog, containing a predicted pterin molybdenum cofactor binding domain typical of TorA/TorZ family proteins. In *Vibrio* spp. there are two potential TMAO respiration systems, *torECA* and *torYZ*, with TorC or TorY as the NapC/NirT superfamily pentaheme quinone oxidoreductase (204). We hypothesize the CymA homologs identified previously by genomic analysis are not dedicated for EET, but are potentially TorY homologs.

Physiological role of EET in *V. natriegens* and ecological insights

Vibrio spp. are not commonly recovered in enrichments for EET capable microorganisms. Although this observation may in part be a bias in enrichment conditions, the benefit to performing EET in the versatile heterotrophic fermenting *V. natriegens* remained unclear. EET dependent extended survival has been previously shown in glucose fermenting *Pseudomonas aeruginosa* and fructose fermenting *Bacillus* sp. (241, 252). We hypothesized the ability to perform EET by *V. natriegens* could provide a survival benefit after exhaustion of fermentable substrates, dependent on the CymA/PdsA/MtrCAB pathway (Fig 19). Wild-type *V. natriegens* survived longer in the presence of Fe(III) citrate than without (Fig 19A and 19B). This increased survival was dependent on a functional EET pathway, as *pdsA-cymA* and *mtrCAB* mutants did not survive as long as wild-type (Fig 19A and 19B). In conditions without Fe(III) citrate, the wild-type survived slightly longer and reached a higher final density compared to EET deficient mutants (Fig 19A). Redox-active mineral and medium components could have served as residual electron acceptor for EET which the mutant strains could not utilize. Addition of nutritional iron in the form of $FeCl_2$ did not result in increased survival for wild-type or mutant strains of *V. natriegens* (Fig 19C), although both mutant and wild-type strains reached a higher cell density in conditions with Fe(III) citrate, suggesting that even without EET there was an undefined benefit with Fe(III) citrate (Fig 19). The data from electron donor and survival experiments has led to the following hypothesized model during gluconate fermentation and Fe(III) citrate reduction in wild-type *V. natriegens*. Gluconate fermentation supports growth and as cells reach late exponential phase, iron reduction begins at approximately 8 hours post-inoculation (Fig 19A, 19D and Fig 14). As cells enter stationary phase, iron reduction begins (Fig 19A and Fig 19D) potentially via the fermentation byproduct, formate (Fig 11A). Cell viability is maintained until Fe(III) is depleted and cell death begins (Fig 19B and 19D).

The ability to perform EET extends survival in laboratory incubations of *V. natriegens*, but the extracellular acceptor *Vibrio* spp. encounter in their natural habitats is unknown. *Vibrio* spp. are ubiquitous in marine environments where Fe(III) can be in many different forms depending on the source, complexation, redox potential and location of the Fe(III) (253). Insoluble environmental iron oxides may be poor electron acceptors for *Vibrionaceae*. Previous *Vibrio* spp. isolates examined for EET only reduced <6% of added $FeCl_3$ (216, 217), and *V. natriegens* reduced 21.6±0.03% of the available Fe(III) oxide (Fig 16). Electron shuttling humic acids could facilitate EET *in situ* as salt marsh grasses, such as *Spartina alterniflora*, are known producers of humic acids (254), and N_2 fixing *V. natriegens* and *V. parahaemolyticus* are enriched in the rhizosphere of these grasses (197). Further studies examining the importance of EET in *Vibrio* spp. is needed to better understand how these ubiquitous microorganisms utilize anaerobic strategies to persist in the environment.

3.5 Materials and Methods

Bacterial strains and growth conditions. Strains and plasmids used in this study are found in Table 1. *V. natriegens* ATCC 14048 was obtained from the American Type Culture Collection (Manassas, VA). *S. oneidensis* strain MR-1 was originally isolated from Lake Oneida in New York State (178). All chemicals were obtained from Sigma-Aldrich (St. Louis, MO). *S. oneidensis* and *Escherichia coli* were grown aerobically in Lysogeny Broth (LB) during routine manipulation and strain construction with the supplementation of 50 μg/mL of kanamycin and 250 μM 2,6-diamiopimelic acid (DAP) as necessary. *V. natriegens* was grown aerobically in LB with 20 g/L of NaCl (LBV) during routine manipulation and strain construction with the supplementation of 100 μg/mL of kanamycin or 5 μg/mL chloramphenicol as necessary. *S. oneidensis* was grown in *Shewanella* basal medium (SBM) for growth and metal reduction experiments, containing (per L) 0.225 g K_2HPO_4, 0.225 g KH_2PO_4, 0.46 g NaCl, 0.225 g $(NH_4)SO_4$, 0.117 g $MgSO_4$•7H2O, 2.38 g HEPES, 10 mL of 100x mineral mix (179), 10 mL 100x vitamin mix excluding riboflavin (180), 0.5 g Casamino Acids, and 20 mM lactate at pH 7.2. *V. natriegens* was grown in *Vibrio* basal medium (VBM) for growth and metal reduction experiments, containing (per L) 0.68 g Na_2HPO_4, 0.3 g KH_2PO_4, 20.5 g NaCl, 1 g NH_4Cl, 0.24 g $MgSO_4$ anhydrous, 0.01 g $CaCl_2$, 23.8 g HEPES, 10 mL of mineral mix (179), 10 mL 100x vitamin mix excluding riboflavin (180), 10 mM selected carbon source at pH 7.0. Media was made anaerobic when necessary by purging with Argon gas

passed over a heated copper column to remove trace oxygen. Cultures were grown at 30°C (*S. oneidensis* and *V. natriegens*) or 37°C (*E. coli*) and shaken at 250 rpm when grown aerobically. Electron donors and acceptors were provided in the following final concentrations: 20 mM lactate, 10 mM gluconate, 40 mM sodium fumarate, 50 mM dimethylsulfoxide (DMSO), 3 mM $NaNO_3$, 5 mM Fe(III) citrate, and 5 mM Fe(III) oxide. The Fe(III) oxide was prepared as Schwertmannite (255), added to media, degassed and autoclaved.

Plasmid and mutant construction. Primers used to construct plasmids are listed in Table 2. Construction of chloramphenicol resistance cassette replacement mutants in *V. natriegens* was performed as previously described (256). Briefly, gene knockout cassettes were constructed consisting of a chloramphenicol resistance gene bounded by 3 kb homology arms directed to the genetic loci of interest, replacing the coding sequence from start to stop codon. *V. natriegens* cells were rendered naturally competent and transformed with the linear knockout cassettes essentially as described by (257). Chloramphenicol-resistant transformants were screened by colony PCR to verify the replacement of the gene of interest with the chloramphenicol resistance gene. Complementation strains were constructed using pBBR1MCS-2 (185). All constructs and mutants were sequence verified by ACGT, Inc (Wheeling IL).

Metal reduction assays. Metal reduction assays using *S. oneidensis* strains were performed as previously described (214). Metal reduction assays using *V. natriegens* were performed in anaerobic conditions in VBM with 10 mM gluconate as electron donor and carbon source and either 5 mM Fe(III) citrate or 5 mM Fe(III) oxide. Single colonies freshly streaked from frozen stocks were inoculated into aerobic VBM with 10 mM gluconate and grown overnight with 100 μg/mL of kanamycin as necessary. Cells were washed once in VBM and resuspended to an OD_{600} of 1 and inoculated 1:100 into 10 mL of anaerobic media lacking antibiotics. For carbon source utilization experiments, cells were prepared as described above except single colonies were inoculated into LB supplemented with 1 mM $FeSO_4$ to ensure sufficient iron for heme maturation and grown overnight. Carbon sources were prepared as concentrated stocks in 10 mM HEPES at pH 7.0, sterile filtered and added to autoclaved medium for a final concentration of 10 mM electron donor. At each time point, 0.1 mL of culture was anaerobically removed and samples were diluted 1:10 into 0.5 N HCl to prevent the oxidation of Fe(II) (187). Fe(II)

was measured by diluting the acid-fixed sample 1:10 into a solution containing 2 g/L ferrozine buffered in 100 mM HEPES (188) and OD_{562} was measured. Standard curves for Fe(II) were made from $FeSO_4$ dissolved in 0.5 N HCl.

Genome comparison and phylogeny. The Integrated Microbial Genomes (IMG) database (https://img.jgi.doe.gov/cgi-bin/m/main.cgi) was used to compare both draft and finished *Vibrionales* genomes. Amino acid sequences from *V. natriegens* ATCC 14048 (accession number NZ_CP009977) MtrC, MtrA, MtrB, PdsA and CymA were used to identify homologs in other sequenced *Vibrionales* genomes using the Homolog Toolkit with a minimum cut off of 20% amino acid identity. Strains with incomplete contigs of the predicted *cymA/pdsA/mtrCAB* gene cluster were removed from further analysis. Strains encoding homologs for each MtrC, MtrA, MtrB, PdsA and CymA were cross compared and analyzed for the presence of all homologs. For the phylogenetic tree, CymA, NapC and NrfH sequences were obtained from IMG from representative species. The genomic neighborhoods of representative NapC sequences were screened for the presence of *napAB* and other accessory nitrate reduction genes (*napD/E/F/G/H*) encoded in the same cluster with *napC*. Sequences were aligned using ClustalOmega 1.2.3 using mbed algorithm as a guide tree with a cluster size of 100 (258). Sequences with greater than 97% similarity using BLOSUM62 matrix were considered duplicates and were eliminated from Bayesian analysis. The phylogenetic tree was built using Mr. Bayes 3.2.6 using Poisson matrix with gamma rate variation and annotated using FigTree 1.4.3 (192, 259). Sequence alignments were visualized using JalView version 2.11.0 (260).

Survival Experiments. Survival of *V. natriegens* was assayed by measuring colony forming units per mL (CFU/mL). VBM containing 10 mM gluconate with and without 5 mM Fe(III) citrate, or 100 μM $FeCl_2$ were inoculated as described above. Cultures were anaerobically sampled at each timepoint by removing 0.2 mL, 0.1 mL for Fe(II) quantification (as described above) and 0.1 mL for CFU/mL dilutions. Cultures were diluted in VBM and 10 μL of dilutions were spotted and tilted onto pre-warmed LBV agar plates. Dilution plates were incubated at room temperature for 24 hours and then enumerated.

Table 3. Strains and plasmids for the studies described in chapter 3

Strain or Plasmid	Genotype, relevant characteristics	Source or reference
Strains		
JG274	*S. oneidensis* MR-1, wild-type	(178)
JG687	JG274 with empty pBBR1MCS-2 (pEV), Km^r	(179)
JG1453	JG274 Δ*mtrABC*/Δ*mtrDEF*/ Δ*omcA*/ Δ*dmsE*/ ΔSO4360/ Δ*cctA*	(164)
JG3584	JG1453 with empty pBBR1MCS-2 (pEV), Km^r	(214)
JG3996	JG1453 with pVn_*mtrCAB*, Km^r	This study
JG1064	JG274 Δ*cymA*	(183)
JG1224	JG1064 with empty pBBR1MCS-2 (pEV), Km^r	(214)
JG3796	JG1064 with pSo_*cymA*, Km^r	(214)
JG3997	JG1064 with pVn_*pdsA-cymA,* Km^r	This study
JG4188	JG1064 with pVn_*cymA,* Km^r	This study
JG3745	Δ*cymA*Δ*fccA*Δ*cctA*	(214)
JG3752	JG3745 with empty pBBR1MCS-2 (pEV), Km^r	(214)
JG3998	JG3745 with pVn_*pdsA-cymA,* Km^r	This study
JG4235	JG3745 with pVn_*cymA,* Km^r	This study
JG3980	*V. natriegens* ATCC 14048	ATCC (194, 195)
JG4076	JG3980 Δ*mtrCAB*::Cm^r (PN96_07570-07580), Cm^r	This study
JG4077	JG3980 Δ*pdsA-cymA*::Cm^r (PN96_07460-07465), Cm^r	This study
JG4078	JG3980 Δ*cymA*::Cm^r (PN96_07460), Cm^r	This study
JG4079	JG3980 Δ*pdsA*::Cm^r (PN96_07465), Cm^r	This study
JG4149	JG3980 with empty pBBR1MCS-2 (pEV), Km^r	This study
JG4175	JG4077 with empty pBBR1MCS-2 (pEV), Cm^r Km^r	This study
JG4171	JG4077 with pVn_*pdsA-cymA,* Cm^r, Km^r	This study
JG4303	JG4077 with pVn_*pdsA,* Cm^r, Km^r	This study
JG4304	JG4077 with pVn_*cymA,* Cm^r, Km^r	This study
JG4172	JG4077 with pAh_*pdsA-netBCD,* Cm^r, Km^r	This study
JG4173	JG4077 with pAh_*netBCD,* Cm^r, Km^r	This study

JG4184	JG4079 with empty pBBR1MCS-2 (pEV), Cm^r Km^r	This study
JG4181	JG4079 with pVn_*pdsA,* Cm^r, Km^r	This study
JG4180	JG4078 with empty pBBR1MCS-2 (pEV), Cm^r Km^r	This study
JG4176	JG4078 with pVn_*cymA,* Cm^r, Km^r	This study
JG4179	JG4078 with pSo_*cymA*, Cm^r, Km^r	This study
JG4177	JG4078 with pAh_*netBCD,* Cm^r, Km^r	This study
UQ950	*E. coli* DH5α λ(pir) host for cloning, F^-Δ(*argF-lac*)*169* ϕ80*dlacZ58*(ΔM15) *glnV44*(AS) *rfbD1 gyrA96*(NalR) *recA1 endA1 spoT1 thi-1 hsdR17 deoR* λ*pir*$^+$	(184)
WM3064	*E. coli* donor strain for conjugation, *thrB1004 pro thi rpsL hsdS lacZ*Δ M15 RP4–1360 Δ(*araBAD*)*567* Δ*dapA*1341::[*erm pir*(wt)]	(184)
Plasmids		
pBBR1MCS-2	Broad-host range cloning vector, Km^r (pEV)	(185)
pSo_*cymA*	*cymA* in pBBR1MCS-22 with 12 bp upstream and 78 bp downstream in pBBR1MCS-2	Lab stock
pAh_*pdsA-netBCD*	*pdsA* and *netBCD* (AHA_2760-63) with 35 bp upstream and 77 bp downstream in pBBR1MCS-2	(214)
pAh_*netBCD*	*netBCD* with 62 bp upstream and 42 bp downstream in pBBR1MCS-2	(214)
pVn_*pdsA-cymA*	*pdsA* and *cymA* (PN96_07460-07465) with 135 bp upstream and 40 bp downstream in pBBR1MCS-2	This study
pVn_*pdsA*	*pdsA* (PN96_07465) with 49 bp upstream and 14 bp downstream in pBBR1MCS-2	This study
pVn_*cymA*	*cymA* (PN96_07460) with 29 bp upstream and 7 bp downstream in pBBR1MCS-2	This study
pVn_*mtrCAB*	*mtrCAB* (PN96_07470-07480) with 78 bp upstream and 20 bp downstream in pBBR1MCS-2	This study

Table 4. Primers for the studies described in chapter 3

Complementation primers and restriction sites		
Vn*mtrCAB*_F	NNNNNNAAGCTTAGAGCCGAAAATTCAATAAG	HindIII
Vn*mtrCAB*_R	NNNNNNTCTAGAGTTTTAACAACGCACATTGG	XbaI
Vn*pdsA-cymA*_F	NNNNNNAAGCTTAAGAAAGCGTTGGTTTAGCA	HindIII
Vn*pdsA-cymA*_R	NNNNNNTCTAGAAGGCAGCCATACTTTATACT	XbaI
Vn*pdsA*_F	NNNNNNAAGCTTCTAGTTCTCACTGTCTTTCA	HindIII
Vn*pdsA*_R	NNNNNNTCTAGATGCCAGTGATTGATTTATTG	XbaI
Vn*cymA*_F	NNNNNNAAGCTTTCAATCACTGGCAAGGTGGA	HindIII
Vn*cymA*_R	NNNNNNTCTAGAAGAATCAATTAACCATAGCG	XbaI

3.6 Acknowledgements

This work was supported by a grant from the National Science Foundation (DEB-1542513) to JAG and DRB. BEC was partially supported by the Doctoral Dissertation Fellowship from the University of Minnesota.

Chapter 4: Evidence for horizontal and vertical transmission of Mtr-mediated extracellular electron transfer among the Bacteria

Bridget E. Conley, Isabel R. Baker, Peter R. Girguis, Jeffrey A. Gralnick

4.1 Summary

Some bacteria and archaea have evolved the means to use extracellular electron donors and acceptors for energy metabolism, a phenomenon broadly known as extracellular electron transfer (EET). One such EET mechanism is the transmembrane electron conduit MtrCAB, which has been shown to transfer electrons derived from metabolic substrates to electron acceptors, like Fe (III) and Mn(IV) oxides, outside the cell. Though most studies of MtrCAB-mediated EET have been conducted in *Shewanella oneidensis* MR-1, recent investigations in *Vibrio* and *Aeromonas* species have revealed that the electron-donating proteins that support MtrCAB in *Shewanella* are not as representative as previously thought. This begs the question of how widespread the capacity for MtrCAB-mediated EET is, the changes it has accrued in different lineages, and where these lineages persist today. Here we employed a phylogenetic and comparative genomics approach to identify the MtrCAB system across all domains of life. We found *mtrCAB* in the genomes of numerous diverse Bacteria from a wide range of environments, and the patterns therein strongly suggest that *mtrCAB* is a mobile genetic element that has been transmitted through both vertical and horizontal transmission, and in cases followed by modular diversification of both its core and accessory components. Our data point to an emerging evolutionary story about metal-oxidizing and -reducing metabolism, demonstrates that this capacity for EET has broad relevance to a diversity of taxa and the biogeochemical cycles they drive, and lays the foundation for further studies to shed light on how this mechanism may have co-evolved with Earth's redox landscape.

4.2 Introduction

Bacteria and archaea are the biological drivers of Earth's ecological and geochemical evolution. Their far-reaching impact on our planet is rooted in their incredible physiological diversity. They are found in every habitat on Earth, defining the edges of the biosphere. One of their metabolic capabilities is the breadth of substrates they can use to harness energy. Some bacteria and archaea have even evolved the

means to use exogenous electron donors and acceptors for energy metabolism, such as reduced and oxidized iron-containing minerals. This phenomenon is broadly known as extracellular electron transfer (EET). EET has been implicated as a major agent of environmental change, including the oxidation of methane (a potent greenhouse gas (261–264)), the rise of oxygen on early Earth (265–268), and the remediation of materials considered toxic to most other forms of life (269–272). EET can occur in both the reductive or oxidative direction depending on the microorganism and source of electrons. However, extracellular redox reactions are accompanied by a unique physiological challenge: electrons must be efficiently transferred between environment and cell across insulating protective barriers.

Several seemingly independently evolved modes of EET have been identified in a range of microorganisms.(264, 273–282) Of these, two taxa have become the primary models for studying the biochemistry and physiology of EET: *Shewanella* spp. and *Geobacter* spp.(63, 283, 284) EET in *Shewanella spp*. is mediated by the MtrCAB system, in which electrons derived from metabolic activity are transported from the inner membrane through a tetraheme quinol dehydrogenase, CymA, to periplasmic cytochromes CctA or FccA, which then deliver electrons to the decaheme *c*-type cytochrome MtrA, insulated within the beta-barrel protein MtrB located in the outer membrane (43). The MtrAB complex transmits electrons to the extracellular decaheme cytochrome MtrC, which donates those electrons to an electron acceptor outside the cell (43) Most investigations of MtrCAB have focused on its physiology and biochemistry in *Shewanella oneidensis* MR-1, which was originally isolated as an iron- and manganese-reducer, but has since been shown to employ MtrCAB when respiring other electron acceptors, such as electrodes, chromium, cobalt, technetium, uranium, and vanadium(41). The genes encoding this metabolic capacity are clustered together in the order of *mtrC*, *mtrA,* and *mtrB* in the *S. oneidensis* MR-1 genome. Immediately upstream of *mtrCAB* is *omcA* (a homolog of *mtrC*), which is preceded by the genes *mtrD, mtrE,* and *mtrF* – homologs of *mtrA*, *mtrB*, and *mtrC* respectively (285).

Recent genomic analyses identified homologs of MtrCAB in *Aeromonas* and *Vibrio* spp. (44, 45, 284), and subsequent functional experiments confirmed that MtrCAB is essential for metal reduction in examined representatives *Aeromonas hydrophila* and *Vibrio natriegens* (90, 286). While the MtrCAB complex is conserved in metal reducing *Shewanella*, *Aeromonas*, and *Vibrio* spp., the inner membrane quinol dehydrogenase and periplasmic electron carrier proteins differ among these three genera, indicating that

the *Shewanella* model of the Mtr pathway is not as canonical as previously thought. In addition to other Gammaproteobacteria, homologs of MtrA and MtrB (deemed PioA and PioB, respectively) in the phototrophic α-proteobacterium *Rhodopseudomonas palustris* TIE-1 are required for EET in the opposite direction; that is, electrons travel from outside to inside the cell while oxidizing extracellular donors like iron (Fe^{2+}) or cathodes (287–289). Other homologs of MtrAB called MtoAB have also been proposed to function in chemolithoautotrophic iron oxidation by the betaproteobacteria *Gallionella* spp. and *Sideroxydans* spp. (290–293).

These examples of Mtr-linked EET activity found among diverse taxa within the Bacteria point to a shared lineage, the evolution of which could be resolved by knowing how widespread this metabolic capacity is throughout the tree of life. In light of the massive increase in the number of microbial genomes and recent advances in computational tools for analyzing patterns across genomes, we posit that a new survey of the available genomic data paired with careful phylogenetic analysis could A) better constrain how widespread Mtr-mediated EET is among contemporary taxa; B) reveal the scope of this system's variations; and C) reveal connections between MtrCAB's evolution, function, and impact on the environment. Such an effort would represent a significant advance, building upon previous studies (44, 63, 283, 284, 292, 294, 295) that examine the evolution and/or distribution of MtrCAB and related pathways. Here we employ a phylogenetic and comparative genomics approach to look for Mtr-mediated EET across all three domains of life. We find mtrCAB in the genomes of numerous diverse bacteria from a wide range of environments, including among taxa from entire classes and even phyla that, to our knowledge, have never been shown to encode MtrCAB until now. The data further suggest that mtrCAB has been transmitted through several horizontal gene transfer events, each followed by modular diversification of both its core and accessory components. Our findings point to an emerging story about the evolution of EET and the capacity for extracellular metal-oxidizing and -reducing metabolism and lay the foundation to resolve how this mechanism may have co-evolved with Earth's redox landscape and inform biogeochemical models that implicate EET.

4.3 Methods

Sequence Retrieval

MtrA (WP_011706573.1), MtrB (WP_011706574.1), and MtrC (WP_164927685.1) protein sequences from *Aeromonas hydrophila* were queried against the National Center for Biotechnology Information's database of non-redundant protein sequences available on July 28, 2020 using PSI-BLAST. Both metagenomes and genomes were included in the analysis.

Data Curation

Individual amino acid sequences identified through PSI-BLAST were first filtered based on the presence or absence of non-Mtr domains, as determined by NCBI's Conserved Domain Database search tool (296). Hits with additional detected protein domains were discarded for subsequent data culling and analyses. The genomic loci for the remaining curated protein coding sequences were then compared to assess whether they comprised a genuine *mtrCAB* gene cluster. Of the total protein hits, any 2 coding sequences that were within 3,500 base pairs on a genome were marked as part of a single cluster. Those that did not meet this criterion were removed from further analysis. Clusters that did not have a complete set of these three proteins (in any order on the genome) were also removed. In the cases of metagenomes, MtrCAB clusters that comprised the majority of a contig or scaffold (i.e. 3 out of 11 or fewer total coding genes) were removed in the interest of maintaining a high confidence in the taxonomic assignments of each cluster. Taxonomy of the metagenomes were confirmed based on BLAST of additional coding genes in the *mtrCAB* encoding contig or scaffold. Some species had more than one strain or sequenced genome represented at this stage of data curation, in which case one strain or genome was selected at random to remain for further analyses, while the others were removed. *Shewanella* and *Vibrio* hits without a species designation (e.g. *Shewanella* sp. or *Vibrio* sp.) were also discarded to avoid oversampling these relatively highly sequenced genera. The genomic order of remaining *Shewanella* Mtr coding sequences in each cluster was examined; *Shewanella* clusters encoding MtrABC were labelled as D-E-F, based on the delineation between MtrCAB and MtrDEF established in *S. oneidensis* MR-1 (63).

Additional MtrC/OmcA family proteins that were encoded next to a complete *mtrCAB* cluster were identified within strains encoding MtrCAB. *S. oneidensis* MtrC (WP_011071901.1), MtrF (WP_011071903.1), OmcA (WP_011071902.1), *S. piezotolerans* MtrH (WP_020913331.1), *S. loihic*a MtrG (WP_011866320.1), *S. putrefaciens* UndA (WP_011789901.1), *Niveibacterium* sp. 150 COAC-50 MtrC (WP_172203423.1), Gammaproteobacteria bacterium sp. SP163 MtrC (MBA55444.1),

and Wenzhouxiangella sp. XN201 MtrC (WP_164230597.1) were queried against a curated database of proteins from strains encoding MtrCAB. Any identified MtrC/OmcA coding sequences had to be located next to *mtrCAB* or an additional *mtrC/omcA* family protein part of a larger *mtrCAB* gene cluster. Duplicates, hits with E>1x10^{-10}, and proteins with additional detected protein domains were removed.

MtrCAB Maximum Likelihood Tree

Alignments of the MtrA(D), MtrB(E), and MtrC(F) from each gene cluster were generated with ClustalΩ(297) and subsequently concatenated. Distances were calculated using the JTT substitution matrix(298). The maximum likelihood (ML) tree was then built from a Neighbor-Joining (NJ) tree using the WAG rate model(299). Branch lengths were optimized for the WAG model, before calculating bootstrap support and finally visualizing the tree with iTOL(300). Individual ML trees of MtrA, MtrB and MtrC family proteins were also generated. Additional MtrC/OmcA family outer membrane decaheme- and undecaheme-encoding proteins identified in the mtr gene clusters were included in the MtrC family ML tree but were not in the concatenated MtrCAB tree. For perspective MtrAB homologs were added to MtrA and MtrB individual ML trees. MtoA and MtoB coding sequences (CDS) from the iron-oxidizing bacteria *Gallionella capsiferriformans* ES 2 and *Sideroxydans lithotrophicus* ES-1,(292, 301) as well as the PioA and PioB CDS from the photoferrotroph *Rhodopseudomonas palustris* TIE-1,(289) were included in the MtrA and MtrB ML trees, respectively.

Whole Genome Comparisons

Genomes from the same genera encoding MtrCAB and genomes lacking MtrCAB were compared for potential horizontal gene transfer events. Genomes were downloaded from NCBI June 2020, aligned using Progressive Mauve with automatically calculated seed weight and minimum LCB scores (302) using the Geneious Prime 2020.2 plugin. Alignments were visualized for publication using EasyFig(303) and manually annotated in Adobe Illustrator 2020.

4.4 Results

The capacity for MtrCAB-mediated EET is widespread among phylogenetically and physiologically diverse Bacteria.

The MtrCAB outer membrane conduit has been genetically and physiologically implicated in EET among S*hewanella oneidensis*, *Shewanella* sp. ANA-3, *Aeromonas hydrophila*, and *Vibrio natriegens* (43, 45, 90, 286, 304, 305). Accordingly, to begin investigating the prevalence of these genes among other bacteria, we searched for

homologs of the MtrCAB across the entire domain. Given that the MtrCAB-encoding genes are directly adjacent to each other in the aforementioned models, we constrained our search to only include hits in which *mtrC*, *mtrA*, and *mtrB* occur as a cluster – in any order – in a genome (see Methods for more details). With these parameters, we found MtrCAB is encoded in numerous phylogenetically diverse Bacteria, spanning 148 species representing 13 orders, 5 classes, and 3 phyla.

Most of the species identified here belong to the Gammaproteobacteria and Betaproteobacteria, in addition to 5 hits amongst the Acidobacteria and singletons from the Alphaproteobacteria and Gemmatimonadetes. These classes are composed exclusively of Gram-negative Bacteria, with neither Eukaryotes nor Archaeans predicted to encode MtrCAB. These observations suggest that MtrCAB-mediated EET is restricted to Bacteria with an outer membrane. Parallel to these various environmental contexts and taxonomic affinities, the species predicted to encode MtrCAB include those described as chemoorganotrophs, photoheterotrophs, and chemolithoautotrophs capable of aerobic, facultative anaerobic and/or fermentative respiratory strategies (Table 5). These MtrCAB-encoding species were recovered from a wide range of environments, including the waters and sediments from both freshwater and marine settings, hot springs and hydrothermal vents, soda and salt lakes, contaminated wastewater, engineered systems, and host-associated habitats (Figure 23, Table 5).

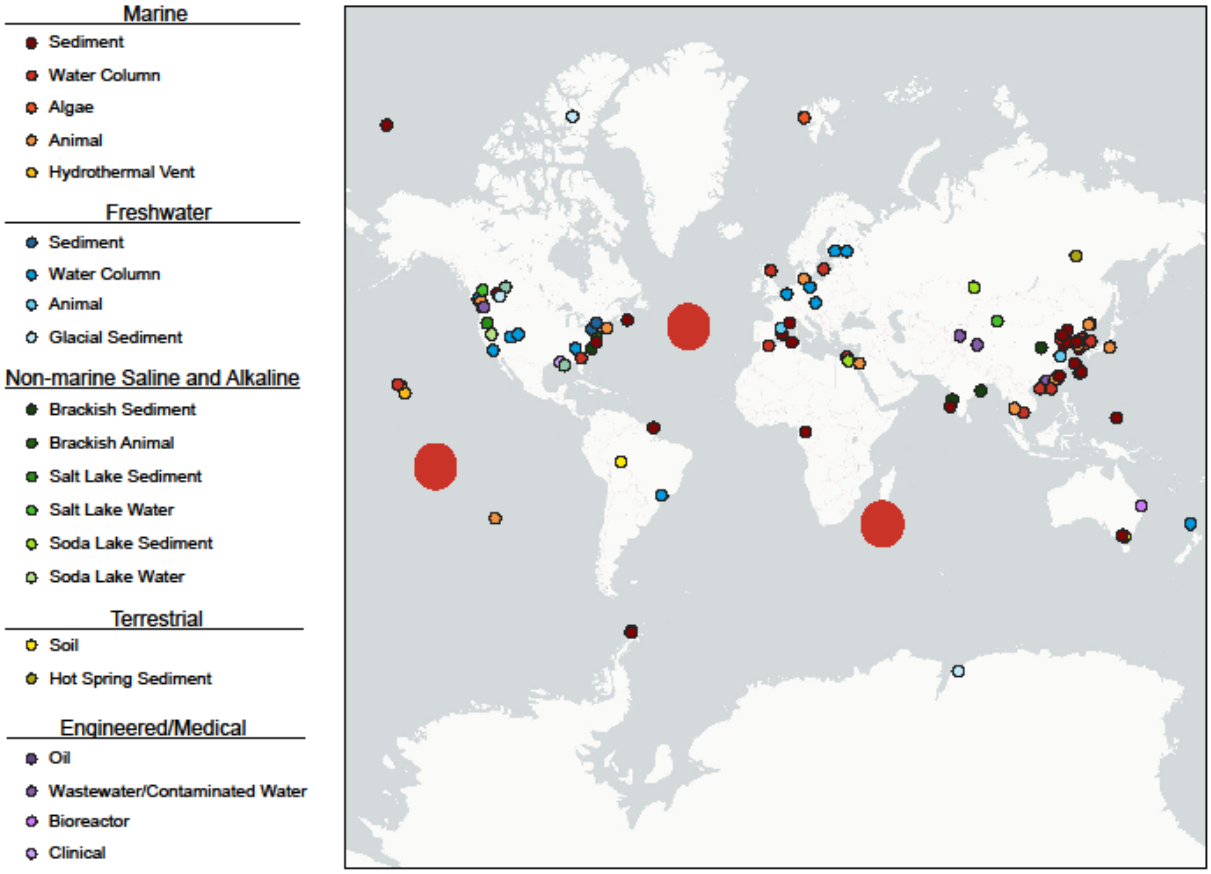

Figure 23. Geographic locales of microorganisms encoding elements of the MtrCAB system. Geographic location of isolation was unavailable for some sequences. Large red circles represent the South Pacific, North Atlantic, and Indian Ocean (Eastern Africa Coastal Province) regions described in Tully et al. (2018) (306). For more details, refer to Table 5.

Notably, 29 of these species have been directly implicated in some form of EET, especially in the reduction of iron and manganese oxides (Supplementary Table 1), although it must be noted that MtrCAB was not explored as the explicit driver of EET in most of these cases. While the majority of these cases belong to the Shewanellaceae and close relative Ferrimonadaceae, these also include *Aeromonas hydrophila* and *Vibrio natriegens* (90, 286). Specifically, evidence for EET was also found in a few of the MtrCAB-encoding Betaproteobacteria identified in our search, including the iron-reducer *Albidoferax ferrireducens* T118 (307, 308) (basonym *Rhodoferax ferrireducens*) and the recently described Ramlibacter lithotrophicus RBP-2, which has been implicated in

oxidative EET and expresses *mtrCAB* when grown on Mn(II) in co-culture with Candidatus *Manganitrophus noduliformans* (309). Other species found to encode MtrCAB, such as Burkholderiales bacterium JOSHI_001 and *Ideonella* sp. A288, have been reported to deposit manganese and iron oxides, respectively, but whether or not they yield energy from these reactions remains to be seen(310, 311). Likewise, some of the MtrCAB-encoding organisms come from metagenomic samples in which EET was implicated through bioelectrochemical experiments or other geochemical observations, but in lieu of experimental validation for individual genotypes we choose not to speculate on whether the organisms we identified in these cases are directly engaged in EET.

Beyond these instances where EET has been directly or indirectly implicated, the majority of MtrCAB-encoding organisms have never been experimentally tested for this metabolic capacity. While the MtrCAB system is typically associated with reductive EET (as opposed to oxidative EET like the PioAB system)(287, 289). MtrCAB has been shown to operate as an oxidizing system in artificial lab settings (312, 313). Thus, we cannot infer the net direction of electron flow for most microorganisms identified in our search because the inherent and environmental controls on electron flow directionality are still poorly understood. Interestingly, one MtrCAB-encoding organism from a metagenome, Gallionellales bacterium RIFCSPLOWO2_02_FULL_59_110, is a member of the same sub-order as the iron-oxidizing bacteria *Gallionella capsiferriformans* ES-2 and *Sideroxydans lithotrophicus* ES-1 that encode homologs of MtrAB but lack MtrC(292, 293).

Moreover, nearly 40% of the species we recovered are members of the *Shewanella Paraferrimonas-Ferrimonas* group, for which almost all of the genome assemblies that we analyzed included the MtrCAB gene cluster (Table 6). Vertical transmission of MtrCAB within the *Shewanella-Paraferrimonas-Ferrimonas* group would be consistent with the observed patterns of inheritance; although further phylogenetic work resolving the relationships between these genera is required, as discussed below. In general, however, the remaining species which we did recover are not unique to a single bacterial clade; those that do possess MtrCAB are generally the minority amongst their genus, family, order, or even class or phylum (Table 6). Horizontal gene transfer (HGT) is one mechanism that could explain the sporadic phylogenetic representation amongst the species encoding MtrCAB; the fact that we find the *mtrCAB* gene cluster scattered amongst many unrelated species is inconsistent with vertical transmission.

Horizontal and vertical transmission of *mtrCAB*: a story of evolving gene flow among distinct clades.

Relationships between MtrCAB sequences are incongruent with species phylogeny.

Beyond antibiotic resistance, HGT has been shown to mobilize metabolic pathways, such as genes encoding chlorate reduction (314), perchlorate reduction (315), and photosynthesis (316, 317). We hypothesized that the capacity for MtrCAB-mediated EET was horizontally transferred based on the breadth and scattering of phylogenetic diversity in our curated search. As incongruent phylogenetic relationships between gene and species trees are a hallmark of HGT (318), we built a tree of the identified MtrCAB sequences to test our hypothesis. In addition to building individual MtrA/D, MtrB/E, and MtrC/F trees, we also concatenated the MtrA(D), MtrB(E), and MtrC(F) sequences for each identified cluster and used these concatenated sequences to build a maximum likelihood tree.

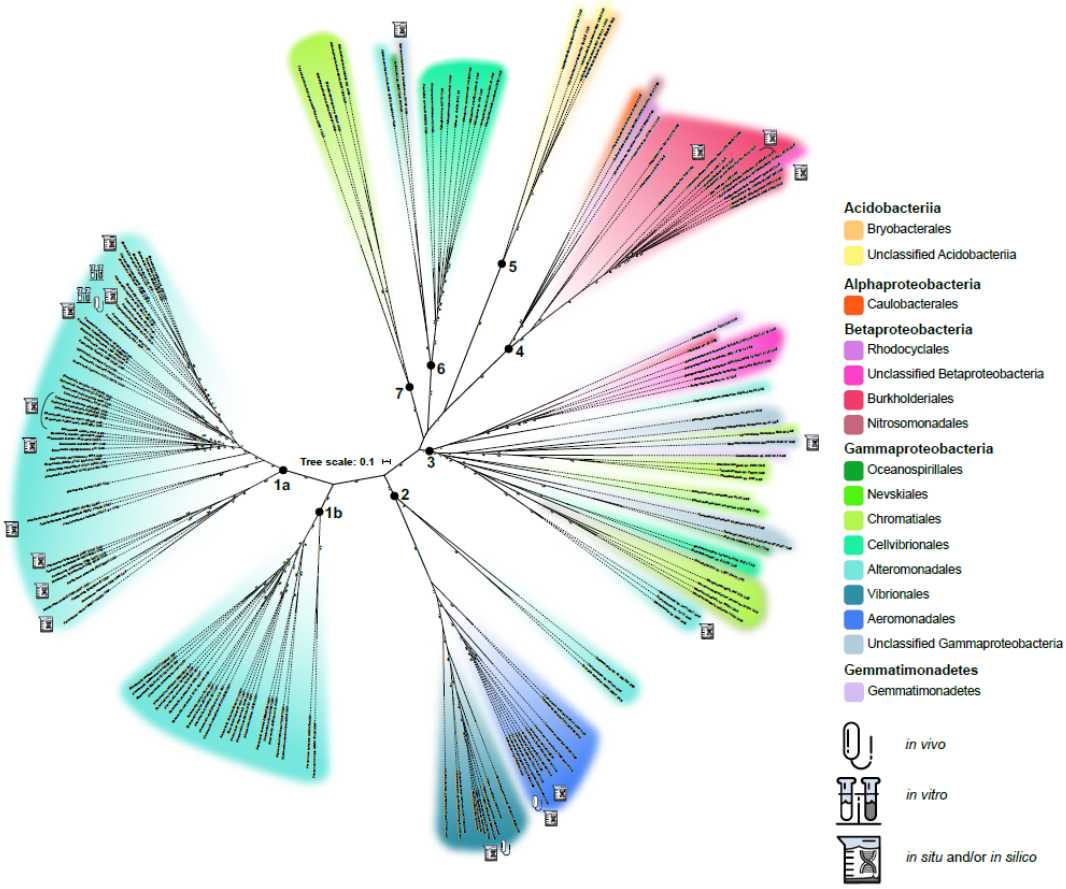

Figure 24. Phylogenomic relationships amongst MtrCAB coding sequences. This maximum likelihood tree contains 177 concatenated MtrA(D), MtrB(E), and MtrC(F) amino acid sequences encoded in the genomes of 148 species. Each node represents a single concatenated MtrCAB (MtrDEF) sequence. Color codes were assigned by taxonomic order. Bootstrap values are indicated along branchpoints. Bolded numbers 1-7 indicate MtrCAB groups referenced throughout this paper. Groups 1a and 1b represent MtrCAB and MtrDEF, respectively, in the *Shewanella* spp. and Ferrimonadaceae. Sequences derived from species with previous evidence of MtrCAB/DEF dependent EET are noted in the “Investigations of Mtr” section in Table 5. Genetic, *in vivo* evidence is denoted with a bacterium symbol and biochemical, *in vitro* evidence is denoted with a test tube symbol.

The results of the MtrCAB maximum likelihood tree (Figure 24) imply seven distinct clades, or diversifications, of the MtrCAB system, hereon referenced to as Group 1-7. Group 1 is comprised mostly of *Shewanella* spp, with the remainder representing the closely related family *Ferrimonadaceae*(319). The majority of species represented in Group 1 had both MtrCAB and its paralog MtrDEF, which were incorporated into the tree-building process as separate sequences. MtrCAB and MtrDEF formed separate clades on the tree and are distinguished as Groups 1a and 1b, respectively. Group 2 contains MtrCAB sequences mostly from species of *Vibrio* and *Aeromonas* in addition to a few *Photobacterium*, *Thalassotalea* and *Colwellia* species. While Group 3 did not include any experimentally validated cases of EET, it was the most phylogenetically diverse cluster representing numerous *Thioalkalkivibrio spp.* and *Wenzhouxiangella spp., Marinobacter spp.*, unclassified Gammaproteobacteria and Betaproteobacteria, and a member of the phylum Gemmatimonadetes. Group 4 is almost completely populated by betaproteobacteria, most of which are Burkholderiales, as well as singletons from the unclassified Betaproteobacteria, the orders Rhodocyclales and Nitrosomonadales (Gallionellales), and 1 alphaproteobacterium from the order Caulobacterales. Group 5 is made up exclusively of sequences from the Acidobacteriia that are unclassified or belong to the order Bryobacterales. Sequences from the Cellvibrionales *Halieaceae* family comprised the majority of Group 6 with single additional representatives from Oceanospirillales, Alteromonadales and unclassified Gammaproteobacteria. Lastly, Group 7 contained MtrCAB sequences from the family Ectothiorhodospiraceae.

By and large, the MtrCAB gene tree does not align with the phylogenetic relationships of the species predicted to encode MtrCAB identified here, consistent with the hypothesis that HGT played a role in the dispersal of MtrCAB to the species represented in Figure 24. These apparent relationships between MtrCAB clades are generally mirrored in the individual MtrA, MtrB, and MtrC trees (Figures 25-26).

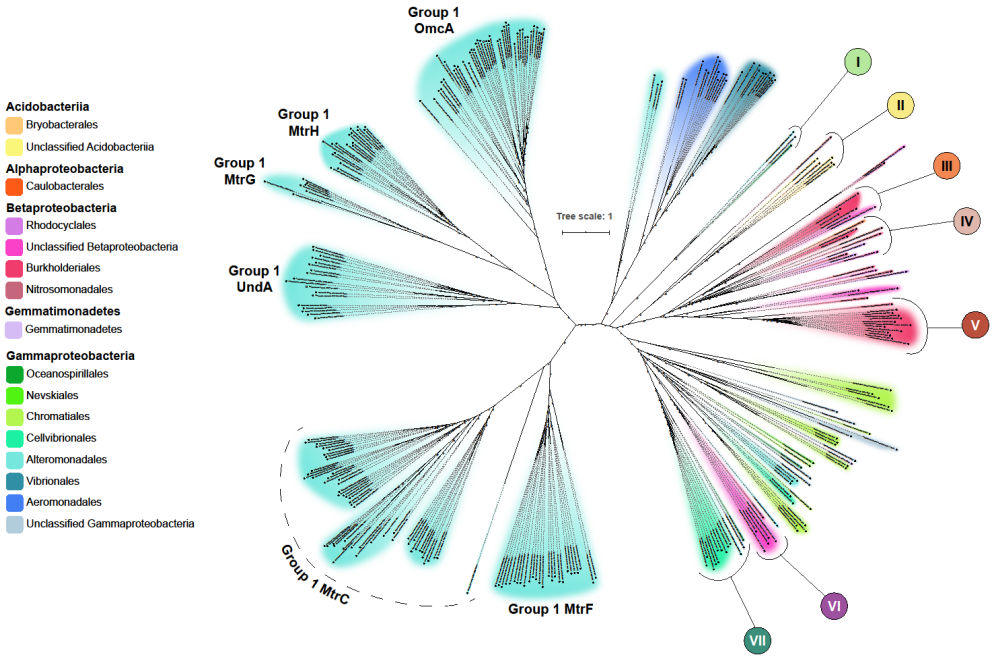

Figure 25. MtrC maximum likelihood tree generated from amino acid sequences encoded by all core *mtrC*(*mtrF*) genes (those encoded directly adjacent to *mtrAB*) as well as those *mtrC* genes encoded next to core *mtrCAB* clusters. Numbered, colored circles correspond to numbered, colored arrows in Figure 33. Bootstrap values are indicated along branchpoints.

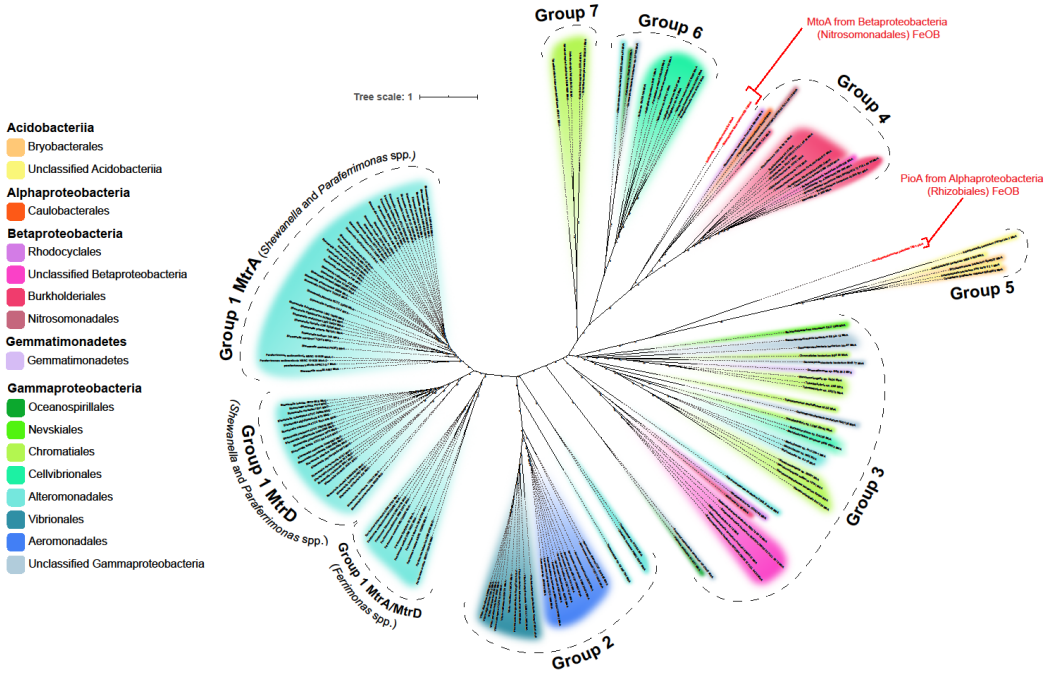

Figure 26. MtrA maximum likelihood tree generated from amino acid sequences encoded by all *mtrA*(*mtrD*) sequences in the *mtrCAB* clusters identified in our study. Homologs of MtrA from chemolithotrophic iron-oxidizing betaproteobacteria (labelled as MtoA) and a phototrophic iron-oxidizing alphaproteobacterium (labelled as PioA) were also included in building the tree and are indicated in red. Bootstrap values are indicated along branchpoints.

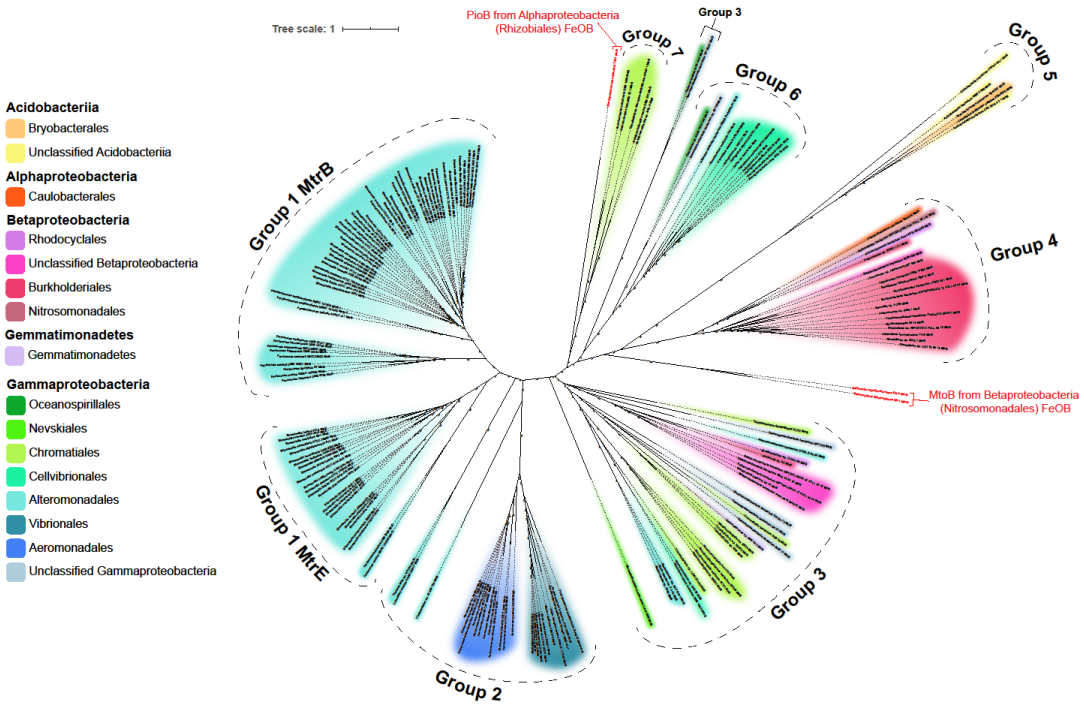

Figure 27. MtrB maximum likelihood tree generated from amino acid sequences encoded by all *mtrB*(*mtrE*) sequences in the *mtrCAB* clusters identified in our study. Homologs of MtrB from chemolithotrophic iron-oxidizing betaproteobacteria (labelled as MtoB) and a phototrophic iron-oxidizing alphaproteobacterium (labelled as PioB) were also included in building the tree and are indicated in red. Bootstrap values are indicated along branchpoints.

Examples of phylogenetic incongruences are most apparent in Group 3, which include distantly related taxa belonging to the Betaproteobacteria, Gammaproteobacteria, and Gemmatimonadetes. While the Betaproteobacteria and Gammaproteobacteria do form distinct clades within Group 3 (excluding MtrCAB from Alteromonadaceae bacterium 2753L.S.0a.02 and *Gemmatimonas* sp. SG8_38_2,

which groups with the Betaproteobacteria and Gammaproteobacteria, respectively), the relationships amongst MtrCAB within these classes are largely discordant with their host species' relationships. Within the Group 3 Gammaproteobacteria, for example, one subset of MtrCAB from *Thioalkalivibrio* and *Wenzhouxiangella* sp. (order Chromatiales) appear to be sister to MtrCAB from *Marinimicrobium* sp. (order Cellvibrionales), while another subset of the same Chromatiales genera group with *Gemmatimonas* sp. SG8_38_2, which isn't a Proteobacterium at all, but rather a member of the phylum Gemmatimonadetes (320). Another example of MtrCAB-species phylogeny incongruence is the Alteromonadales species (*Colwellia and Thalassotalea* spp.) represented in Group 2, which is otherwise comprised of sister orders Vibrionales and Aeromonadales (321, 322). A similar instance can be found in Group 6, which features MtrCAB from an Alteromonadales, Oceanospirillales, and an unclassified Gammaproteobacterium in an otherwise Halieaceae-dominated group.

Conversely, the high species representation of *Shewanella* in Group 1 (40 MtrCAB+ species out of the 45 *Shewanella* species with genome assemblies available at the time of this study, see Methods for details) and the close topological alignment with the *Shewanella* species phylogeny (284, 323) suggests that MtrCAB is vertically transmitted among *Shewanella* spp. The Ferrimonadaceae represented in Group 1 also suggest a history of *mtrCAB* being vertically transmitted, with all available *Ferrimonas* genome assemblies and 2 out of 3 *Paraferrimonas* genomes encoding MtrCAB. However, the family-level relationships between the Shewanellaceae and Ferrimonadaceae still require further resolution; some studies point toward the Shewanellaceae and Ferrimonadaceae as being sister to one another(319, 324), while other studies suggest that the Shewanellaceae are in fact more closely related to the MtrCAB-lacking Moritellaceae than they are to the Ferrimonadaceae (104, 325). Additionally, the Shewanellaceae species *Psychrobium* and *Parashewanella* do not encode MtrCAB. Thus, it is not yet possible to resolve the evolutionary order of events that led to the transmission of MtrCAB amongst the Shewanellaceae and Ferrimonadaceae; it's possible that the Shewanellaceae-Moritellaceae Ferrimonadaceae ancestor possessed *mtrCAB* but was later lost in the Moritellaceae lineage, or that separate HGT events led to the Shewanellaceae and Ferrimonadaceae ancestors acquiring *mtrCAB* separately. This latter scenario does not preclude the possibility that the ancestor of either of these two families transferred *mtrCAB* via HGT to the other.

Beyond phylogenetic discrepancies in the individual MtrCAB groups, the overall diversity and topology of the MtrCAB tree suggest a complicated evolutionary history driven in large part by HGT. With the exception of the Shewanellaceae and Ferrimonadaceae, the species predicted to encode MtrCAB are not representative of the majority of their sequenced representatives; that is, few or no other members of the same taxonomic group encode MtrCAB. It has been previously noted, for example, that the genetic potential to perform EET is unevenly dispersed within the genera *Aeromonas* and *Vibrio* with certain clades predominantly maintaining *mtrCAB* in the genome and other strains as the single MtrCAB-encoding representative (90, 286). This sporadic representation of MtrCAB-encoding species suggests two potential evolutionary histories: multiple secondary losses in the majority of lineages, or more likely, insertion into the genomes of the strains we identified in our search.

Genomic comparisons suggest that *mtrCAB* is highly mobile.

To address the two scenarios mentioned above, we examined the context of the *mtr* locus by comparing genomes of strains carrying *mtrCAB* with genomes from closely related species that apparently lack *mtrCAB*. These comparisons revealed genomic “scars” indicative of events where *mtrCAB* might have been inserted or lost in the past (Figure 28, Supplementary Figure 4). In general, we found that *mtrCAB* seemingly interrupted the otherwise syntenic region in the *mtrCAB*-lacking genome, suggesting that *mtrCAB* was inserted in these sites. In other instances, the aligning regions between two genomes revealed transposases, integrases, endonucleases, and/or recombinases in place of *mtrCAB*, perhaps indicating a prior loss of *mtrCAB* from the genome. Below, we describe several representative examples that demonstrate the mobility of *mtrCAB* and linked accessory genes.

One notable example is the *mtrCAB*-lacking genome of *Marinobacter atlanticus* CP1, a member of a cathodically-enriched electroactive community (326–330), which has multiple transposases and restriction endonucleases in the same genomic locus that encodes *mtrCAB* in fellow *Marinobacter* species, *Marinobacter* sp. W62 and sp. PJ-16 (Figure 28A). In contrast to gene loss evidence based on the presence of mobility-associated elements, alignments of the MtrCAB-encoding *Aeromonas veronii* AMC34 genome revealed a genomic inversion in the region of *mtrCAB* insertion relative to the same region in *A. veronii* B565 lacking *mtrCAB* (Figure 28B). The

genomic inversion may indicate a past transposase-mediated event at the *mtrCAB* locus in *A. veronii* AMC34 as genomic inversion can result from recombination between inverted repeated sequences which flank transposable elements (331).

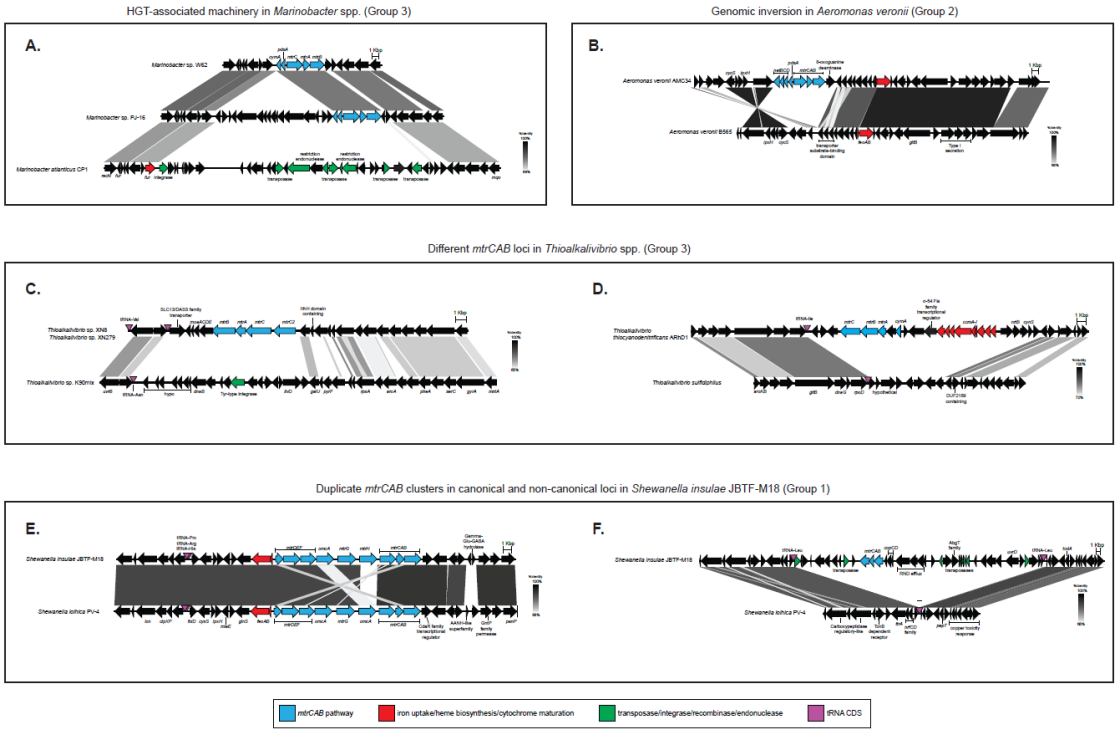

Figure 28. Genomic comparisons of *mtrCAB* loci in MtrCAB-encoding organisms and syntenic regions in MtrCAB-lacking relatives highlights mobility of *mtrCAB*.

Thioalkalivbrio spp. have acquired at least two different homologs of *mtrCAB*. The MtrCAB CDS from *Thioalkalivibrio thiocyanodentrificans* ARhD1 lays in a distant clade amongst other similarly related Ectothiorhodospiraceae sequences on the MtrCAB tree (Group 7, Figure 24). In contrast, MtrCAB from *Thioalkalivbrio* sp. XN8, sp. XN279, and sp. LCM1.Bin42 fall into a diverse clade (Group 3, Figure 24) comprised of Chromatiaceae and other gammaproteobacterial sequences. Even within Group 3, MtrCAB from *Thioalkalivibrio* sp. XN8 and XN279 and *Thioalkalivibrio* sp. LCM1.Bin42 branch into discrete clusters with two different sets of *Wenzhouxiangella* spp. In addition to belonging to different groups on the MtrCAB tree, the genomic context of *mtrCAB* is also different between *Thioalkalivbrio* sp. XN8 and XN279, *Thioalkalivibrio* sp. LCM1.Bin42, and *T. thiocyanodentrificans* ARhD1 (Figure 28C, D). In parallel to these differences, the Mtr genes are arranged as C-A-B in the genomes of *Thioalkalivbrio* sp. XN8, XN279, and LCM1.Bin42, but appear in the order

of A-B-C in *T. thiocyanodentrificans* ARhD1's genome. The differences in genomic context and affinity on the MtrCAB tree between these *Ectothiorhodospiraceae* species may indicate two divergent mobile elements targeting different insertion sites within this family of Gammaproteobacteria.

Another example of *mtrCAB* mobility was observed in *Shewanella insulae* JBTF-M18's genome, which contains two non-syntenic *mtrCAB* gene clusters. One copy of *mtrCAB* is located in the conserved location upstream of *feoAB* as observed in the closely related *S. loihica* PV-4 (Figure 28E, F). The other *mtrCAB* cluster is flanked by transposase CDS and lacks the additional *mtrC*/*omcA* family homologs that are normally observed in *Shewanella* spp. *mtrCAB* loci. Additionally, this extraneous cluster is located on a segment of DNA between two tandem tRNA Leu encoding genes, which can be recognized by certain transposases as insertion sites (331). That said, both copies of MtrCAB from *S. insulae* share more sequence identity with each other than with any other MtrCAB CDS, suggesting that the mobility of *mtrCAB* in this instance was not from a phylogenetically distant donor, but instead may indicate an internal duplication event following by recombination. A similar phenomenon was observed in the 2 *Photobacterium* recovered in our search, as both *P. lutimaris* JCM 13586 and *P. gaetbulicola* Gung47 have *mtrCAB* 382 in identical regions on chromosome, but *P. gaetbulicola* Gung47 has a second copy of *mtrCAB* in a different region on chromosome 2 (Figure 29).

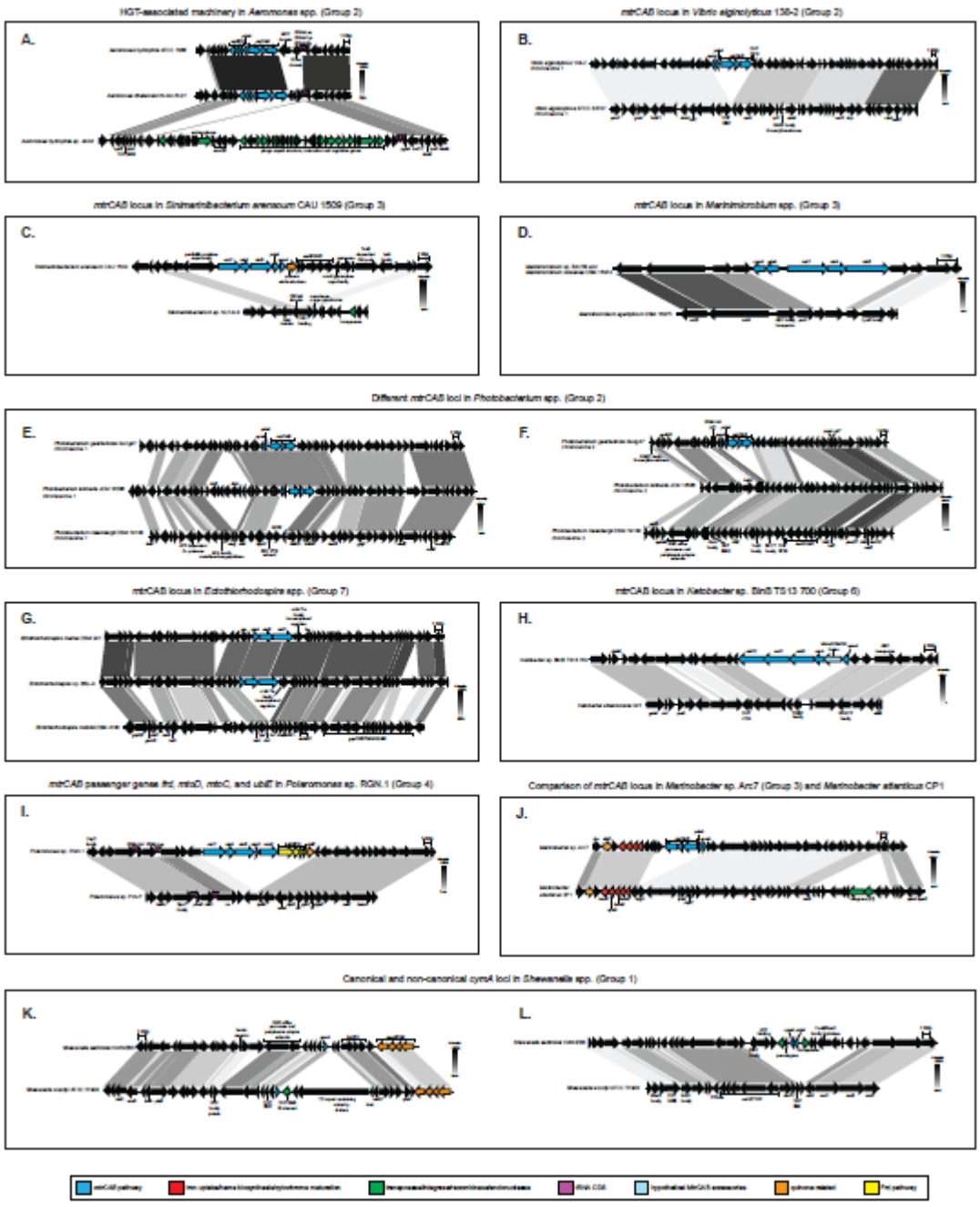

Figure 29. Additional genomic comparisons between *mtrCAB* loci in MtrCAB encoding organisms and syntenic regions in MtrCAB-lacking relatives.

Genomic context reveals passenger genes that mobilize with *mtrCAB*.

We observed that syntenic genes that co-occur with *mtrCAB* but are similarly lacking from closely related MtrCAB-less genomes (Figure 30). The genes therein

included other members of the MtrCAB EET pathway that have been functionally characterized (90, 286, 332, 333), such as the inner membrane quinol dehydrogenases CymA or NetBCD or the periplasmic diheme cytochrome PdsA (Figures 28A, 28B, 28D, Figure 29). Transfer of the *mtrCAB/pdsA/cymA[netBCD]* gene cluster to another organism would equip the receiving species with a full suite of machinery to perform EET, provided that the receiving genome already contains the appropriate *c*-type cytochrome maturation and menaquinone biosynthetic genes. Other genes clustered with *mtrCAB* included *mtoC* and *mtoD* (290), the putative inner membrane quinone oxidoreductase and periplasmic electron carrier, respectively, that are hypothesized to play a role in extracellular electron uptake in the MtoAB system in *Sideroxydans lithotrophicus* ES-1 and other related iron-oxidizing betaproteobacteria (44, 334) (Figure 30A-C, Figure 29).

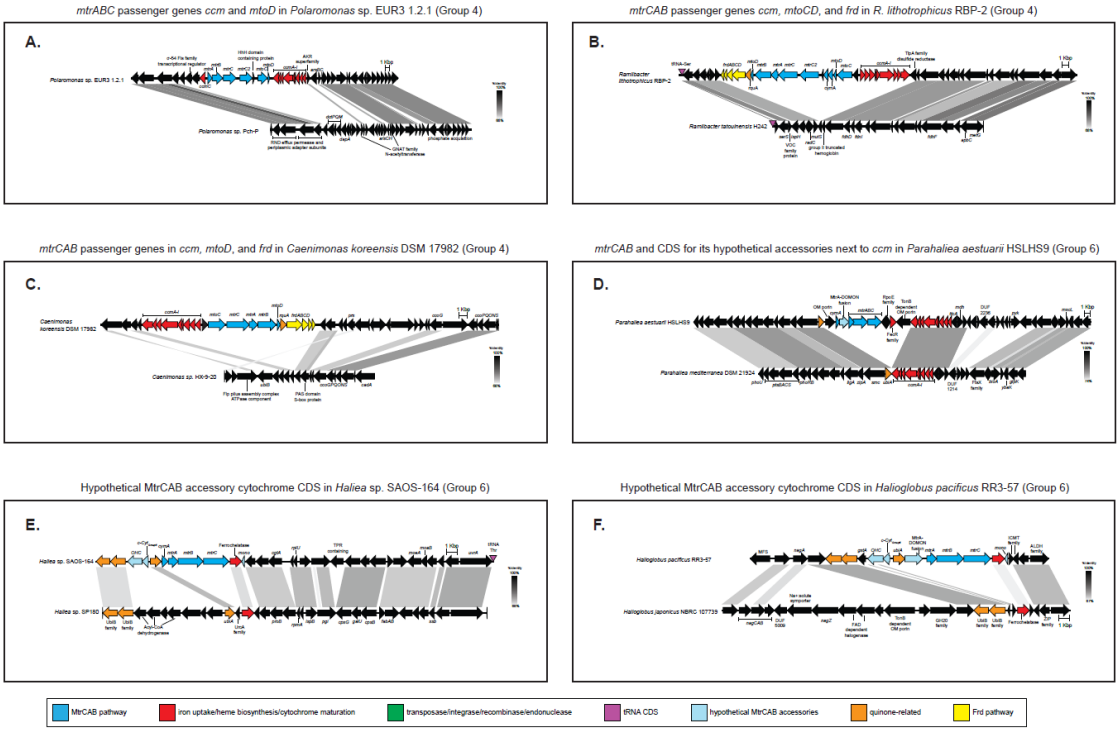

Figure 30. Putative *mtrCAB* passenger genes genomic comparisons of *mtrCAB* loci in MtrCAB-encoding organisms and syntenic regions in MtrCAB-lacking relatives reveal putative *mtrCAB* passenger genes and provide further evidence for *mtrCAB*'s mobility and distribution through HGT.

Moreover, we discovered novel putative cytochrome-encoding genes adjacent to MtrCAB that are shared amongst subsets of our newly detected species encoding MtrCAB (Figure 30D-F, Figure 29). While the function of these proposed accessory genes is not yet verified, they are typically predicted to be localized to the periplasm, outer membrane, inner membrane, or extracellular space, which would be important if they function in the transmission of electrons between the cell and the extracellular environment. Additionally, the fact that these genes are not found in the MtrCAB lacking genomes points toward some level of involvement in the MtrCAB pathway. These features may suggest that certain genes travel together with *mtrCAB*, reminiscent of passenger genes carried by mobile elements (335).

To that same end, both verified and putative accessory cytochromes alike–as well as MtrC homologs (see next section)–seem to track with MtrCAB tree-groups rather than with species affinity (Figure 31). Excluding the Group 1 representatives, which encode CymA and other relevant cytochromes (FccA, CctA) in regions non-syntenic with the core *mtrCAB* locus, we found that specific cytochromes encoded next to *mtrCAB* were unique to one or two groups, possibly indicating episodic evolutionary events in a group ancestor, suggesting that the MtrCAB evolves in a modular fashion. For example, *pdsA* is found in all members of Group 2 and most Gammaproteobacteria in Group 3,but is absent from other MtrCAB groups (Figures 28A-B, 31). Likewise, *mtoC* and *mtoD* homologs are found almost exclusively in the betaproteobacteria dominated Group 4 (Figure 30A-C, Figure 31), with just one other representative (also a betaproteobacterium) in Group 3 also possessing *mtoD* adjacent to *mtrCAB*. There were also instances of group-specific putative cytochromes that were not found in members of other groups. The Group 5 Acidobacteriia all encoded a predicted periplasmic tetraheme cytochrome (*c cyt*$_{Group5}$) immediately downstream of *mtrB* (Figure 31). Group 6 *mtrCAB* clusters were neighbored by up to 4 encoded cytochromes unique to these *mtrCAB*-encoding species, which to our knowledge, have never been described before (Figure 30D-F, 31). These include a predicted periplasmic nonaheme MtrA-family cytochrome with a DOMON domain (*mtrA-DOMON)*, an inner-membrane tetraheme cytochrome (*c-cyt*$_{Group6}$), a periplasmic monoheme protein (*mono*), and a periplasmic octaheme c-type cytochrome (*ohc*). The one commonality to almost all groups was that at least one group member encoded a CymA homolog as part of the

mtrCAB gene cluster, excluding the Group 5 Acidobacteriia which did not encode any putative inner membrane quinone oxidoreductases near the MtrCAB CDS (Figure 31).

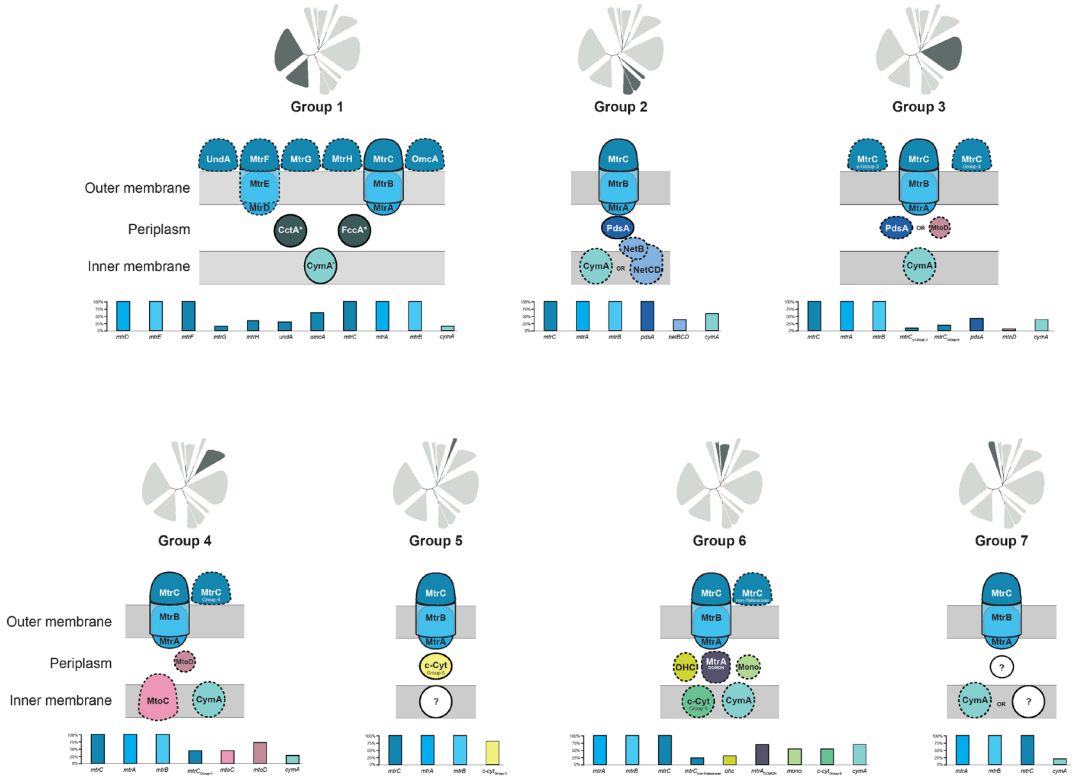

Figure 31. Hypothetical models of MtrCAB and accessory components encoded in *mtrCAB* gene clusters show group-specific diversifications. Protein localization along the cell envelope was predicted with PSORTb. (336) Proteins outlined with a solid line are found in every species in the MtrCAB group, while dotted lines indicate that the protein is encoded in at least one, but not all members of the MtrCAB group. White circles with a question mark indicate that a putative protein in that cellular location was not encoded in the *mtrCAB* cluster in all or most members of that MtrCAB group. Barplots show the percentage of members in a given group that encode each *mtrCAB* component. *CymA, FccA, and CctA are not encoded adjacent to the mtrCAB cluster in *Shewanella* species nor most Ferrimonadaceae species but are included here due to their well-established role in MtrCAB-mediated EET in members of these species.

We did not search the genome beyond the identified *mtrCAB* loci for *cymA* or the other depicted accessory cytochromes in other organisms.

Mobility of additional EET-associated genes was also observed in multiple *Shewanella* genomes (Figure 29). In *Shewanella sediminis* HAW-EB3, for example, CymA is encoded in a conserved location upstream of *menECHD,* as observed in close relative *S. woodyi* ATCC 51908 and other MtrCAB-encoding *Shewanella* spp. (Figure 29). In a separate region of the *S. sediminis* HAW-EB3 genome however, an additional *cymA* was observed directly next to the periplasmic electron shuttle *pdsA*, the role of which is normally fulfilled by FccA or CctA (46, 337) in the *Shewanella* Mtr pathway (90, 286). Furthermore, the *cymA-pdsA* region in *S. sediminis* (Figure 29) is flanked by encoded transposases and both of these *S. sediminis* genes align most closely with homologs from *Vibrio* spp. These genomic features further support the hypothesis of this system being mobile and prone to horizontal transfer, potentially in a modular fashion.

While the majority of sequenced *Shewanella* spp. encode MtrCAB, there are 2 species, *S. violacea* DSSS12 and *S. denitrificans* OS217, that do not encode Mtr homologs (Figure 32) and are unable to reduce extracellular acceptors (338, 339). Given that the other genes involved in or required for the MtrCAB pathway have been especially well studied in *Shewanella* spp., we were able to compare these 2 genomes to their MtrCAB-encoding counterparts to look for further indications of gene loss. A genomic inversion is observed at the site of *cctA* loss in *S. denitrificans* OS217 (not shown). Loss of *menECHD*, which encodes proteins required for synthesis of menaquinone, was observed in *S. denitrificans* but not in *S. violacea*, while *cymA* was missing from both species (Figure 32).

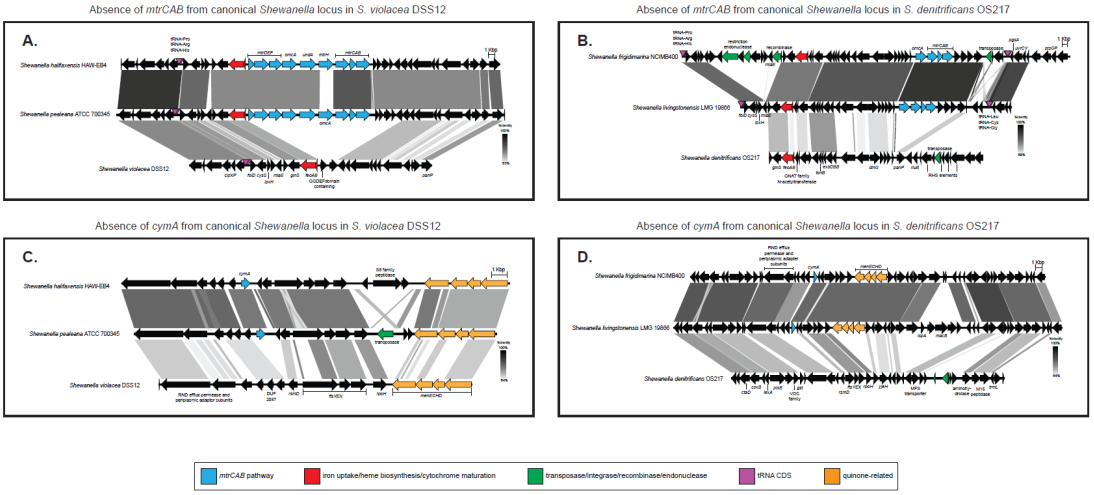

Figure 32. *mtrCAB* and *cymA* loss in canonical genomic regions in 2 species of *Shewanella*, a genus where *mtrCAB* was most likely vertically transmitted.

Lastly, in addition to electron-carrying cytochromes, alignments between genomes encoding and lacking MtrCAB revealed other potential passenger genes specifically involved in or related to cytochrome synthesis. After all, even if a species encodes MtrCAB, it cannot be utilized without the proper machinery to manufacture and localize functional components of the electron conduit. System I cytochrome maturation, CcmA-I, for example, is essential for maturation of MtrA and MtrC and subsequent EET activity in *S. oneidensis* (340, 341). System I may have other biological roles besides heme maturation (342) and can serve as a heme reservoir when iron is unavailable for heme synthesis (343). Additionally, system I requires reduction of the oxidized Fe-heme before cytochrome maturation, unlike system II, which protects reduced Fe-heme from oxidation (344) and functions at a lower concentration of iron than system II (345).

Six of the *mtrCAB* gene clusters (*Thioalkalivibrio thiocyanodenitrificans* ARhD1, *Ramlibacter lithotrophicus* RBP-2, Betaproteobacteria bacterium SpSt-328, *Polaromonas* sp. EUR3 1.2.1, *Parahaliea aestuarii* HSLHS9, and *Caenimonas koreensis* DSM 17982) were genomically adjacent to the complete *ccmA-I* operon (representatives illustrated in Figure 28D, 30A-D, 29). *Aquincola* sp. S2 and *Thioalkalivibrio* sp. LCM1.Bin42 *mtrCAB* were also neighbored by partial *ccm* operons that were interrupted at the end of a contig. We did not find duplicate system I

cytochrome maturation genes in the other genome assemblies encoding CcmA-I next to MtrCAB, although 4 strains (*Thioalkalivibrio thiocyanodenitrificans* ARhD1, *Ramlibacter lithotrophicus* RBP-2, Betaproteobacteria bacterium SpSt-328, and *Aquincola* sp. S2) encoded system II cytochrome maturation genes (*ccsAB*/*resBC*) elsewhere on the genome adjacent to other putative cytochrome-encoding genes. While the rest of these cases indicate that *ccmA-I* is linked with *mtrCAB* in its mobility, this is not the case for *ccmA-I Parahaliea aestuarii* HSLHS9 (Figure 4D), which appears to be native to the syntenic region in the *mtrCAB*-lacking *Parahaliea mediterranea* DSM 21924.

Most of those *mtrCAB* clusters flanked by *ccmA-I* were found in betaproteobacteria belonging to Group 4. Interestingly, Group 4 *mtrCAB* clusters were also often neighbored by the fumarate reductase complex (*frdABCD*), sometimes in tandem with *ccmA-I* (Figure 30B-C, Figure 29). We could not find additional copies of *frdABCD* elsewhere on the genome in these cases, and comparative analyses revealed *frdABCD* was absent in related genomes lacking *mtrCAB*. Upstream of almost all Group 1 *mtr* clusters is *glnS*, which plays an established role in heme biosynthesis by providing glutamate for the synthesis of tetrapyrrole-precursor 5-aminolevulinic acid (346). The *frd* operon could potentially play a parallel role by providing a source of succinate, which, if converted to succinyl-CoA, can also generate 5-aminolevulinic acid (347). Another possible function of FrdABCD in conjunction with Mtr would be to support EET in both the oxidative and reductive directions, an intriguing possibility that warrants further study.

Other genes encoding proteins for heme synthesis, cytochrome maturation, and iron uptake were also observed alongside *mtrCAB*, but do not always follow group-specific patterns or are also found in the same region in their *mtrCAB*-lacking relatives, such as with the *ccmA-I* example in *Parahaliea aestuarii* HSLHS9 detailed above. The menaquinone-dependent protoporphyrinogen IX dehydrogenase gene *hemG* is in the vicinity of *mtrCAB* in *Albidoferax ferrireducens* T118, *Rhodoferax* sp. Bin2_7, and Betaproteobacteria bacterium SpSt 328. Gammaproteobacterium MnB_17 encodes another member of the *hem* operon, oxygen-independent coproporphyrinogen III oxidase HemN, upstream of its *mtr* gene cluster. The *Marinobacter* sp. Arc7 *mtrCAB* cluster is neighbored by a larger suite of heme synthesis genes (*hemY*, *cysG*, *hemD*, and *hemC*), although these genes are also present in the syntenic region in its *mtrCAB*-

-lacking relative *M. atlanticus* CP-1 mentioned earlier (Figure 29). Similarly, all of the Group 6 *mtrCAB* clusters from Halieaceae species (excluding *Parahaliea aestuarii* HSLHS9 and *Halioglobus* sp. NAT121) are immediately upstream of ferrochelatase-encoding *hemH* which catalyzes the final step of heme synthesis (346), but the same regions identified through alignments in Halieaceae species missing *mtrCAB* encode *hemH* as well (Figure 30E, F).

MtrCAB is prone to modular evolution – the curious case of *mtrC*.

Duplications of *mtrC* reveal previous gene flow between *mtrCAB* groups. In addition to the core *mtrA*, *mtrB*, and *mtrC* genes in each cluster, many *mtrCAB* clusters were neighbored by additional MtrC-coding sequences. While only the *mtrC* sequences directly adjacent to *mtrAB* were incorporated into the concatenated MtrCAB tree (Figure 24), all identified duplicates of *mtrC* proximal to the *mtrCAB* gene cluster were included in building the MtrC tree (Figure 23). The distribution of these MtrC sequences in different species and their placement relative to each other and relative to their phylogenetic affinity on the MtrC tree (Figure 25) yielded further insights into the transfer and modular evolution of the MtrCAB system.

Of the *mtrCAB* gene clusters identified in this study, 44% had at least one additional *mtrC* immediately next to the core *mtrCAB*. The number of adjacent *mtrC* duplicates clustered with *mtrCAB* ranged from one to as many as four duplicates outside of the core *mtrC* directly adjacent to *mtrAB*. That said, *mtrC* duplications were not observed in any members of Group 2 (gammaproteobacteria belonging to *Aeromonadaceae, Vibrionaceae, and Alteromonadaceae*), Group 5 (*Bryobacteraceae* and other unclassified acidobacteriia), nor Group 7 (*Ectothiorhodospiraceae* of the gammaproteobacteria). In contrast, every representative of Group 1 (*Shewanellaceae* and *Ferrimonadaceae*) had at least one additional *mtrC* outside of *mtrCAB* and *mtrDEF*, save for 1 of the 2 *mtrCAB* clusters identified in *Shewanella insulae* JBTF-M18 (which likely arose from an internal whole-*mtrCAB* duplication and recombination, discussed in previous section) as well as the *mtrCAB* from *Shewanella polaris* SM1901. Likewise, the 3 non-Halieaceae species in Group 6 have two copies of *mtrC* neighboring *mtrAB*, and 29% and 44% of Groups 3 and 4, respectively, also had representatives with at least one additional *mtrC* neighboring *mtrCAB* in the genome.

We found that in many of these cases, the affinity of the accessory *mtrC* coding sequences on the MtrC tree revealed vestiges of prior HGT and diversification events.

The three non-Halieaceae representatives in Group 6, for example, each possess 2 MtrC-encoding genes, though the other Halieaceae Group 6 representatives only have 1 MtrC coding sequence in their *mtrCAB* clusters. Interestingly, in these non-Halieceae members, it is the *mtrC* that is *not* genomically adjoining *mtrAB*, but rather the second *mtrC* neighboring the core *mtrCAB* cluster, that groups with the rest of the Group 6 MtrCs (Figure 31, 33A, 25). The core MtrC in these 3 individuals instead forms an independent clade that appears to be more closely related to the MtrCs in Groups 4 and 5, although the clade's branch point is relatively deep. One possible scenario that led to this topology would be the transfer of the Group 6 non-Halieacae *mtrCAB* cluster to the ancestor of the Group 6 Halieaceae, followed by gene loss of the non Halieaceae *mtrC*. Alternatively, the non-Halieacae *mtrC* could have arisen as a duplication of the Halieacae *mtrC* following horizontal transmission from the Halieaceae to the non-Halieaceae Group 6 members.

Similarly, Gallionellales bacterium RIFCSPLOWO2_02_FULL_59_110 (Group 4) has 2 copies of *mtrC* as part of its *mtr* gene cluster; one of these coding sequences grouped with the other Group 4 betaproteobacteria MtrCs (Figure 5, 6B, Supplementary Figure 1), while the other MtrC clustered with the Group 5 MtrCs. This could indicate gene flow between Groups 4 and 5 and, based on the lack of other MtrC duplicates in Acidobacteriia, could represent a previous loss event that removed what might have been a functionally irrelevant paralog. Such instances of genome reduction by paralog loss are not uncommon and have been well-studied in other systems (348–350), in which a gene is duplicated and subsequently neofunctionalized, followed by a loss of one of the two copies.

There is also clear gene flow and downstream MtrC diversification that connects the betaproteobacteria of the otherwise gamma-dominated Group 3 with the betaproteobacteria represented in Group 4 (Figure 31, 33C, 25). The core MtrC found in the Group 3 betaproteobacteria (excluding *Niveibacterium* sp. COAC-50) sits amongst the other Group 3 MtrCs (Figure 25). This is also consistent with the individual MtrA and MtrB trees (Figures 26 and 27) which place these select betaproteobacteria amongst Group 3 (including *Niveibacterium* sp. COAC-50). Interestingly, *Niveibacterium* sp. COAC-50's sole MtrC (and thus the one incorporated in the

concatenated MtrCAB tree, Figure 24) groups with the rest of the Group 4 MtrCs, but the strong affinity of the MtrA and MtrB sequences for Group 3 (Figures 24, -26) were apparently sufficient enough to overwhelm any Group 4 affinity lent by its MtrC. Group 3 betaproteobacterium *Aquincola* sp. S2, which possesses the Group 3-centric MtrC, also has the same Group 4-type MtrC as *Niveibacterium* sp. COAC-50. In both *Niveibacterium* and *Aquincola*, the Group 4-type MtrC coding sequence (denoted by the pink arrow in Figure 33C) is followed by a putative gene encoding a Helix-hairpin-Helix (HhH) gene; in the *Aquincola* genome, this HhH CDS sits between the two *mtrC*s, while it adjoins the sole *mtrC* and *mtrAB* coding sequences in *Niveibacterium*. The retention of this *HhH* beside the Group 4-type *mtrC* and the Group 3-leaning nature of *Niveibacterium*'s *mtrAB* is consistent with a deletion of the Group 3-type *mtrC* in *Niveibacterium*.

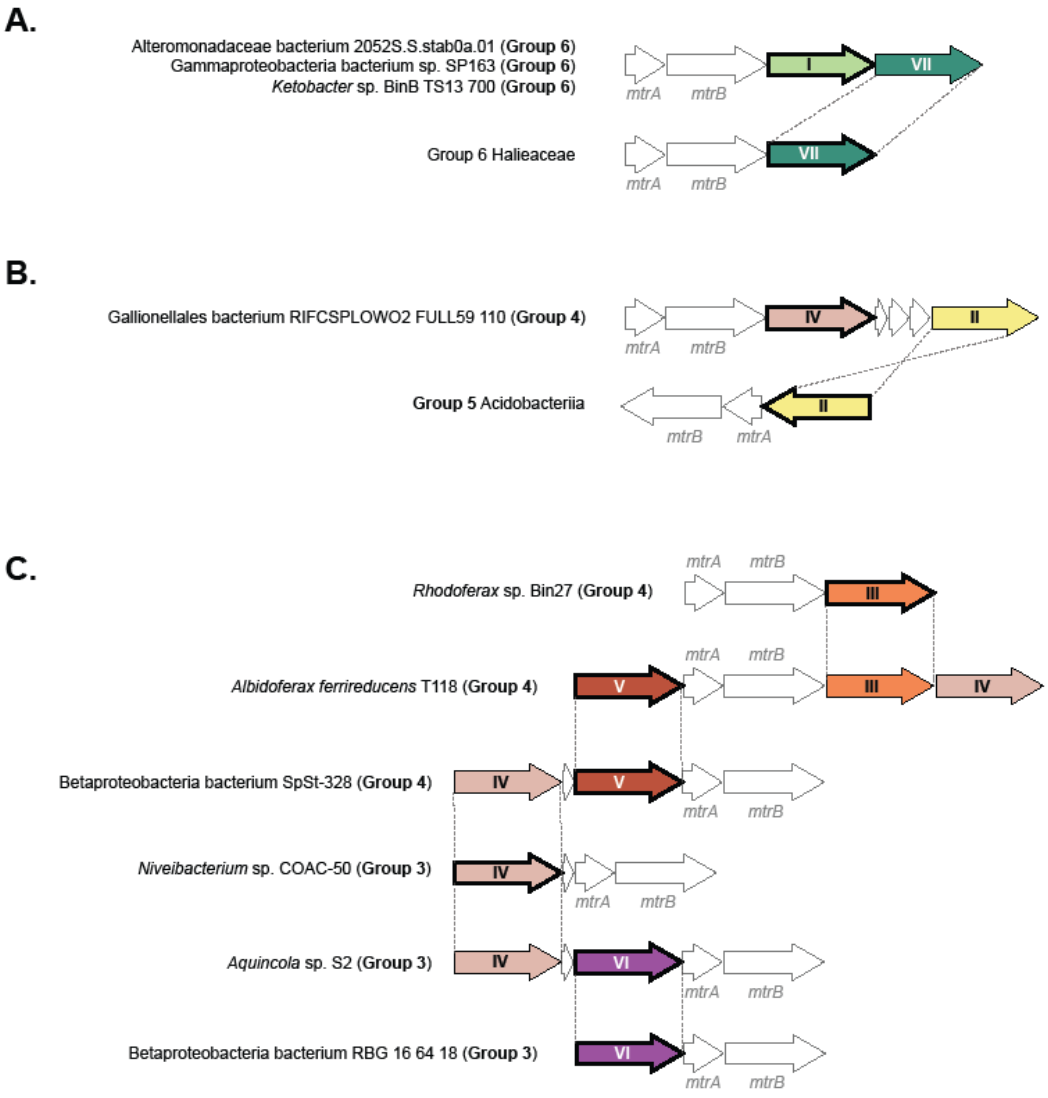

Figure 33. Tracking *mtrC* homologs reveal finer scale gene flow between MtrCAB-encoding species. Arrows filled with color represent *mtrC* sequences. Colors correspond to the numbered circles (I-VII) in Figure 25. Bolded outlines indicate the core *mtrC* whose translated coding sequence was incorporated into the concatenated MtrCAB tree (Figure 24). Unlabeled white arrows in C represent a conserved HhH encoded in some *mtrCAB* clusters.

This apparent deletion however, is not the only instance of overlap between the betaproteobacteria of Groups 3 and 4. In fact, many of the Group 3 betaproteobacteria genomes also contain MtrC coding sequences that are missing from all other Group 3 genomes yet are abundant in the Group 4 MtrCAB gene clusters. It must be noted,

however, that there is one clade of MtrCs each in the Group 3 betaproteobacteria and in Group 4 that are unique to the representatives of the respective *mtrCAB* group genomes. All of the group 3 betaproteobacteria (except *Niveibacterium* sp. COAC 50) have a core MtrC (represented by the purple arrows in Figure 33C) that is not present in any of the Group 4 genomes. Likewise, a subset of the group 4 betaproteobacteria have a core MtrC (represented as orange arrows in Figure 33C) that is not present in any of the Group 3 genomes.

MtrC has diversified and formed distinct clades in Group 1

Relative to these other MtrC groupings, the MtrC family proteins encoded in the Group 1 (*Shewanella* spp., *Ferrimonas* spp., and *Paraferrimonas* spp.) *mtrCAB/DEF* gene clusters formed exceptionally distinct clades (Figures 25, 33). We named these MtrC family clades (MtrC, MtrF, OmcA, UndA, MtrG, MtrH) based on previously published descriptions and characterizations (337, 351–360), however, there are naming discrepancies in the literature for MtrH, OmcA, and UndA (44, 63, 284, 361). To reconcile these discrepancies, we propose updating the naming conventions for this family of proteins based on our MtrC tree (Figures 25, 33; Table 5), which was built from significantly more sequence data than what previous analyses had available at their time of publication (63, 284).

The number (0-5) and subfamily (MtrC, MtrF, OmcA, UndA, MtrG, MtrH) of MtrC family proteins encoded in *mtr* gene clusters varied widely across Group 1, but all species encoded MtrC. MtrC associates with MtrAB at a 1:1 ratio in the outer membrane and is reduced by MtrA (43, 362). Based on structural and sequence homology to MtrC, MtrF likely associates with MtrDE, in a manner similar to MtrCAB (353). MtrF was present in 49% of Group 1 species and was always encoded immediately downstream from *mtrDE*, in the same way that *mtrC* is always observed immediately upstream of *mtrAB* (Figure 34). MtrF formed a sister clade to MtrC (Figure 25), recapitulating the relationship observed in the concatenated MtrCAB tree (Figure 24) and supporting previous hypotheses about their heritage (45). The shared ancestry of both the individual MtrC/MtrF coding sequences and the MtrCAB/MtrDEF clusters indicates that *mtrDEF* and *mtrCAB* formed through a duplication of the entire gene cluster, rather than through duplications of the individual

mtrA/D, mtrB/E, and *mtrC/F* genes. However, the order of operations that led to the birth of these two gene clusters--that is, whether *mtrDEF* arose as a duplication and reconfiguration of *mtrCAB* or vice versa--remains to be determined.

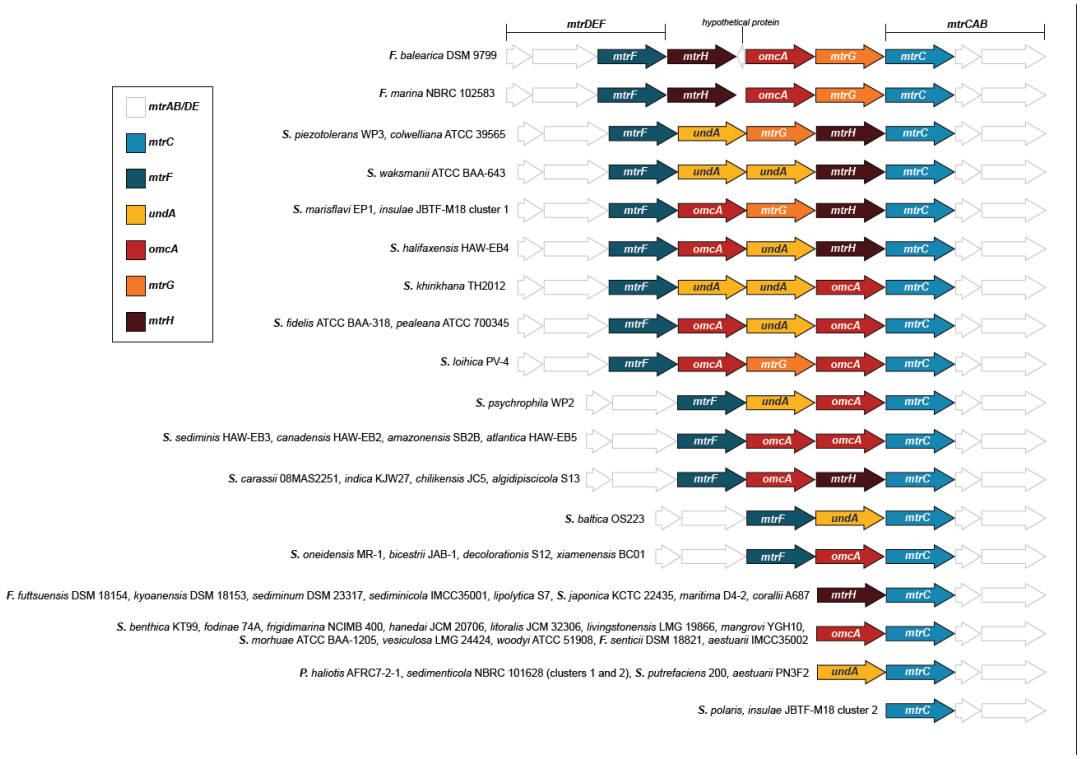

Figure 34. Genomic arrangement of *mtrC* homologs in Group 1 *mtrCAB* clusters. Gene names are based on corresponding placement in the MtrC tree (Figure 25).

Conversely, the other MtrC family proteins that we uncovered in Group 1 (OmcA, UndA, MtrG, MtrH) do not appear to have co-evolved with a complementing *mtrAB/DE* but, based on their observed relationships (Figure 25), have emerged through individual duplications and diversifications of an ancestral MtrC family protein. OmcA was the most common unanchored MtrC family protein encoded in Group 1, with 64% of species encoding at least one copy and several species encoding two non-syntenic *omcA* homologs (Figures 25, 33; Table 5). UndA, another previously reported MtrC family protein (63, 355, 361), was encoded in 30% of Group 1 species and also displayed duplications within some *mtr* gene clusters. *mtrG* and *mtrH* encode uncharacterized MtrC family proteins that are predicted to localize to the extracellular

space like OmcA and UndA and occurred in 11% and 34% of Group 1 species, respectively.

None of the *mtr* clusters in the Group 1 species encoded all 6 of the MtrC family proteins that we identified. That said, except for *S. polaris* and cluster 2 in *S. insulae* JBTF-M18 (as mentioned at the beginning of this section), all Group 1 clusters included at least one unanchored MtrC family protein. Gene clusters that included both *mtrCAB* and *mtrDEF* always had at least one unanchored MtrC family protein (OmcA, UndA, MtrG, MtrH) encoded between the 2 complete modules. OmcA and UndA were the only MtrC family proteins encoded between *mtrCAB* and *mtrDEF* when only one unanchored MtrC family gene was present. In clusters lacking *mtrDEF*, the MtrC family protein encoded next to *mtrCAB* was either MtrH, OmcA, or UndA, but never MtrG. Beyond these parameters, there were no 'rules' as to the combination of genes encoding different MtrC family proteins in a given *mtr* cluster (i.e. the presence of a specific clade of MtrC family gene was not dependent on the presence of another).

4.5 Discussion

In this study, we set out to determine the prevalence of *mtrCAB* genes throughout all three domains of the tree of life, with the broader goals of A) capturing the prevalence of these transmembrane systems among all taxa; B) understanding the evolution and mobility of *mtrCAB*-mediated EET; and C) providing a roadmap for the empirical assessment of EET among those taxa with the *mtrCAB* genes. With the only requirement being that the *mtrC, mtrA,* and *mtrB* genes occur in close succession together in a given genome, we found that the genomic potential for EET is broadly distributed amongst Gram-negative Bacteria from a wide range of environments and geographic locales (Figure 23, Table 5). The sporadic phylogenetic representation (Table 6) amongst various orders of Gammaproteobacteria, Betaproteobacteria, Alphaproteobacteria, Acidobacteriia, and Gemmatimonadetes led us to hypothesize that this system was dispersed largely through horizontal gene transfer. The incongruences in the concatenated MtrCAB phylogenetic tree (Figure 24) support this hypothesis, as seen in the topology both within and between tree groups. Part of this mismatch between species phylogeny and relationships amongst MtrCAB coding sequences can be attributed to the fact that the overwhelming majority of genera

(excluding *Shewanella* spp. and the Ferrimonadaceae in which *mtrCAB* was likely vertically transmitted to all species following an ancestral HGT) represented in our tree contain mostly MtrCAB-lacking species (Table 6), not to mention the genera and orders interspersed between those in our tree in which MtrCAB is completely absent.

That said, these closely related genomes lacking *mtrCAB* afforded us the opportunity to further assess the HGT hypothesis through a comparative genomics approach. These comparisons further supported HGT as the main mechanism by which *mtrCAB* spread. In addition to revealing footprints from prior recombination or transposition events (Figures 28 and 30), this method revealed putative genes that are linked with MtrCAB, potentially as passenger genes, should *mtrCAB* comprise a mobile element as our data suggests. In addition to genes likely associated with maturation of MtrCAB and its associates, analysis of the genes neighboring *mtrCAB* revealed coding sequences for putative hemoproteins predicted to localize along the cell envelope (Figures 28, 30 and 31). These include periplasmic and inner-membrane electron carriers with established functions in some species (i.e. CymA, PdsA, NetBCD), as well as proteins implicated in iron oxidation (i.e. MtoC, MtoD), and other putative cytochromes that, to our knowledge, have not been reported before. The fact that some of these hypothesized ancillary MtrCAB components are group-specific (Figure 31) strongly suggests that these components co-evolved with MtrCAB and highlight the capacity for MtrCAB and its accessories to change in a modular fashion. This also includes the duplications and diversification of MtrC (Figure 33).

In the following sections, we address 2 pressing questions that were prompted by our findings: A) what evolutionary events in the past led to the relationships amongst MtrCAB modules observed today, and B) do the modular innovations associated with MtrCAB reflect adaptations to the environments in which they emerged?

An emerging evolutionary story

The relationships between MtrCAB coding sequences (Figure 24-27), largely confounded by their incongruencies with species phylogeny, do not lend themselves to an especially clear portrait of their evolutionary history. As discussed throughout this paper, we hypothesize that *mtrCAB* comprises a mobile genetic element. Consistent with the selfish operon theory (363, 364), *mtrCAB* and its accessories exist as a succinct, contiguous cluster of genes, making it possible to transfer this metabolic

capacity as a single functional package. Not only do the genes required for the reduction of specific electron acceptors often occur in close succession like *mtrCAB* (315, 365–367), the most phylogenetically distant transfers are typically limited to those encoding metabolic genes (368, 369). In addition to enabling the easy mobilization of clusters like *mtrCAB*, this modular arrangement also minimizes disruption to other metabolic networks if suddenly lost from the genome (363).

This still does not explain why *mtrCAB* appears to be missing from some genera or even entire phyla. The main limiting factor as to whether or not *mtrCAB* is maintained in a genome is not discernible from our present analyses, but studies of other mobile elements have revealed that their retention in a recipient genome is just as contingent on compatibility with the recipient's ecology, physiology, and cell architecture as it is on phylogenetic proximity of the HGT donor species (370–372). This principle very likely explains why we did not detect *mtrCAB* in the genomes of Gram-positive bacteria, archaea, or eukaryotes; organisms cannot mature and assemble an outer membrane cytochrome complex like MtrCAB without an outer membrane to which it can be localized. Should one of these organisms that lack an outer membrane receive *mtrCAB* through HGT, the protein products would have to be adapted to fit into a very different kind of cell envelope, and the evolutionary time (or cost) required for these changes to arise may be too large for the genes to be retained in the new host's genome, *even* if they would incur a fitness boost in the long-term. That said, if these accommodations to the cell envelope have arisen in some organisms lacking an outer membrane, it is very likely that our current detection method—which is certainly biased toward MtrCAB as it exists in gram-negative bacteria—would have missed these extremely diverged MtrCAB sequences.

Beyond the limits of cell envelope architecture, the factors determining the genomic retention of *mtrCAB* are not known. Among the *Shewanella* spp., in which *mtrCAB* was likely vertically disseminated (Figure 35A), the species *S. denitrificans* and *S. violaceae* provide two independent examples of possible environment-dependent conditional dispensability of EET (93). *S. violaceae* was isolated from the upper layers of deep-sea sediment, and genomic analysis suggests that it has shifted from a CymA-dependent anaerobic metabolism to an aerobic one, facilitated by inhabiting the oxygenated sediment-water interface (338). *S. denitrificans* was similarly isolated from an oxic-anoxic interface in the central Baltic Sea and is capable of denitrification (339).

In regards to the retention of *mtrCAB* received by horizontal transfer, any adaptive advantage lent by MtrCAB could be voided by detrimental pleiotropic effects (370), mismatch between *mtrCAB*'s regulatory regions and the new host's transcriptional machinery could lead to deleterious over expression of *mtrCAB* (372), or the selection pressure may be too weak to drive retention or altogether limited by genetic drift before it can establish footing in a genome (373). Thus, when *mtrCAB* is received by horizontal gene transfer, any fitness cost incurred by the expression of these foreign genes would need to be minimal or resolvable through "domestication" of these genes and/or through compensatory evolution of other loci in the host genome that alleviate harm incurred by the foreign genes (370, 374), along with strong positive selection pressure for it to remain in the genome (375).

Such adaptations are potentially represented in our findings as accessory cytochromes (Figure 31, Table 5), MtrC diversifications (Figure 33, 25, 34), and the accompaniment of genetic modules involved in heme and cytochrome production (Figures 28-32). Once accrued to fit the ecophysiology of its new host, these changes would then be propagated to downstream HGT recipients and most likely to be retained in recipients with ecophysiology similar to that of its own. We speculate that this is what led to the relatively mono-familial MtrCAB clades like Groups 2, 4, 5, 6, and 7; these contemporary relationships are the product of extensive HGT over long phylogenetic distances to various ancestral organisms, followed by short-distance HGT events to genetically and ecophysiologically similar species (Figure 35B), as was similarly proposed by Zhong et al. (2018)(284). This would also explain why other species in these genera lack *mtrCAB*, although as mentioned above in the case of *Shewanella* spp., as well as the Ferrimonadaceae, it is still possible for *mtrCAB* to be vertically transmitted, then secondarily lost in some lineages (Figure 33A).

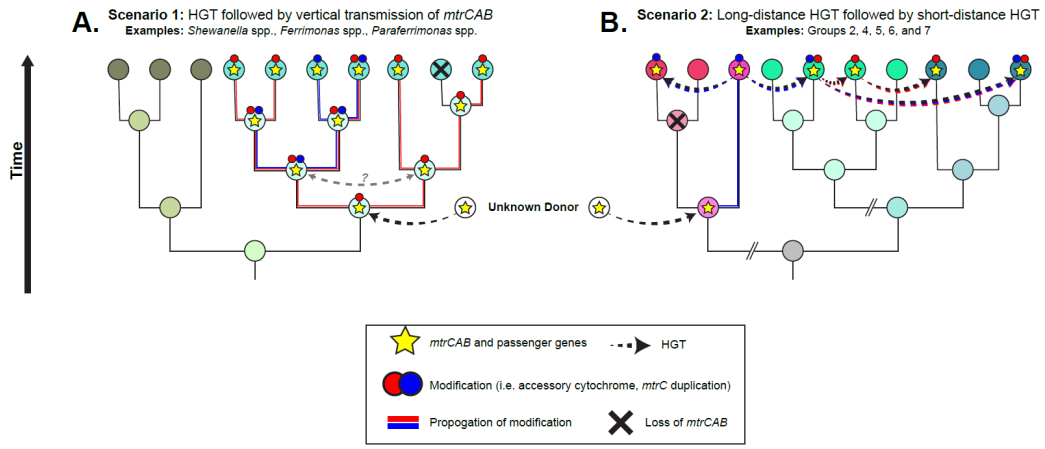

Figure 36. A hypothetical model representing two possible modes of *mtrCAB*'s dissemination to the species identified in our study.

Revisiting the modularity of MtrCAB

The data here provide insights into the diversification and thus potential adaptation of genes in the *mtr* gene cluster. Our analyses show that the core MtrAB module (Figures 26, 27) is relatively conserved, while the systems that support them (MtrC and accessory cytochromes) seem to vary (Figures 25, 31, 33). In contrast to the MtrC tree (Figure 25), the individual protein trees for MtrA (Figure 26) and MtrB (Figure 27) rarely deviate from the topology and clade assignments in the MtrCAB tree (Figure 24). This may be because the evolutionary trajectories of MtrA and MtrB are inextricably linked through molecular structure – any substantial change in one would break the entire MtrAB association without a parallel, compatible change in the other (43, 305). Conversely, because the majority of MtrC is relegated to the extracellular space and the only structural demands in relation to MtrAB are placement in the outer membrane and co-localization with MtrAB, MtrC may have more flexibility in its sequence and structure evolution. Indeed, this may be corollary to the diverse functionality of MtrC in reducing a wide range of substrates, while MtrAB functions as an electron delivery system to MtrC.

This underscores the modularity of this system; MtrAB may be a core system that can be modified and adapted through the diversification and addition of MtrC

homologs and other novel cytochromes. That said, our data on *mtrCAB*'s ubiquity, diversity, and the patterns that lay therein begs the question of how these various changes to the MtrAB ancillary system translate to function. Do these represent specialized components that operate optimally under different conditions? How do they affect the availability and nature of different extracellular electron acceptors and variations in their redox potential, crystallinity, and solubility? Accordingly, we can turn to the research on *S. oneidensis* MR-1 and other *Shewanella* spp., which have been studied in the lab for decades.

Previous studies differentiating MtrCAB, MtrDEF, and MtrC family proteins allows us to explore the relationship between modularity, evolution, and the associated physiology of these gene products as they function in Mtr-facilitated EET. OmcA, UndA, MtrG, and MtrH are not predicted to form a complex with MtrAB homologs (354), but instead are thought to be reduced extracellularly by MtrC or MtrF anchored in their respective outer membrane conduits. The functional role of these unanchored extracellular cytochromes in metal reduction may be accessory, as *Shewanella* spp. mutants lacking only *omcA* or *undA* are still capable of EET (361) and these genes are transcribed from promoters separate from *mtrCAB* and *mtrDEF* (351). Genetic and biophysical analysis suggests substrate specificity could be an accessory function for these proteins (45). OmcA, for example, is thought to enhance adherement to solid substrates like electrodes (45, 376), hematite (357, 377), and goethite (378), while UndA may specialize in facilitating electron transfer to soluble substrates like ligand-bound Fe^{3+} (43, 361). MtrCAB and MtrDEF may be adapted to different conditions as well, as MtrCAB is preferentially expressed under iron-limited or O_2-limited conditions, while MtrDEF prevails under iron-replete conditions or when cells are aggregated (379–381).

Revisiting our domain-wide data through the same lens of diversification and adaptation submits that the modular deviations from the core *mtrCAB* model could similarly represent condition specific adaptations. These questions and principles extend beyond MtrCAB to other systems utilizing MtrAB homologs at their core, such as DmsEF in extracellular DMSO respiration (49), PioAB in phototrophic iron oxidation (287, 289), and MtoAB implicated in chemolithoautotrophic iron oxidation (292, 295, 382). The latter two instances may lead one to think that MtrC is responsible for conferring reductive capacity to an otherwise presumably oxidatively-

inclined MtrAB/MtoAB/PioAB core, especially because MtoA/PioA and MtoB/PioB do not form a separate “function-specific” clade on the individual MtrA and MtrB trees but instead group with MtrA and MtrB homologs belonging to complete MtrCAB modules (Figures 25, 26). Similarly, the distribution of known FeOB-associated and FeRB-associated proteins genomically adjacent to MtrCAB (Figure 31) and MtoAB (290, 295, 334) may hint at a possible evolutionary model for the functional diversification of Mtr as an oxidizing or reducing system. However, laboratory experiments have shown that MtrCAB of *S. oneidensis* MR-1 can be coerced to transmit electrons in the opposite direction of its traditional anodic ways (312, 383). In parallel, Bücking et al. (2012) showed that point mutations in MtrA and MtrB can rescue iron-reducing capability in an *S. oneidensis* mutant devoid of outer membrane cytochromes (384). Thus, even with our expanded catalog of MtrCAB and the changes that have accompanied it throughout its distribution to different lineages, we still lack sufficient functional data to inform the physiological capacity conveyed by these changes. We encourage future studies to focus on assessing whether electron flow directionality is a consequence of machinery, metabolism, environmental chemistry, or a combination of all.

A unifying quest in the field of geobiology is to understand the co-evolution of life and Earth, and our findings further signify the importance of this pursuit. In light of the central role that known EET-capable organisms such as *Shewanella*, *Geobacter*, *Desulfuromonas*, and *Rhodopseudomonas* spp. play in key elemental cycles such as iron, sulfur, manganese, and carbon cycling (280, 385, 386), it is appropriate to consider whether this vast diversity of taxa that the MtrCAB system play a comparable role to the aforementioned microorganisms. At the moment, we do not know how the newly identified microorganisms use the Mtr system, nor do we know what role the environment has played in the diversification of MtrCAB and its associated machinery, nor under what conditions these adaptations have arisen. Many of the organisms identified in our study live at the oxic-anoxic interface where they are faced with fluctuating oxygen concentrations and consequent changes in mineral solubility and redox potential. Mtr-linked EET may serve as an adaptation that permit r-selected strategists to persist in these types of habitats. Furthermore, we know that the global supply of Fe (II), Fe (III), and O_2 have changed dramatically over the past 4 billion years, and, prior to the rise of O_2, Fe (II) was possibly one of the most important electron donors for anoxygenic photosynthesis (265, 269, 387–389). Should these adaptations in MtrCAB reflect changes in the environment like shifts in redox chemistry,

understanding the timing of their emergence may shine light on major biogeochemical transitions in Earth history and address the first-order question of whether they can even be implicated in the ancient biogeochemical cycles that transformed Earth's surface and habitability.

Table 5. MtrCAB encoding species identified with references and descriptions.

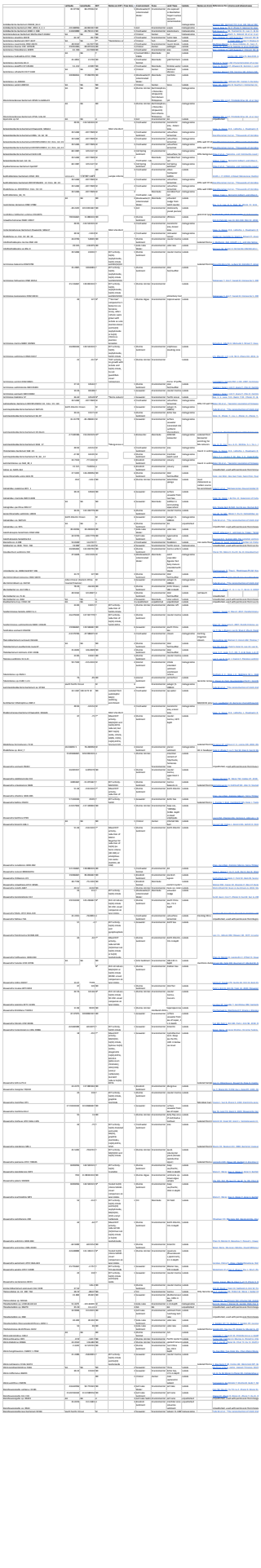

Table 6. Phylogenies of *mtrCAB* encoding strains and their prevalence among the corresponding genera

Phylum	Class	Order	Family	Genus	Available Assemblies	Number with MtrCAB
Proteobacteria	Betaproteobacteria	Burkholderiales	Burkholderiaceae	Limnobacter	20	1
			Comamonadaceae	Ramlibacter	16	1
				Aquincola	4	1
				Albidoferax/Rhodoferax	45	4
				Caenimonas	4	1
				nclassified Comamonadacea	NA	1
				Ideonella	8	1
				Polaromonas	46	2
				Ramlibacter	21	1
			Unclassified Burkholderiales		NA	3
		odocycla	Rhodocyclaceae	Niveibacterium	1	1
				Unclassified Rhodocyclaceae	NA	1
		adales/G	Unclassified Gallionellales		30	1
		Unclassified Betaproteobacteria			NA	5
	Gammaproteobacteria	omonad	Aeromonadaceae	nclassified Aeromonadacea	NA	1
				Aeromonas	68	11
		Alteromonadales	lteromonadacea	Marinobacter	151	3
				nclassified Alteromonadace	NA	2
			Ferrimonadaceae	Ferrimonas	9	9
				Paraferrimonas	3	2
			Shewanellaceae	Shewanella	45	40
			Colwelliaceae	Colwellia	50	1
				Thalassotalea	12	2
		Cellvibrionales	Halieaceae	Haliea	15	1
				alioglobus/Seongchinamell	12	5
				Kineobactrum	2	1
				Parahaliea	2	1
			Cellvibrionaceae	Marinimicrobium	4	2
		Chromatiales	othiorhodospirac	Ectothiorhodospira	7	2
				Halorhodospira	7	2
				Thioalkalivibrio	111	4
				Thiohalomonas	1	1
			nzhouxiangellac	Wenzhouxiangella	22	4
				assified Wenzhouxiangella	NA	1
		ievskiale	Sinobacteraceae	Sinimarinibacterium	3	1
		anospiril	Alcanivoracaceae	Ketobacter	7	1
			Kangiellaceae	Pleionea	2	1
		Unclassified Gammaproteobacteria			NA	7
		ibrionale	Vibrionaceae	Photobacterium	41	2
				Vibrio	120	8
	proteoba	obacter	Caulobacteraceae	Phenylobacterium	28	1
	Unclassified Acidobacteriia				NA	3
dobact	dobacte	obactera	Bryobacteraceae	Unclassified Bryobacteracea	NA	1
				Candidatus Solibacter	8	1
atimon	atimona	aatimona	mmatimonadace	Gemmatimonas	21	1
						146

Bibliography

1. Beblawy S, Bursac T, Paquete C, Louro R, Clarke TA, Gescher J. 2018. Extracellular reduction of solid electron acceptors by *Shewanella oneidensis*. Mol Microbiol 109:571–583.

2. Reguera G, Kashefi K. 2019. The electrifying physiology of *Geobacter* bacteria, 30 years on. Adv Microb Physiol 74:1–96.

3. Logan BE, Rossi R, Ragab A, Saikaly PE. 2019. Electroactive microorganisms in bioelectrochemical systems. Nat Rev Microbiol 17:307–319.

4. Koch C, Harnisch F. 2016. Is there a Specific Ecological Niche for Electroactive Microorganisms? ChemElectroChem 3:1282–1295.

5. Sayed ET, Tsujiguchi T, Nakagawa N. 2012. Catalytic activity of baker's yeast in a mediatorless microbial fuel cell. Bioelectrochemistry 86:97–101.

6. Logan BE. 2012. Essential Data and Techniques for Conducting Microbial Fuel Cell and other Types of Bioelectrochemical System Experiments. ChemSusChem 5:988–994.

7. Light SH, Su L, Rivera-Lugo R, Cornejo JA, Louie A, Iavarone AT, Ajo-Franklin CM, Portnoy DA. 2018. A flavin-based extracellular electron transfer mechanism in diverse Gram-positive bacteria. Nature 562:140–144.

8. McAllister SM, Moore RM, Gartman A, Luther GW, Emerson D, Chan CS. 2019. The Fe(II)-oxidizing *Zetaproteobacteria* : historical, ecological and genomic perspectives. FEMS Microbiol Ecol 95.

9. Zavarzina DG, Sokolova TG, Tourova TP, Chernyh NA, Kostrikina NA, Bonch-Osmolovskaya EA. 2007. *Thermincola ferriacetica* sp. nov., a new anaerobic, thermophilic, facultatively chemolithoautotrophic bacterium capable of dissimilatory Fe(III) reduction. Extremophiles 11:1–7.

10. Renslow RS, Babauta JT, Dohnalkova AC, Boyanov MI, Kemner KM, Majors PD, Fredrickson JK, Beyenal H. 2013. Metabolic spatial variability in electrode-respiring *Geobacter sulfurreducens* biofilms. Energy Environ Sci 6:1827.

11. Michelson K, Alcalde RE, Sanford RA, Valocchi AJ, Werth CJ. 2019. Diffusion-based recycling of flavins allows *Shewanella oneidensis* MR-1 to yield energy from metal reduction across physical separations. Environ Sci Technol 53:3480–3487.

12. Torres CI, Kato Marcus A, Rittmann BE. 2008. Proton transport inside the biofilm limits electrical current generation by anode-respiring bacteria. Biotechnol Bioeng 100:872–881.

13. Erben J, Pinder ZA, Lüdtke MS, Kerzenmacher S. 2021. Local acidification limits the current production and biofilm formation of *Shewanella oneidensis* MR-1 with electrospun anodes. Front Microbiol 12:660474.

14. Chadwick GL, Jiménez Otero F, Gralnick JA, Bond DR, Orphan VJ. 2019. NanoSIMS imaging reveals metabolic stratification within current-producing biofilms. Proc Natl Acad Sci 116:20716–20724.

15. Kees ED, Levar CE, Miller SP, Bond DR, Gralnick JA, Dean AM. 2021. Survival of the first rather than the fittest in a *Shewanella* electrode biofilm. Commun Biol 4:536.

16. Thormann KM, Saville RM, Shukla S, Spormann AM. 2005. Induction of rapid detachment in *Shewanella oneidensis* MR-1 biofilms. J Bacteriol 187:1014–1021.

17. Joshi K, Kane AL, Kotloski NJ, Gralnick JA, Bond DR. 2019. Preventing hydrogen disposal increases electrode utilization efficiency by *Shewanella oneidensis*. Front Energy Res 7:95.

18. Levar CE, Hoffman CL, Dunshee AJ, Toner BM, Bond DR. 2017. Redox potential as a master variable controlling pathways of metal reduction by *Geobacter sulfurreducens*. ISME J 11:741–752.

19. Huang B, Gao S, Xu Z, He H, Pan X. 2018. The functional mechanisms and application of electron shuttles in extracellular electron transfer. Curr Microbiol 75:99–106.

20. Glasser NR, Saunders SH, Newman DK. 2017. The colorful world of extracellular electron shuttles. Annu Rev Microbiol 71:731–751.

21. Doyle LE, Yung PY, Mitra SD, Wuertz S, Williams RBH, Lauro FM, Marsili E. 2017. Electrochemical and genomic analysis of novel electroactive isolates obtained via potentiostatic enrichment from tropical sediment. J Power Sources 356:539–548.

22. Pham et al. - 2003 - A novel electrochemically active and Fe(III)-reduc.pdf.

23. Sharma SCD, Feng C, Li J, Hu A, Wang H, Qin D, Yu C-P. 2016. Electrochemical characterization of a novel exoelectrogenic bacterium strain SCS5, isolated from a mediator-less microbial fuel cell and phylogenetically related to *Aeromonas jandaei*. Microbes Environ 31:213–225.

24. Chung K, Okabe S. 2009. Characterization of electrochemical activity of a strain ISO2-3 phylogenetically related to *Aeromonas* sp. isolated from a glucose-fed microbial fuel cell. Biotechnol Bioeng 104:901–910.

25. Li S-W, He H, Zeng RJ, Sheng G-P. 2017. Chitin degradation and electricity generation by *Aeromonas hydrophila* in microbial fuel cells. Chemosphere 168:293–299.

26. Ishii S, Suzuki S, Yamanaka Y, Wu A, Nealson KH, Bretschger O. 2017. Population dynamics of electrogenic microbial communities in microbial fuel cells started with three different inoculum sources. Bioelectrochemistry 117:74–82.

27. Ishii S, Suzuki S, Norden-Krichmar TM, Phan T, Wanger G, Nealson KH, Sekiguchi Y, Gorby YA, Bretschger O. 2014. Microbial population and functional dynamics associated with surface potential and carbon metabolism. ISME J 8:963–978.

28. Knight V, Blakemore R. 1998. Reduction of diverse electron acceptors by *Aeromonas hydrophila*. Arch Microbiol 169:239–248.

29. Cao F, Liu TX, Wu CY, Li FB, Li XM, Yu HY, Tong H, Chen MJ. 2012. Enhanced biotransformation of DDTs by an iron- and humic-reducing bacteria *Aeromonas hydrophila* HS01 upon addition of Goethite and anthraquinone-2,6-disulphonic disodium salt (AQDS). J Agric Food Chem 60:11238–11244.

30. Kooli WM, Junier T, Shakya M, Monachon M, Davenport KW, Vaideeswaran K, Vernudachi A, Marozau I, Monrouzeau T, Gleasner CD, McMurry K, Lienhard R, Rufener L, Perret J-L, Sereda O, Chain PS, Joseph E, Junier P. 2019. Remedial treatment of corroded iron objects by environmental *Aeromonas* isolates. Appl Environ Microbiol 85.

31. Lam BR, Barr CR, Rowe AR, Nealson KH. 2019. Differences in applied redox potential on cathodes enrich for diverse electrochemically active microbial isolates from a marine sediment. Front Microbiol 10:1979.

32. Nivens DE, Nichols PD, Henson JM, Geesey GG, White DC. 1986. Reversible Acceleration of the Corrosion of AISI 304 Stainless Steel Exposed to Seawater Induced by Growth and Secretions of the Marine Bacterium *Vibrio Natriegens*. CORROSION 42:204–210.

33. Jones JG, Gardener S, Simon BM. 1984. Reduction of Ferric Iron by Heterotrophic Bacteria in Lake Sediments. Microbiology 130:45–51.

34. Jones JG, Gardener S, Simon BM. 1983. Bacterial Reduction of Ferric Iron in a Stratified Eutrophic Lake. Microbiology 129:131–139.

35. Jones JG, Davison W, Gardener S. 1984. Iron reduction by bacteria: range of organisms involved and metals reduced. FEMS Microbiol Lett 21:133–136.

36. Wee SK, Burns JL, DiChristina TJ. 2014. Identification of a molecular signature unique to metal-reducing *Gammaproteobacteria*. FEMS Microbiol Lett 350:90–99.

37. Woźnica A, Dzirba J, Mańka D, Łabużek S. 2003. Effects of electron transport inhibitors on iron reduction in Aeromonas hydrophila strain KB1. Anaerobe 9:125–130.

38. Lovley DR. 1987. Organic matter mineralization with the reduction of ferric iron: A review. Geomicrobiol J 5:375–399.

39. Lovley DR, Phillips EJP. 1988. Novel Mode of Microbial Energy Metabolism: Organic Carbon Oxidation Coupled to Dissimilatory Reduction of Iron or Manganese. Appl Environ Microbiol 54:1472–1480.

40. Wang Y, Kern SE, Newman DK. 2010. Endogenous Phenazine Antibiotics Promote Anaerobic Survival of Pseudomonas aeruginosa via Extracellular Electron Transfer. J Bacteriol 192:365–369.

41. Beblawy S, Bursac T, Paquete C, Louro R, Clarke TA, Gescher J. 2018. Extracellular reduction of solid electron acceptors by *Shewanella oneidensis*. Mol Microbiol 109:571–583.

42. Edwards MJ, Richardson DJ, Paquete CM, Clarke TA. 2020. Role of multiheme cytochromes involved in extracellular anaerobic respiration in bacteria. Protein Sci 29:830–842.

43. Edwards MJ, White GF, Butt JN, Richardson DJ, Clarke TA. 2020. The Crystal Structure of a Biological Insulated Transmembrane Molecular Wire. Cell 181:665-673.e10.

44. Shi L, Rosso KM, Zachara JM, Fredrickson JK. 2012. Mtr extracellular electron-transfer pathways in Fe(III)-reducing or Fe(II)-oxidizing bacteria: a genomic perspective. Biochem Soc Trans 40:1261–1267.

45. Coursolle D, Gralnick JA. 2010. Modularity of the Mtr respiratory pathway of *Shewanella oneidensis* strain MR-1. Mol Microbiol no-no.

46. Sturm G, Richter K, Doetsch A, Heide H, Louro RO, Gescher J. 2015. A dynamic periplasmic electron transfer network enables respiratory flexibility beyond a thermodynamic regulatory regime. ISME J 9:1802–1811.

47. Alves MN, Neto SE, Alves AS, Fonseca BM, Carrêlo A, Pacheco I, Paquete CM, Soares CM, Louro RO. 2015. Characterization of the periplasmic redox network that sustains the versatile anaerobic metabolism of *Shewanella oneidensis* MR-1. Front Microbiol 6.

48. Delgado VP, Paquete CM, Sturm G, Gescher J. 2019. Improvement of the electron transfer rate in *Shewanella oneidensis* MR-1 using a tailored periplasmic protein composition. Bioelectrochemistry 129:18–25.

49. Gralnick JA, Vali H, Lies DP, Newman DK. 2006. Extracellular respiration of dimethyl sulfoxide by *Shewanella oneidensis* strain MR-1. Proc Natl Acad Sci 103:4669–4674.

50. Mestre M, Höfer J. 2021. The Microbial Conveyor Belt: Connecting the Globe through Dispersion and Dormancy. Trends Microbiol 29:482–492.

51. Greening C, Grinter R, Chiri E. 2019. Uncovering the Metabolic Strategies of the Dormant Microbial Majority: towards Integrative Approaches. mSystems 4.

52. Pinto D, Santos MA, Chambel L. 2015. Thirty years of viable but nonculturable state research: Unsolved molecular mechanisms. Crit Rev Microbiol 41:61–76.

53. Kees ED, Pendleton AR, Paquete CM, Arriola MB, Kane AL, Kotloski NJ, Intile PJ, Gralnick JA. 2019. Secreted Flavin Cofactors for Anaerobic Respiration of

Fumarate and Urocanate by *Shewanella oneidensis*: Cost and Role. Appl Environ Microbiol 85.

54. Liu D-F, Li W-W. 2020. Potential-dependent extracellular electron transfer pathways of exoelectrogens. Curr Opin Chem Biol 59:140–146.

55. Levar CE, Chan CH, Mehta-Kolte MG, Bond DR. 2014. An Inner Membrane Cytochrome Required Only for Reduction of High Redox Potential Extracellular Electron Acceptors. mBio 5:e02034-14.

56. Myers CR, Myers JM. 1993. Role of menaquinone in the reduction of fumarate, nitrate, iron(III) and manganese(IV) by *Shewanella putrefaciens* MR-1. FEMS Microbiol Lett 114:215–222.

57. McMillan DGG, Marritt SJ, Butt JN, Jeuken LJC. 2012. Menaquinone-7 Is Specific Cofactor in Tetraheme Quinol Dehydrogenase CymA. J Biol Chem 287:14215–14225.

58. Hirose A, Kasai T, Aoki M, Umemura T, Watanabe K, Kouzuma A. 2018. Electrochemically active bacteria sense electrode potentials for regulating catabolic pathways. Nat Commun 9:1083.

59. Hirose A, Kouzuma A, Watanabe K. 2021. Hydrogen-dependent current generation and energy conservation by *Shewanella oneidensis* MR-1 in bioelectrochemical systems. J Biosci Bioeng 131:27–32.

60. Stairs CW, Eme L, Muñoz-Gómez SA, Cohen A, Dellaire G, Shepherd JN, Fawcett JP, Roger AJ. 2018. Microbial eukaryotes have adapted to hypoxia by horizontal acquisitions of a gene involved in rhodoquinone biosynthesis. eLife 7:e34292.

61. Anand A, Chen K, Yang L, Sastry AV, Olson CA, Poudel S, Seif Y, Hefner Y, Phaneuf PV, Xu S, Szubin R, Feist AM, Palsson BO. 2019. Adaptive evolution reveals a tradeoff between growth rate and oxidative stress during naphthoquinone-based aerobic respiration. Proc Natl Acad Sci 116:25287–25292.

62. Johnston JM, Bulloch EM. 2020. Advances in menaquinone biosynthesis: sublocalisation and allosteric regulation. Curr Opin Struct Biol 65:33–41.

63. Fredrickson JK, Romine MF, Beliaev AS, Auchtung JM, Driscoll ME, Gardner TS, Nealson KH, Osterman AL, Pinchuk G, Reed JL, Rodionov DA, Rodrigues JLM, Saffarini DA, Serres MH, Spormann AM, Zhulin IB, Tiedje JM. 2008. Towards environmental systems biology of *Shewanella*. Nat Rev Microbiol 6:592–603.

64. Lemaire ON, Méjean V, Iobbi-Nivol C. 2020. The *Shewanella* genus: ubiquitous organisms sustaining and preserving aquatic ecosystems. FEMS Microbiol Rev 44:155–170.

65. Knight V, Caccavo F, Wudyka S, Blakemore R. 1996. Synergistic iron reduction and citrate dissimilation by *Shewanella alga* and *Aeromonas veronii*. Arch Microbiol 166:269–274.

66. Zago V, Veschetti L, Patuzzo C, Malerba G, Lleo MM. 2020. Resistome, Mobilome and Virulome Analysis of *Shewanella algae* and *Vibrio* spp. Strains Isolated in Italian Aquaculture Centers. Microorganisms 8:572.

67. Loftie-Eaton W, Crabtree A, Perry D, Millstein J, Baytosh J, Stalder T, Robison BD, Forney LJ, Top EM. 2021. Contagious Antibiotic Resistance: Plasmid Transfer among Bacterial Residents of the Zebrafish Gut. Appl Environ Microbiol 87:15.

68. Paulick A, Koerdt A, Lassak J, Huntley S, Wilms I, Narberhaus F, Thormann KM. 2009. Two different stator systems drive a single polar flagellum in *Shewanella oneidensis* MR-1. Mol Microbiol 71:836–850.

69. Huys G. 2014. The Family Aeromonadaceae, p. 27–57. *In* Rosenberg, E, DeLong, EF, Lory, S, Stackebrandt, E, Thompson, F (eds.), The Prokaryotes. Springer Berlin Heidelberg, Berlin, Heidelberg.

70. Gomez-Gil et al. - 2014 - The Famlily Vibrionaceae.pdf.

71. Girguis P. 2016. Microbial ecology: Here, there and everywhere. Nat Microbiol 1:16123.

72. Gomez-Gil B, Thompson CC, Matsumura Y, Sawabe T, Iida T, Christen R, Thompson F, Sawabe T. 2014. The Famlily Vibrionaceae, p. 659–747. *In* Rosenberg, E, DeLong, EF, Lory, S, Stackebrandt, E, Thompson, F (eds.), The Prokaryotes. Springer Berlin Heidelberg, Berlin, Heidelberg.

73. Pérez-Brocal V, Latorre A, Moya A. 2011. Symbionts and Pathogens: What is the Difference?, p. 215–243. *In* Dobrindt, U, Hacker, JH, Svanborg, C (eds.), Between Pathogenicity and Commensalism. Springer Berlin Heidelberg, Berlin, Heidelberg.

74. Diner RE, Kaul D, Rabines A, Zheng H, Steele JA, Griffith JF, Allen AE. 2021. Pathogenic *Vibrio* Species Are Associated with Distinct Environmental Niches and Planktonic Taxa in Southern California (USA) Aquatic Microbiomes. mSystems https://doi.org/10.1128/mSystems.00571-21.

75. Takemura AF, Chien DM, Polz MF. 2014. Associations and dynamics of Vibrionaceae in the environment, from the genus to the population level. Front Microbiol 5.

76. Visick KL, Stabb EV, Ruby EG. 2021. A lasting symbiosis: how *Vibrio fischeri* finds a squid partner and persists within its natural host. Nat Rev Microbiol https://doi.org/10.1038/s41579-021-00557-0.

77. Diner et al. - 2021 - Pathogenic Vibrio Species Are Associated wi.pdf.

78. Richardson DJ. Bacterial respiration : a flexible process for a changing environment 21.

79. Bueno E, Pinedo V, Cava F. 2020. Adaptation of *Vibrio cholerae* to hypoxic environments. Front Microbiol 11:739.

80. Proctor LM, Gunsalus RP. 2000. Anaerobic respiratory growth of Vibrio harveyi, Vibrio fischeri and Photobacterium leiognathi with trimethylamine N-oxide, nitrate and fumarate: ecological implications. Environ Microbiol 2:399–406.

81. Kado T, Kashimoto T, Yamazaki K, Ueno S. 2017. Importance of fumarate and nitrate reduction regulatory protein for intestinal proliferation of *Vibrio vulnificus*. FEMS Microbiol Lett 364:fnw274.

82. Kaila VRI, Wikström M. 2021. Architecture of bacterial respiratory chains. Nat Rev Microbiol 19:319–330.

83. Fenchel T, Finlay B. 2008. Oxygen and the Spatial Structure of Microbial Communities. Biol Rev https://doi.org/10.1111/j.1469-185X.2008.00054.x.

84. Brune A. 2000. Life at the oxic–anoxic interface: microbial activities and adaptations. FEMS Microbiol Rev 24:691–710.

85. Blaut M. 2011. Ecology and Physiology of the Intestinal Tract, p. 247–272. *In* Dobrindt, U, Hacker, JH, Svanborg, C (eds.), Between Pathogenicity and Commensalism. Springer Berlin Heidelberg, Berlin, Heidelberg.

86. Steinsiek S, Stagge S, Bettenbrock K. 2014. Analysis of Escherichia coli Mutants with a Linear Respiratory Chain. PLoS ONE 9:e87307.

87. Gunsalus RP, Park S-J. 1994. Aerobic-anaerobic gene regulation in Escherichia coli: control by the ArcAB and Fnr regulons. Res Microbiol 145:437–450.

88. Chen K, Anand A, Olson C, Sandberg TE, Gao Y, Mih N, Palsson BO. 2021. Bacterial fitness landscapes stratify based on proteome allocation associated with discrete aero-types. PLOS Comput Biol 17:e1008596.

89. Bueno E, Sit B, Waldor MK, Cava F. 2020. Genetic Dissection of the Fermentative and Respiratory Contributions Supporting Vibrio cholerae Hypoxic Growth. J Bacteriol 202.

90. Conley BE, Weinstock MT, Bond DR, Gralnick JA. 2020. A Hybrid Extracellular Electron Transfer Pathway Enhances the Survival of *Vibrio natriegens*. Appl Environ Microbiol 86:e01253-20, /aem/86/19/AEM.01253-20.atom.

91. Journal of Bacteriology-1962-Eagon-736.full.pdf.

92. Spring S, Scheuner C, Göker M, Klenk H-P. 2015. A taxonomic framework for emerging groups of ecologically important marine gammaproteobacteria based on

the reconstruction of evolutionary relationships using genome-scale data. Front Microbiol 6.

93. Albalat R, Cañestro C. 2016. Evolution by gene loss. Nat Rev Genet 17:379–391.

94. de Groot DH, van Boxtel C, Planqué R, Bruggeman FJ, Teusink B. 2019. The number of active metabolic pathways is bounded by the number of cellular constraints at maximal metabolic rates. PLOS Comput Biol 15:e1006858.

95. Wang Z, O'Shaughnessy TJ, Soto CM, Rahbar AM, Robertson KL, Lebedev N, Vora GJ. 2012. Function and Regulation of Vibrio campbellii Proteorhodopsin: Acquired Phototrophy in a Classical Organoheterotroph. PLoS ONE 7:e38749.

96. Le Roux F, Blokesch M. 2018. Eco-evolutionary Dynamics Linked to Horizontal Gene Transfer in Vibrios. Annu Rev Microbiol 72:89–110.

97. Martin WF, Sousa FL. 2016. Early Microbial Evolution: The Age of Anaerobes. Cold Spring Harb Perspect Biol 8:a018127.

98. Ligrone R. 2019. The Great Oxygenation Event, p. 129–154. *In* Biological Innovations that Built the World. Springer International Publishing, Cham.

99. Knoll AH, Nowak MA. 2017. The timetable of evolution. Sci Adv 3:e1603076.

100. Lin W, Paterson GA, Zhu Q, Wang Y, Kopylova E, Li Y, Knight R, Bazylinski DA, Zhu R, Kirschvink JL, Pan Y. 2017. Origin of microbial biomineralization and magnetotaxis during the Archean. Proc Natl Acad Sci 114:2171–2176.

101. Osborne CD, Haritos VS. 2018. Horizontal gene transfer of three co-inherited methane monooxygenase systems gave rise to methanotrophy in the Proteobacteria. Mol Phylogenet Evol 129:171–181.

102. Mus F, Colman DR, Peters JW, Boyd ES. 2019. Geobiological feedbacks, oxygen, and the evolution of nitrogenase. Free Radic Biol Med 140:250–259.

103. Tao Q, Tamura K, Kumar S. 2020. Efficient Methods for Dating Evolutionary Divergences, p. 197–219. *In* Ho, SYW (ed.), The Molecular Evolutionary Clock. Springer International Publishing, Cham.

104. Marin J, Battistuzzi FU, Brown AC, Hedges SB. 2016. The Timetree of Prokaryotes: New Insights into Their Evolution and Speciation. Mol Biol Evol msw245.

105. Waite DW, Vanwonterghem I, Rinke C, Parks DH, Zhang Y, Takai K, Sievert SM, Simon J, Campbell BJ, Hanson TE, Woyke T, Klotz MG, Hugenholtz P. 2017. Comparative Genomic Analysis of the Class Epsilonproteobacteria and Proposed Reclassification to Epsilonbacteraeota (phyl. nov.). Front Microbiol 8:682.

106. Waite DW, Chuvochina M, Pelikan C, Parks DH, Yilmaz P, Wagner M, Loy A, Naganuma T, Nakai R, Whitman WB, Hahn MW, Kuever J, Hugenholtz P. 2020. Proposal to reclassify the proteobacterial classes Deltaproteobacteria and Oligoflexia, and the phylum Thermodesulfobacteria into four phyla reflecting major functional capabilities. Int J Syst Evol Microbiol 70:5972–6016.

107. Sheridan PP, Freeman KH, Brenchley JE. 2003. Estimated Minimal Divergence Times of the Major Bacterial and Archaeal Phyla. Geomicrobiol J 20:1–14.

108. Battistuzzi FU, Feijao A, Hedges SB. 2004. A genomic timescale of prokaryote evolution: insights into the origin of methanogenesis, phototrophy, and the colonization of land. BMC Evol Biol 4:44.

109. Wang S, Luo H. 2021. Dating Alphaproteobacteria evolution with eukaryotic fossils. Nat Commun 12:3324.

110. Degli Esposti M, Mentel M, Martin W, Sousa FL. 2019. Oxygen Reductases in Alphaproteobacterial Genomes: Physiological Evolution From Low to High Oxygen Environments. Front Microbiol 10:499.

111. Retchless AC, Lawrence JG. 2007. Temporal Fragmentation of Speciation in Bacteria. Science 317:1093–1096.

112. Lorén JG, Farfán M, Fusté MC. 2018. Species Delimitation, Phylogenetic Relationships, and Temporal Divergence Model in the Genus Aeromonas. Front Microbiol 9:770.

113. Gruen DS, Wolfe JM, Fournier GP. 2019. Paleozoic diversification of terrestrial chitin-degrading bacterial lineages. BMC Evol Biol 19:34.

114. Martin RE, Servais T. 2020. Did the evolution of the phytoplankton fuel the diversification of the marine biosphere? Lethaia 53:5–31.

115. Shi L, Dong H, Reguera G, Beyenal H, Lu A, Liu J, Yu H-Q, Fredrickson JK. 2016. Extracellular electron transfer mechanisms between microorganisms and minerals. Nat Rev Microbiol 14:651–662.

116. Gralnick JA, Newman DK. 2007. Extracellular respiration. Mol Microbiol 65:1–11.

117. Bird LJ, Bonnefoy V, Newman DK. 2011. Bioenergetic challenges of microbial iron metabolisms. Trends Microbiol 19:330–340.

118. Weber KA, Achenbach LA, Coates JD. 2006. Microorganisms pumping iron: anaerobic microbial iron oxidation and reduction. Nat Rev Microbiol 4:752–764.

119. Brutinel ED, Gralnick JA. 2012. Shuttling happens: soluble flavin mediators of extracellular electron transfer in *Shewanella*. Appl Microbiol Biotechnol 93:41–48.

120. Shi L, Richardson DJ, Wang Z, Kerisit SN, Rosso KM, Zachara JM, Fredrickson JK. 2009. The roles of outer membrane cytochromes of *Shewanella* and *Geobacter* in extracellular electron transfer. Environ Microbiol Rep 1:220–227.

121. Lovley DR, Holmes DE, Nevin KP. 2004. Dissimilatory Fe(III) and Mn(IV) reduction. Adv Microb Physiol 49:221–286.

122. Marritt SJ, Lowe TG, Bye J, McMillan DGG, Shi L, Fredrickson J, Zachara J, Richardson DJ, Cheesman MR, Jeuken LJC, Butt JN. 2012. A functional description of CymA, an electron-transfer hub supporting anaerobic respiratory flexibility in *Shewanella*. Biochem J 444:465–474.

123. Myers JM, Myers CR. 2000. Role of the tetraheme cytochrome CymA in anaerobic electron transport in cells of *Shewanella putrefaciens* MR-1 with normal levels of menaquinone. J Bacteriol 182:67–75.

124. Leys D, Meyer TE, Tsapin AS, Nealson KH, Cusanovich MA, Van Beeumen JJ. 2002. Crystal structures at atomic resolution reveal the novel concept of “electron-harvesting” as a role for the small tetraheme cytochrome *c*. J Biol Chem 277:35703–35711.

125. Sturm G, Richter K, Doetsch A, Heide H, Louro RO, Gescher J. 2015. A dynamic periplasmic electron transfer network enables respiratory flexibility beyond a thermodynamic regulatory regime. ISME J 9:1802–1811.

126. Leys D, Tsapin AS, Nealson KH, Meyer TE, Cusanovich MA, Van Beeumen JJ. 1999. Structure and mechanism of the flavocytochrome *c* fumarate reductase of *Shewanella putrefaciens* MR-1. Nat Struct Biol 6:1113–1117.

127. Hartshorne RS, Reardon CL, Ross D, Nuester J, Clarke TA, Gates AJ, Mills PC, Fredrickson JK, Zachara JM, Shi L, Beliaev AS, Marshall MJ, Tien M, Brantley S, Butt JN, Richardson DJ. 2009. Characterization of an electron conduit between bacteria and the extracellular environment. Proc Natl Acad Sci 106:22169–22174.

128. Ross DE, Ruebush SS, Brantley SL, Hartshorne RS, Clarke TA, Richardson DJ, Tien M. 2007. Characterization of protein-protein interactions involved in iron reduction by *Shewanella oneidensis* MR-1. Appl Environ Microbiol 73:5797–5808.

129. Edwards MJ, White GF, Lockwood CW, Lawes M, Martel A, Harris G, Scott DJ, Richardson D, Butt JN, Clarke TA. 2018. Structural model of a porin-cytochrome electron conduit from the outer membrane of a metal reducing bacterium suggests electron transfer via periplasmic redox partners. J Biol Chem 293:8103–8112.

130. Von Canstein H, Ogawa J, Shimizu S, Lloyd JR. 2008. Secretion of flavins by *Shewanella* species and their role in extracellular electron transfer. Appl Environ Microbiol 74:615–623.

131. Marsili E, Baron DB, Shikhare ID, Coursolle D, Gralnick JA, Bond DR. 2008. *Shewanella* secretes flavins that mediate extracellular electron transfer. Proc Natl Acad Sci U S A 105:3968–3973.

132. Edwards MJ, White GF, Norman M, Tome-Fernandez A, Ainsworth E, Shi L, Fredrickson JK, Zachara JM, Butt JN, Richardson DJ, Clarke TA. 2015. Redox linked flavin sites in extracellular decaheme proteins involved in microbe-mineral electron transfer. Sci Rep 5:11677.

133. Okamoto A, Hashimoto K, Nealson KH, Nakamura R. 2013. Rate enhancement of bacterial extracellular electron transport involves bound flavin semiquinones. Proc Natl Acad Sci 110:7856–7861.

134. Levar CE, Chan CH, Mehta-Kolte MiG, Bond DR. 2014. An inner membrane cytochrome required only for reduction of high redox potential extracellular electron acceptors. mBio 5:02034–14.

135. Levar CE, Hoffman CL, Dunshee AJ, Toner BM, Bond DR. 2016. Redox potential as a master variable controlling pathways of metal reduction by *Geobacter sulfurreducens*. ISME J 11:741–752.

136. Zacharoff L, Chan CH, Bond DR. 2016. Reduction of low potential electron acceptors requires the CbcL inner membrane cytochrome of *Geobacter sulfurreducens*. Bioelectrochemistry 107:7–13.

137. Lloyd JR, Leang C, Myerson ALH, Coppi M V., Cuifo S, Methe B, Sandler SJ, Lovely DR. 2003. Biochemical and genetic characterization of PpcA, a periplasmic *c*-type cytochrome in *Geobacter sulfurreducens*. Biochem J 369:153–161.

138. Morgado L, Brulx M, Pessanha M, Londer YY, Salgueiro CA. 2010. Thermodynamic characterization of a triheme cytochrome family from *Geobacter sulfurreducens* reveals mechanistic and functional diversity. Biophys J 99:293–301.

139. Ueki T, DiDonato LN, Lovley DR. 2017. Toward establishing minimum requirements for extracellular electron transfer in *Geobacter sulfurreducens*. FEMS Microbiol Lett 364:1–7.

140. Jiménez Otero F, Chan CH, Bond DR. 2018. Identification of different putative outer membrane electron conduits necessary for Fe(III) citrate, Fe(III) oxide, Mn(IV) oxide, or electrode reduction by Geobacter sulfurreducens. J Bacteriol JB.00347-18.

141. Liu Y, Wang Z, Liu J, Levar C, Edwards MJ, Babauta JT, Kennedy DW, Shi Z, Beyenal H, Bond DR, Clarke TA, Butt JN, Richardson DJ, Rosso KM, Zachara JM, Fredrickson JK, Shi L. 2014. A trans-outer membrane porin-cytochrome protein complex for extracellular electron transfer by *Geobacter sulfurreducens* PCA. Environ Microbiol Rep 6:776–785.

142. Koch C, Harnisch F. 2016. Is there a specific ecological niche for electroactive microorganisms? ChemElectroChem 3:1282–1295.

143. Chung K, Okabe S. 2009. Characterization of electrochemical activity of a strain ISO2-3 phylogenetically related to *Aeromonas* sp. isolated from a glucose-fed microbial fuel cell. Biotechnol Bioeng 104:901–910.

144. Chandra Dev Sharma S, Feng C, Li J, Hu A, Wang H, Qin D, Yu C-P. 2016. Electrochemical characterization of a novel exoelectrogenic bacterium strain SCS5, isolated from a mediator-less microbial fuel cell and phylogenetically related to *Aeromonas jandaei*. Microbes Environ 00:1–13.

145. Knight V, Blakemore R. 1998. Reduction of diverse electron acceptors by *Aeromonas hydrophila*. Arch Microbiol 169:239–248.

146. Ishii S, Suzuki S, Norden-Krichmar TM, Phan T, Wanger G, Nealson KH, Sekiguchi Y, Gorby YA, Bretschger O. 2014. Microbial population and functional dynamics associated with surface potential and carbon metabolism. ISME J 8:963–978.

147. Ishii S, Suzuki S, Yamanaka Y, Wu A, Nealson KH, Bretschger O. 2017. Population dynamics of electrogenic microbial communities in microbial fuel cells started with three different inoculum sources. Bioelectrochemistry 117:74–82.

148. Janda JM, Abbott SL. 2010. The genus *Aeromonas*: taxonomy, pathogenicity, and infection. Clin Microbiol Rev 23:35–73.

149. Strom AR, Larsen H. 1979. Anaerobic fish spoilage by bacteria I. biochemical changes in herring extracts. J Appl Bacteriol 46:531–543.

150. Lerke P, Adams R, Farber L. 1965. Bacteriology of spoilage of fish muscle. Appl Microbiol 13:625–630.

151. Barrett, E L and Kwan HS. 1985. Bacterial reduction of trimethylamine oxide. Annu Rev Microbiol 39:131–149.

152. Macfarlane GT, Herbert RA. 1984. Dissimilatory nitrate reduction and nitrification in estuarine sediments. Microbiology 130:2301–2308.

153. Cole JA, Brown CM. 1980. Nitrite reduction to ammonia by fermentative bacteria: A short circuit in the biological nitrogen cycle. FEMS Microbiol Lett 7:65–72.

154. McLeod ES, Dawood Z, Macdonald R, Oosthuizen MC, Graf J, Steyn PL, Brözel VS. 1998. Isolation and identification of sulphite- and iron reducing, hydrogenase positive facultative anaerobes from cooling water systems. Syst Appl Microbiol 21:297–305.

155. Gray SJ. 1984. *Aeromonas hydrophila* in livestock: incidence, biochemical charactenstics and antibiotic susceptibility. J Hyg (Lond) 92:365–375.

156. Gosling PJ. 1996. *Aeromonas* species in diseases of animals, p. 121–175. *In* Austin, B. Altwegg, M., Gosling, P. J., and Joseph, SW (ed.), The genus *Aeromonas*, 1st ed. John Wiley & Sons, Ltd., Chichester, United Kingdom.

157. Coursolle D, Gralnick JA. 2010. Modularity of the Mtr respiratory pathway of *Shewanella oneidensis* strain MR-1. Mol Microbiol 77:995–1008.

158. Shi L, Rosso KM, Zachara JM, Fredrickson JK. 2012. Mtr extracellular electron-transfer pathways in Fe(III)-reducing or Fe(II)-oxidizing bacteria: a genomic perspective. Biochem Soc Trans 40:1261–1267.

159. Lovley DR, Fraga JL, Blunt-Harris EL, Hayes LA, Phillips EJP, Coates JD. 1998. Humic substances as a mediator for microbially catalyzed metal reduction. Acta Hydrochim Hydrobiol 26:152–157.

160. Kelly L, Mezulis S, Yates CM, Wass MN, Sternberg MJ. 2015. The Phyre2 web portal for protein modelling, prediction, and analysis. Nat Protoc 10:845–858.

161. Edwards MJ, Baiden NA, Johs A, Tomanicek SJ, Liang L, Shi L, Fredrickson JK, Zachara JM, Gates AJ, Butt JN, Richardson DJ, Clarke TA. 2014. The X-ray crystal structure of *Shewanella oneidensis* OmcA reveals new insight at the microbe-mineral interface. FEBS Lett 588:1886–1890.

162. Edwards MJ, Hall A, Shi L, Fredrickson JK, Zachara JM, Butt JN, Richardson DJ, Clarke TA. 2012. The crystal structure of the extracellular 11-heme cytochrome

UndA reveals a conserved 10-heme motif and defined binding site for soluble iron chelates. Structure 20:1275–1284.

163. Clarke TA, Edwards MJ, Gates AJ, Hall A, White GF, Bradley J, Reardon CL, Shi L, Beliaev AS, Marshall MJ, Wang Z, Watmough NJ, Fredrickson JK, Zachara JM, Butt JN, Richardson DJ. 2011. Structure of a bacterial cell surface decaheme electron conduit. Proc Natl Acad Sci U S A 108:9384–9.

164. Coursolle D, Gralnick JA. 2012. Reconstruction of extracellular respiratory pathways for iron(III) reduction in *Shewanella oneidensis* strain MR-1. Front Microbiol 3:1–11.

165. Simon J, Kroneck PMH. 2014. The production of ammonia by multiheme ctochromes *c*, p. 211–236. *In* Metal Ions in Life Sciences 14.

166. Eaves DJ, Grove J, Staudenmann W, James P, Poole RK, White SA, Griffiths I, Cole JA. 1998. Involvement of products of the *nrfEFG* genes in the covalent attachment of haem *c* to a novel cysteine-lysine motif in the cytochrome *c*552 nitrite reductase from *Escherichia coli*. Mol Microbiol 28:205–216.

167. Sebban-Kreuzer C, Dolla A, Guerlesquin F. 1998. The formate dehydrogenase-cytochrome *c*553 complex from *Desulfovibrio vulgaris* Hildenborough. Eur J Biochem 253:645–652.

168. Ho KK, Kerfeld CA, Krogmann D. 2011. The water soluble cytochromes of Cyanobacteria, p. 515–540. *In* Bioenergetic Processes of Cyanobacteria.

169. Kurth JM, Brito JA, Reuter J, Flegler A, Koch T, Franke T, Klein EM, Rowe SF, Butt JN, Denkmann K, Pereira IAC, Archer M, Dahl C. 2016. Electron accepting units of

the diheme cytochrome *c* TsdA, a bifunctional thiosulfate dehydrogenase/tetrathionate reductase. J Biol Chem 291:24804–24818.

170. Denkmann K, Grein F, Zigann R, Siemen A, Bergmann J, van Helmont S, Nicolai A, Pereira IAC, Dahl C. 2012. Thiosulfate dehydrogenase: A widespread unusual acidophilic *c*-type cytochrome. Environ Microbiol 14:2673–2688.

171. Myers CR, Myers JM. 1997. Cloning and sequence of *cymA*, a gene encoding a tetraheme cytochrome *c* required for reduction of iron(III), fumarate, and nitrate by *Shewanella putrefaciens* MR-1 . J Bacteriol 179:1143–1152.

172. Schwalb C, Chapman SK, Reid GA. 2003. The tetraheme cytochrome CymA is required for anaerobic respiration with dimethyl sulfoxide and nitrite in *Shewanella oneidensis*. Biochemistry 42:9491–9497.

173. Simon J. 2002. Enzymology and bioenergetics of respiratory nitrite ammonification. FEMS Microbiol Rev 26:285–309.

174. Hussain H, Grove J, Griffiths L, Busby S, Coie J. 1994. A seven-gene operon essential for formate-dependent nitrite reduction to ammonia by enteric bacteria. Mol Microbiol 12:153–163.

175. Clarke TA, Cole JA, Richardson DJ, Hemmings AM. 2007. The crystal structure of the pentahaem *c* -type cytochrome NrfB and characterization of its solution-state interaction with the pentahaem nitrite reductase NrfA 30:19–30.

176. Butler JE, Kaufmann F, Coppi M V, Núñez C, Lovley DR. 2004. MacA , a diheme *c*-type cytochrome involved in Fe (III) reduction by *Geobacter sulfurreducens*. J Bacteriol 186:4042–4045.

177. Seidel J, Hoffmann M, Ellis KE, Seidel A, Spatzal T, Gerhardt S, Elliott SJ, Einsle O. 2012. MacA is a second cytochrome *c* peroxidase of *Geobacter sulfurreducens*. Biochemistry 51:2747–2756.

178. Myers CR, Nealson KH. 1988. Bacterial manganese reduction and growth with manganese oxide as the sole electron acceptor. Science 240:1319–1321.

179. Hau HH, Gilbert A, Coursolle D, Gralnick JA. 2008. Mechanism and consequences of anaerobic respiration of cobalt by *Shewanella oneidensis* strain MR-1. Appl Environ Microbiol 74:6880–6886.

180. Balch WE, Fox GE, Magrum LJ, Woese CR, Wolfe RS. 1979. Methanogens: reevaluation of a unique biological group. Microbiol Rev 43:260–296.

181. Lovley DR, Phillips EJP. 1986. Organic matter mineralization with reduction of ferric iron in anaerobic sediments. Appl Envir Microbiol 51:683–689.

182. Chan CH, Levar CE, Zacharoff L, Badalamenti JP, Bond DR. 2015. Scarless genome editing and stable inducible expression vectors for *Geobacter sulfurreducens*. Appl Environ Microbiol 81:7178–7186.

183. Ross DE, Flynn JM, Baron DB, Gralnick JA, Bond DR. 2011. Towards electrosynthesis in *Shewanell*a: energetics of reversing the Mtr pathway for reductive metabolism. PLoS ONE 6:e16649.

184. Saltikov CW, Newman DK. 2003. Genetic identification of a respiratory arsenate reductase. Proc Natl Acad Sci U S A 100:10983–8.

185. Kovach ME, Elzer PH, Steven Hill D, Robertson GT, Farris MA, Roop RM, Peterson KM. 1995. Four new derivatives of the broad-host-range cloning vector pBBR1MCS, carrying different antibiotic-resistance cassettes. Gene 166:175–176.

186. Rietsch A, Vallet-Gely I, Dove SL, Mekalanos JJ. 2005. ExsE, a secreted regulator of type III secretion genes in *Pseudomonas aeruginosa*. Proc Natl Acad Sci 102:8006–8011.

187. Coursolle D, Baron DB, Bond DR, Gralnick JA. 2010. The Mtr respiratory pathway is essential for reducing flavins and electrodes in *Shewanella oneidensis*. J Bacteriol 192:467–474.

188. Stookey LL. 1970. Ferrozine---a new spectrophotometric reagent for iron. Anal Chem 42:779–781.

189. Thompson JD, Higgins DG, Gibson TJ. 1994. CLUSTAL W: Improving the sensitivity of progressive multiple sequence alignment through sequence weighting, position-specific gap penalties and weight matrix choice. Nucleic Acids Res 22:4673–4680.

190. Jones DT, Taylor WR, Thornton JM. 1992. The rapid generation of mutation data matricies from protein sequences. Comput Appl Biosci 8:275–282.

191. Kumar S, Stecher G, Tamura K. 2016. MEGA7: Molecular evolutionary genetics analysis version 7.0 for bigger datasets. Mol Biol Evol 33:1870–1874.

192. Drummond AJ. 2009. FigTree. http://tree.bio.ed.ac.uk/software/figtree/ Accessed 2018-01-04.

193. Eagon R. G. 1962. *Pseudomonas natriegens*, a marine bacterium with a generation time of less than 10 minutes. J Bacteriol 83:736–737.

194. Payne WJ, Eagon RG, Williams AK. 1961. Some observations on the physiology of *Pseudomonas natriegens* nov. spec. Antonie Van Leeuwenhoek 27:121–128.

195. Payne WJ. 1958. Studies on bacterial utilization of uronic acids III. induction of oxidative enzymes in a marine isolate. J Bacteriol 2337.

196. Neori A, Agami M. 2017. The functioning of rhizosphere biota in wetlands – a review. Wetlands 37:615–633.

197. Takemura AF, Chien DM, Polz MF. 2014. Associations and dynamics of *Vibrionaceae* in the environment, from the genus to the population level. Front Microbiol 5:1–26.

198. Richardson DJ. 2000. Bacterial respiration: a flexible process for a changing environment. Microbiol Read Engl 146:551–571.

199. Proctor LM, Gunsalus RP. 2000. Anaerobic respiratory growth of *Vibrio harveyi*, *Vibrio fischeri* and *Photobacterium leiognathi* with trimethylamine N-oxide, nitrate and fumarate: ecological implications. Environ Microbiol 2:399–406.

200. Macfarlane GT, Herbert RA. 1982. Nitrate dissimilation by *Vibrio* spp. isolated from estuarine sediments. J Gen Microbiol 128:2463–2468.

201. Braun M, Thöny-Meyer L. 2005. Cytochrome *c* maturation and the physiological role of *c*-type cytochromes in *Vibrio cholerae*. J Bacteriol 187:5996–6004.

202. Li Y, Wang Y, Fu L, Gao Y, Zhao H, Zhou W. 2017. Aerobic-heterotrophic nitrogen removal through nitrate reduction and ammonium assimilation by marine bacterium *Vibrio* sp. Y1-5. Bioresour Technol 230:103–111.

203. Lee KM, Park Y, Bari W, Yoon MY, Go J, Kim SC, Lee H Il, Yoon SS. 2012. Activation of cholera toxin production by anaerobic respiration of trimethylamine N-oxide in *Vibrio cholerae*. J Biol Chem 287:39742–39752.

204. Dunn AK, Stabb E V. 2008. Genetic analysis of trimethylamine N-oxide reductases in the light organ symbiont *Vibrio fischeri* ES114. J Bacteriol 190:5814–5823.

205. Bueno E, Sit B, Waldor MK, Cava F. 2018. Anaerobic nitrate reduction divergently governs population expansion of the enteropathogen *Vibrio cholerae*. Nat Microbiol 3:1346–1353.

206. Kado T, Kashimoto T, Yamazaki K, Ueno S. 2017. Importance of fumarate and nitrate reduction regulatory protein for intestinal proliferation of *Vibrio vulnificus*. FEMS Microbiol Lett 364:1–5.

207. Fredrickson JK, Romine MF, Beliaev AS, Auchtung JM, Driscoll ME, Gardner TS, Nealson KH, Osterman AL, Pinchuk G, Reed JL, Rodionov DA, Rodrigues JLM, Saffarini DA, Serres MH, Spormann AM, Zhulin IB, Tiedje JM. 2008. Towards environmental systems biology of *Shewanella*. Nat Rev Microbiol 6:592–603.

208. Beblawy S, Bursac T, Paquete C, Louro R, Clarke TA, Gescher J. 2018. Extracellular reduction of solid electron acceptors by *Shewanella oneidensis*. Mol Microbiol 109:571–583.

209. Fonseca B, Paquete C, Neto S, Pacheco I, Soares C, Louro R. 2013. Mind the gap: cytochrome interactions reveal electron pathways across the periplasm of *Shewanella oneidensis* MR-1. Biochem J 108:101–108.

210. Edwards MJ, White GF, Butt JN, Richardson DJ, Clarke TA. 2020. The crystal structure of a biological insulated transmembrane molecular wire. Cell 181:1–9.

211. Lies DP, Mielke RE, Gralnick JA, Newman DK. 2005. *Shewanella oneidensis* MR-1 uses overlapping pathways for iron reduction at a distance and by direct contact under conditions relevant for biofilms. Appl Environ Microbiol 71:4414–4426.

212. Marsili E, Baron DB, Shikhare ID, Coursolle D, Gralnick JA, Bond DR. 2008. *Shewanella* secretes flavins that mediate extracellular electron transfer. Proc Natl Acad Sci 105:3968–3973.

213. Mevers E, Su L, Pishchany G, Baruch M, Cornejo J, Hobert E, Dimise E, Ajo-Franklin CM, Clardy J. 2019. An elusive electron shuttle from a facultative anaerobe. eLife 8:1–15.

214. Conley BE, Intile PJ, Bond DR, Gralnick JA. 2018. Divergent Nrf family proteins and MtrCAB homologs facilitate extracellular electron transfer in *Aeromonas hydrophila*. Appl Environ Microbiol 84:e02134-18.

215. Jones JG, Davison W, Gardener S. 1984. Iron reduction by bacteria range of organisms involved and metals reduced. FEMS Microbiol Lett 21:133–136.

216. Jones JG, Gardener S, Simon BM. 1983. Bacterial reduction of ferric iron in a stratified eutrophic lake. J Gen Microbiol 129:131–139.

217. Jones JG, Gardener S, Simon BM. 1984. Reduction of ferric iron by heterotrophic bacteria in lake sediments. J Gen Microbiol 130:45–51.

218. Wee SK, Burns JL, Dichristina TJ. 2014. Identification of a molecular signature unique to metal-reducing Gammaproteobacteria. FEMS Microbiol Lett 350:90–99.

219. Nivens DE, Nichols PD, Henson JM, Geesey GG, White DC. 1986. Reversible acceleration of the corrosion of AISI 304 stainless steel exposed to seawater induced by growth and secretions of the marine bacterium *Vibrio natriegens*. Natl Assoc Corros Eng 42:204–210.

220. Dowling NJE, Guezennec J, Lemoine ML, Tunlid A, White DC. 1988. Analysis of carbon steels affected by bacteria using electrochemical impedance and direct current techniques. Corrosion 44:869–874.

221. Benbouzid-Rollet ND, Conte M, Guezennec J, Prieur D. 1991. Monitoring of a *Vibrio natriegens* and *Desulfovibrio vulgaris* marine aerobic biofilm on a stainless steel surface in a laboratory tubular flow system. J Appl Bacteriol 71:244–251.

222. Lam BR, Barr CR, Rowe AR, Nealson KH. 2019. Differences in applied redox potential on cathodes enrich for diverse electrochemically active microbial isolates from a marine sediment. Front Microbiol 10:1–17.

223. Zhong C, Han M, Yu S, Yang P, Li H, Ning K. 2018. Pan-genome analyses of 24 *Shewanella* strains re-emphasize the diversification of their functions yet evolutionary dynamics of metal-reducing pathway. Biotechnol Biofuels 11:1–13.

224. Zhong Y, Shi L. 2018. Genomic analyses of the quinol oxidases and/or quinone reductases involved in bacterial extracellular electron transfer. Front Microbiol 9:1–12.

225. Shi L, Rosso KM, Zachara JM, Fredrickson JK. 2012. Mtr extracellular electron-transfer pathways in Fe(III)-reducing or Fe(II)-oxidizing bacteria: A genomic perspective. Biochem Soc Trans 40:1261–1267.

226. Kosman DJ. 2013. Iron metabolism in aerobes: Managing ferric iron hydrolysis and ferrous iron autoxidation. Coord Chem Rev 257:210–217.

227. Gescher JS, Cordova CD, Spormann AM. 2008. Dissimilatory iron reduction in *Escherichia coli*: Identification of CymA of *Shewanella oneidensis* and NapC of *E. coli* as ferric reductases. Mol Microbiol 68:706–719.

228. Pitts KE, Dobbin PS, Reyes-Ramirez F, Thomson AJ, Richardson DJ, Seward HE. 2003. Characterization of the *Shewanella oneidensis* MR-1 decaheme cytochrome MtrA: Expression in *Escherichia coli* confers the ability to reduce soluble Fe(III) chelates. J Biol Chem 278:27758–27765.

229. Hunt KA, Flynn JM, Naranjo B, Shikhare ID, Gralnick JA. 2010. Substrate-level phosphorylation is the primary source of energy conservation during anaerobic respiration of *Shewanella oneidensis* strain MR-1. J Bacteriol 192:3345–3351.

230. Rodrigues ML, Oliveira TF, Pereira IAC, Archer M. 2006. X-ray structure of the membrane-bound cytochrome c quinol dehydrogenase NrfH reveals novel haem coordination. EMBO J 25:5951–5960.

231. Rodrigues ML, Pereira IA, Archer M. 2011. The NrfH cytochrome *c* quinol dehydrogenase, p. 1–14. *In* Scott, RA (ed.), Encyclopedia of Inorganic and Bioinorganic Chemistry.

232. Hederstedt L, Gorton L, Pankratova G. 2020. Two routes for extracellular electron transfer in *Enterococcus faecalis*. J Bacteriol FIX THIS C:1–18.

233. Light SH, Su L, Rivera-Lugo R, Cornejo JA, Louie A, Iavarone AT, Ajo-Franklin CM, Portnoy DA. 2018. A flavin-based extracellular electron transfer mechanism in diverse Gram-positive bacteria. Nature 562:140–144.

234. Abbott SL, Cheung WKW, Janda JM. 2003. The genus *Aeromonas*: biochemical characteristics, atypical reactions, and phenotypic identification schemes. J Clin Microbiol 41:2348–2357.

235. Minato Y, Fassio SR, Wolfe AJ, Häse CC. 2013. Central metabolism controls transcription of a virulence gene regulator in *Vibrio cholerae*. Microbiology 159:792–802.

236. Studer S V., Mandel MJ, Ruby EG. 2008. AinS quorum sensing regulates the *Vibrio fischeri* acetate switch. J Bacteriol 190:5915–5923.

237. Lee D, Kim EJ, Baek Y, Lee J, Yoon Y, Nair GB, Yoon SS, Kim DW. 2020. Alterations in glucose metabolism in *Vibrio cholerae* serogroup O1 El Tor biotype strains. Sci Rep 10:1–10.

238. Gomez-Gil B, Thompson CC, Matsumura Y, Sawabe T, Iida T, Christen R, Thompson F, Sawabe T. 2014. The family *Vibrionaceae*, p. 659–747. *In*

Rosenberg, E, DeLong, EF, Lory, S, Stackebrandt, E, Thompson, F (eds.), The Prokaryotes.

239. Baumann P, Schubert RH. 1984. The family *Vibrionaceae*, p. 516–550. *In* Bergey's manual of systematic bacteriology.

240. Dong Y, Sanford RA, Chang YJ, McInerney MJ, Fouke BW. 2017. Hematite reduction buffers acid generation and enhances nutrient uptake by a fermentative iron reducing bacterium, *Orenia metallireducens* strain Z6. Environ Sci Technol 51:232–242.

241. Pollock J, Weber KA, Lack J, Achenbach LA, Mormile MR, Coates JD. 2007. Alkaline iron(III) reduction by a novel alkaliphilic, halotolerant, *Bacillus* sp. isolated from salt flat sediments of Soap Lake. Appl Microbiol Biotechnol 77:927–934.

242. List C, Hosseini Z, Lederballe Meibom K, Hatzimanikatis V, Bernier-Latmani R. 2019. Impact of iron reduction on the metabolism of *Clostridium acetobutylicum*. Environ Microbiol 21:3548–3563.

243. Hoffart E, Grenz S, Lange J, Nitschel R, Müller F, Schwentner A, Feith A, Lenfers-lücker M, Takors R, Blombach B. 2017. High substrate uptake rates empower *Vibrio natriegens* as a production host for industrial biotechnology. Appl Environ Mpicrobiology 83:e01614-17.

244. Kane AL, Brutinel ED, Joo H, Maysonet Sanchez R, VanDrisse CM, Kotloski NJ, Gralnick JA. 2016. Formate metabolism in *Shewanella oneidensis* generates proton motive force and prevents growth without an electron acceptor. J Bacteriol 198:JB.00927-15.

245. Simon J, van Spanning RJM, Richardson DJ. 2008. The organisation of proton motive and non-proton motive redox loops in prokaryotic respiratory systems. Biochim Biophys Acta - Bioenerg 1777:1480–1490.

246. Payne SM, Mey AR, Wyckoff EE. 2016. *Vibrio* iron transport: evolutionary adaptation to life in multiple environments. Microbiol Mol Biol Rev 80:69–90.

247. Dohnalkova AC, Marshall MJ, Arey BW, Williams KH, Buck EC, Fredrickson JK. 2011. Imaging hydrated microbial extracellular polymers: Comparative analysis by electron microscopy. Appl Environ Microbiol 77:1254–1262.

248. Turner JW, Tallman JJ, Macias A, Pinnell LJ, Elledge NC, Azadani DN, Nilsson WB, Paranjpye RN, Armbrust E V., Strom MS. 2018. Comparative genomic analysis of *Vibrio diabolicus* and six taxonomic synonyms: A first look at the distribution and diversity of the expanded species. Front Microbiol 9:1–14.

249. Hasan NA, Grim CJ, Lipp EK, Rivera ING, Chun J, Haley BJ, Taviani E, Choi SY, Hoq M, Munk AC, Brettin TS, Bruce D, Challacombe JF, Detter JC, Han CS, Eisen JA, Huq A, Colwell RR. 2015. Deep-sea hydrothermal vent bacteria related to human pathogenic *Vibrio* species. Proc Natl Acad Sci U S A 112:E2813–E2819.

250. Raguénès G, Christen R, Guezennec J, Pignet P, Barbier G. 1997. *Vibrio diabolicus* sp. nov., a new polysaccharide-secreting organism isolated from a deep-sea hydrothermal vent polychaete annelid, *Alvinella pompejana*. Int J Syst Bacteriol 47:989–995.

251. Kees ED, Pendleton AR, Paquete CM, Arriola MB, Kane AL, Kotloski NJ, Intile PJ, Gralnick JA. 2019. Secreted flavin cofactors for anaerobic respiration of fumarate

and urocanate by *Shewanella oneidensis*: Cost and role. Appl Environ Microbiol 85:1–12.

252. Wang Y, Kern SE, Newman DK. 2010. Endogenous phenazine antibiotics promote anaerobic survival of *Pseudomonas aeruginosa* via extracellular electron transfer. J Bacteriol 192:365–369.

253. Tagliabue A, Bowie AR, Boyd PW, Buck KN, Johnson KS, Saito MA. 2017. The integral role of iron in ocean biogeochemistry. Nature 543:51–59.

254. Filip Z, Demnerova K. 2007. Humic substances as a natural factor lowering ecological risk in estuaries, p. 343–353. *In* Linkov, I, Kiker, GA, Wenning, RJ (eds.), Environmental Security in Harbors and Coastal Areas. Springer.

255. Regenspurg S, Brand A, Peiffer S. 2004. Formation and stability of schwertmannite in acidic mining lakes. Geochim Cosmochim Acta 68:1185–1197.

256. Des Soye BJ, Davidson SR, Weinstock MT, Gibson DG, Jewett MC. 2018. Establishing a high-yielding cell-free protein synthesis platform derived from *Vibrio natriegens*. ACS Synth Biol 7:2245–2255.

257. Dalia TN, Hayes CA, Stolyar S, Marx CJ, McKinlay JB, Dalia AB. 2017. Multiplex genome editing by natural transformation (MuGENT) for synthetic biology in *Vibrio natriegens*. ACS Synth Biol 6:1650–1655.

258. Madeira F, Park YM, Lee J, Buso N, Gur T, Madhusoodanan N, Basutkar P, Tivey ARN, Potter SC, Finn RD, Lopez R. 2019. The EMBL-EBI search and sequence analysis tools APIs in 2019. Nucleic Acids Res 47:W636–W641.

259. Huelsenbeck JP, Ronquist F. 2001. MRBAYES: Bayesian inference of phylogenetic trees. Bioinformatics 17:754–755.

260. Waterhouse AM, Procter JB, Martin DMA, Clamp M, Barton GJ. 2009. Jalview Version 2-A multiple sequence alignment editor and analysis workbench. Bioinformatics 25:1189–1191.

261. Aromokeye DA, Kulkarni AC, Elvert M, Wegener G, Henkel S, Coffinet S, Eickhorst T, Oni OE, Richter-Heitmann T, Schnakenberg A, Taubner H, Wunder L, Yin X, Zhu Q, Hinrichs K-U, Kasten S, Friedrich MW. 2020. Rates and Microbial Players of Iron-Driven Anaerobic Oxidation of Methane in Methanic Marine Sediments. Front Microbiol 10:3041.

262. Cai C, Leu AO, Xie G-J, Guo J, Feng Y, Zhao J-X, Tyson GW, Yuan Z, Hu S. 2018. A methanotrophic archaeon couples anaerobic oxidation of methane to Fe(III) reduction. ISME J 12:1929–1939.

263. Ettwig KF, Zhu B, Speth D, Keltjens JT, Jetten MSM, Kartal B. 2016. Archaea catalyze iron-dependent anaerobic oxidation of methane. Proc Natl Acad Sci 113:12792–12796.

264. Gao Y, Lee J, Neufeld JD, Park J, Rittmann BE, Lee H-S. 2017. Anaerobic oxidation of methane coupled with extracellular electron transfer to electrodes. Sci Rep 7:5099.

265. Jelen BI, Giovannelli D, Falkowski PG. 2016. The Role of Microbial Electron Transfer in the Coevolution of the Biosphere and Geosphere. Annu Rev Microbiol 70:45–62.

266. Thompson KJ, Kenward PA, Bauer KW, Warchola T, Gauger T, Martinez R, Simister RL, Michiels CC, Llirós M, Reinhard CT, Kappler A, Konhauser KO, Crowe SA. 2019. Photoferrotrophy, deposition of banded iron formations, and methane production in Archean oceans. Sci Adv 5:eaav2869.

267. Ozaki K, Thompson KJ, Simister RL, Crowe SA, Reinhard CT. 2019. Anoxygenic photosynthesis and the delayed oxygenation of Earth's atmosphere. Nat Commun 10:3026.

268. Kappler A, Pasquero C, Konhauser KO, Newman DK. 2005. Deposition of banded iron formations by anoxygenic phototrophic Fe(II)-oxidizing bacteria. Geology 33:865.

269. Anderson RT, Vrionis HA, Ortiz-Bernad I, Resch CT, Long PE, Dayvault R, Karp K, Marutzky S, Metzler DR, Peacock A, White DC, Lowe M, Lovley DR. 2003. Stimulating the In Situ Activity of *Geobacter* Species To Remove Uranium from the Groundwater of a Uranium-Contaminated Aquifer. Appl Environ Microbiol 69:5884–5891.

270. Liu C, Zachara JM, Zhong L, Heald SM, Wang Z, Jeon B-H, Fredrickson JK. 2009. Microbial Reduction of Intragrain U(VI) in Contaminated Sediment. Environ Sci Technol 43:4928–4933.

271. Lovley DR. 2011. Live wires: direct extracellular electron exchange for bioenergy and the bioremediation of energy-related contamination. Energy Environ Sci 4:4896.

272. Singh VK, Singh AL, Singh R, Kumar A. 2018. Iron oxidizing bacteria: insights on diversity, mechanism of iron oxidation and role in management of metal pollution. Environ Sustain 1:221–231.

273. Butler JE, Young ND, Lovley DR. 2010. Evolution of electron transfer out of the cell: comparative genomics of six Geobacter genomes. BMC Genomics 11:40.

274. Eddie BJ, Wang Z, Malanoski AP, Hall RJ, Oh SD, Heiner C, Lin B, Strycharz-Glaven SM. 2016. 'Candidatus Tenderia electrophaga', an uncultivated electroautotroph from a biocathode enrichment. Int J Syst Evol Microbiol 66:2178–2185.

275. Eddie BJ, Wang Z, Hervey WJ, Leary DH, Malanoski AP, Tender LM, Lin B, Strycharz-Glaven SM. 2017. Metatranscriptomics Supports the Mechanism for Biocathode Electroautotrophy by " *Candidatus* Tenderia electrophaga." mSystems 2.

276. Gupta D, Guzman MS, Bose A. 2020. Extracellular electron uptake by autotrophic microbes: physiological, ecological, and evolutionary implications. J Ind Microbiol Biotechnol 47:863–876.

277. Kashyap S, Holden JF. 2021. Microbe-Mineral Interaction and Novel Proteins for Iron Oxide Mineral Reduction in the Hyperthermophilic Crenarchaeon Pyrodictium delaneyi. Appl Environ Microbiol 87.

278. Larsen S, Nielsen LP, Schramm A. 2015. Cable bacteria associated with long-distance electron transport in New England salt marsh sediment: Cable bacteria in New England salt marsh sediment. Environ Microbiol Rep 7:175–179.

279. Lovley DR. 2017. Syntrophy Goes Electric: Direct Interspecies Electron Transfer. Annu Rev Microbiol 71:643–664.

280. Shi L, Dong H, Reguera G, Beyenal H, Lu A, Liu J, Yu H-Q, Fredrickson JK. 2016. Extracellular electron transfer mechanisms between microorganisms and minerals. Nat Rev Microbiol 14:651–662.

281. Tanaka K, Yokoe S, Igarashi K, Takashino M, Ishikawa M, Hori K, Nakanishi S, Kato S. 2018. Extracellular Electron Transfer via Outer Membrane Cytochromes in a Methanotrophic Bacterium Methylococcus capsulatus (Bath). Front Microbiol 9:2905.

282. Yang Y, Wang Z, Gan C, Klausen LH, Bonné R, Kong G, Luo D, Meert M, Zhu C, Sun G, Guo J, Ma Y, Bjerg JT, Manca J, Xu M, Nielsen LP, Dong M. 2021. Long-distance electron transfer in a filamentous Gram-positive bacterium. Nat Commun 12:1709.

283. Konstantinidis KT, Serres MH, Romine MF, Rodrigues JLM, Auchtung J, McCue L-A, Lipton MS, Obraztsova A, Giometti CS, Nealson KH, Fredrickson JK, Tiedje JM. 2009. Comparative systems biology across an evolutionary gradient within the *Shewanella* genus. Proc Natl Acad Sci 106:15909–15914.

284. Zhong C, Han M, Yu S, Yang P, Li H, Ning K. 2018. Pan-genome analyses of 24 Shewanella strains re-emphasize the diversification of their functions yet evolutionary dynamics of metal-reducing pathway. Biotechnol Biofuels 11:193.

285. Heidelberg JF, Paulsen IT, Nelson KE, Gaidos EJ, Nelson WC, Read TD, Eisen JA, Seshadri R, Ward N, Methe B, Clayton RA, Meyer T, Tsapin A, Scott J, Beanan M, Brinkac L, Daugherty S, DeBoy RT, Dodson RJ, Durkin AS, Haft DH, Kolonay JF,

Madupu R, Peterson JD, Umayam LA, White O, Wolf AM, Vamathevan J, Weidman J, Impraim M, Lee K, Berry K, Lee C, Mueller J, Khouri H, Gill J, Utterback TR, McDonald LA, Feldblyum TV, Smith HO, Venter JC, Nealson KH, Fraser CM. 2002. Genome sequence of the dissimilatory metal ion–reducing bacterium *Shewanella oneidensis*. Nat Biotechnol 20:1118–1123.

286. Conley BE, Intile PJ, Bond DR, Gralnick JA. 2018. Divergent Nrf Family Proteins and MtrCAB Homologs Facilitate Extracellular Electron Transfer in *Aeromonas hydrophila*. Appl Environ Microbiol 84:e02134-18, /aem/84/23/e02134-18.atom.

287. Bose A, Gardel EJ, Vidoudez C, Parra EA, Girguis PR. 2014. Electron uptake by iron-oxidizing phototrophic bacteria. Nat Commun 5:3391.

288. Gupta D, Sutherland MC, Rengasamy K, Meacham JM, Kranz RG, Bose A. 2019. Photoferrotrophs Produce a PioAB Electron Conduit for Extracellular Electron Uptake. mBio 10.

289. Jiao Y, Newman DK. 2007. The pio Operon Is Essential for Phototrophic Fe(II) Oxidation in Rhodopseudomonas palustris TIE-1. J Bacteriol 189:1765–1773.

290. Beckwith CR, Edwards MJ, Lawes M, Shi L, Butt JN, Richardson DJ, Clarke TA. 2015. Characterization of MtoD from Sideroxydans lithotrophicus: a cytochrome c electron shuttle used in lithoautotrophic growth. Front Microbiol 6.

291. Cooper RE, Wegner C-E, McAllister SM, Shevchenko O, Chan CS, Küsel K. 2020. Draft Genome Sequence of Sideroxydans sp. Strain CL21, an Fe(II)-Oxidizing Bacterium. Microbiol Resour Announc 9.

292. Emerson D, Field EK, Chertkov O, Davenport KW, Goodwin L, Munk C, Nolan M, Woyke T. 2013. Comparative genomics of freshwater Fe-oxidizing bacteria: implications for physiology, ecology, and systematics. Front Microbiol 4.

293. Liu J, Wang Z, Belchik SM, Edwards MJ, Liu C, Kennedy DW, Merkley ED, Lipton MS, Butt JN, Richardson DJ, Zachara JM, Fredrickson JK, Rosso KM, Shi L. 2012. Identification and Characterization of MtoA: A Decaheme c-Type Cytochrome of the Neutrophilic Fe(II)-Oxidizing Bacterium Sideroxydans lithotrophicus ES-1. Front Microbiol 3.

294. Garber AI, Nealson KH, Okamoto A, McAllister SM, Chan CS, Barco RA, Merino N. 2020. FeGenie: A Comprehensive Tool for the Identification of Iron Genes and Iron Gene Neighborhoods in Genome and Metagenome Assemblies. Front Microbiol 11:37.

295. He S, Barco RA, Emerson D, Roden EE. 2017. Comparative Genomic Analysis of Neutrophilic Iron(II) Oxidizer Genomes for Candidate Genes in Extracellular Electron Transfer. Front Microbiol 8:1584.

296. Lu S, Wang J, Chitsaz F, Derbyshire MK, Geer RC, Gonzales NR, Gwadz M, Hurwitz DI, Marchler GH, Song JS, Thanki N, Yamashita RA, Yang M, Zhang D, Zheng C, Lanczycki CJ, Marchler-Bauer A. 2020. CDD/SPARCLE: the conserved domain database in 2020. Nucleic Acids Res 48:D265–D268.

297. Madeira F, Park Y mi, Lee J, Buso N, Gur T, Madhusoodanan N, Basutkar P, Tivey ARN, Potter SC, Finn RD, Lopez R. 2019. The EMBL-EBI search and sequence analysis tools APIs in 2019. Nucleic Acids Res 47:W636–W641.

298. Jones DT, Taylor WR, Thornton JM. 1992. The rapid generation of mutation data matrices from protein sequences. Bioinformatics 8:275–282.

299. Whelan S, Goldman N. 2001. A General Empirical Model of Protein Evolution Derived from Multiple Protein Families Using a Maximum-Likelihood Approach. Mol Biol Evol 18:691–699.

300. Letunic I, Bork P. 2019. Interactive Tree Of Life (iTOL) v4: recent updates and new developments. Nucleic Acids Res 47:W256–W259.

301. Emerson D, Moyer C. 1997. Isolation and characterization of novel iron-oxidizing bacteria that grow at circumneutral pH. Appl Environ Microbiol 63:4784–4792.

302. Darling AE, Mau B, Perna NT. 2010. progressiveMauve: Multiple Genome Alignment with Gene Gain, Loss and Rearrangement. PLoS ONE 5:e11147.

303. Sullivan MJ, Petty NK, Beatson SA. 2011. Easyfig: a genome comparison visualizer. Bioinformatics 27:1009–1010.

304. Reyes C, Qian F, Zhang A, Bondarev S, Welch A, Thelen MP, Saltikov CW. 2012. Characterization of Axial and Proximal Histidine Mutations of the Decaheme Cytochrome MtrA from Shewanella sp. Strain ANA-3 and Implications for the Electron Transport System. J Bacteriol 194:5840–5847.

305. Hartshorne RS, Reardon CL, Ross D, Nuester J, Clarke TA, Gates AJ, Mills PC, Fredrickson JK, Zachara JM, Shi L, Beliaev AS, Marshall MJ, Tien M, Brantley S, Butt JN, Richardson DJ. 2009. Characterization of an electron conduit between bacteria and the extracellular environment. Proc Natl Acad Sci 106:22169–22174.

306. Tully BJ, Graham ED, Heidelberg JF. 2018. The reconstruction of 2,631 draft metagenome-assembled genomes from the global oceans. Sci Data 5:170203.

307. Chaudhuri SK, Lovley DR. 2003. Electricity generation by direct oxidation of glucose in mediatorless microbial fuel cells. Nat Biotechnol 21:1229–1232.

308. Finneran KT. 2003. Rhodoferax ferrireducens sp. nov., a psychrotolerant, facultatively anaerobic bacterium that oxidizes acetate with the reduction of Fe(III). Int J Syst Evol Microbiol 53:669–673.

309. Yu H, Leadbetter JR. 2020. Bacterial chemolithoautotrophy via manganese oxidation. Nature 583:453–458.

310. Braun B, Künzel S, Szewzyk U. 2017. Draft Genome Sequence of Ideonella sp. Strain A 288, Isolated from an Iron-Precipitating Biofilm. Genome Announc 5:e00803-17, e00803-17.

311. Schmidt B, Sánchez LA, Fretschner T, Kreps G, Ferrero MA, Siñeriz F, Szewzyk U. 2014. Isolation of *Sphaerotilus - Leptothrix* strains from iron bacteria communities in Tierra del Fuego wetlands. FEMS Microbiol Ecol n/a-n/a.

312. Ross DE, Flynn JM, Baron DB, Gralnick JA, Bond DR. 2011. Towards Electrosynthesis in Shewanella: Energetics of Reversing the Mtr Pathway for Reductive Metabolism. PLoS ONE 6:e16649.

313. Rowe AR, Rajeev P, Jain A, Pirbadian S, Okamoto A, Gralnick JA, El-Naggar MY, Nealson KH. 2018. Tracking Electron Uptake from a Cathode into Shewanella Cells: Implications for Energy Acquisition from Solid-Substrate Electron Donors. mBio 9:e02203-17.

314. Clark IC, Melnyk RA, Engelbrektson A, Coates JD. 2013. Structure and Evolution of Chlorate Reduction Composite Transposons. mBio 4:e00379-13.

315. Melnyk RA, Coates JD. 2015. The Perchlorate Reduction Genomic Island: Mechanisms and Pathways of Evolution by Horizontal Gene Transfer. BMC Genomics 16:862.

316. Lindell D, Sullivan MB, Johnson ZI, Tolonen AC, Rohwer F, Chisholm SW. 2004. Transfer of photosynthesis genes to and from Prochlorococcus viruses. Proc Natl Acad Sci 101:11013–11018.

317. Lindell D, Jaffe JD, Johnson ZI, Church GM, Chisholm SW. 2005. Photosynthesis genes in marine viruses yield proteins during host infection. Nature 438:86–89.

318. Ravenhall M, Škunca N, Lassalle F, Dessimoz C. 2015. Inferring Horizontal Gene Transfer. PLOS Comput Biol 11:e1004095.

319. Ivanova EP, Flavier S, Christen R. 2004. Phylogenetic relationships among marine Alteromonas-like proteobacteria: emended description of the family Alteromonadaceae and proposal of Pseudoalteromonadaceae fam. nov., Colwelliaceae fam. nov., Shewanellaceae fam. nov., Moritellaceae fam. nov., Ferrimonadaceae fam. nov., Idiomarinaceae fam. nov. and Psychromonadaceae fam. nov. Int J Syst Evol Microbiol 54:1773–1788.

320. DeBruyn JM, Nixon LT, Fawaz MN, Johnson AM, Radosevich M. 2011. Global Biogeography and Quantitative Seasonal Dynamics of Gemmatimonadetes in Soil. Appl Environ Microbiol 77:6295–6300.

321. Gao B, Mohan R, Gupta RS. 2009. Phylogenomics and protein signatures elucidating the evolutionary relationships among the Gammaproteobacteria. Int J Syst Evol Microbiol 59:234–247.

322. Williams KP, Gillespie JJ, Sobral BWS, Nordberg EK, Snyder EE, Shallom JM, Dickerman AW. 2010. Phylogeny of Gammaproteobacteria. J Bacteriol 192:2305–2314.

323. Thorell K, Meier-Kolthoff JP, Sjöling Å, Martín-Rodríguez AJ. 2019. Whole-Genome Sequencing Redefines Shewanella Taxonomy. Front Microbiol 10:1861.

324. Urakawa H. 2014. The Family Moritellaceae, p. 477–489. *In* Rosenberg, E, DeLong, EF, Lory, S, Stackebrandt, E, Thompson, F (eds.), The Prokaryotes. Springer Berlin Heidelberg, Berlin, Heidelberg.

325. Satomi M. 2014. The Family Shewanellaceae, p. 597–625. *In* Rosenberg, E, DeLong, EF, Lory, S, Stackebrandt, E, Thompson, F (eds.), The Prokaryotes. Springer Berlin Heidelberg, Berlin, Heidelberg.

326. Bird LJ, Wang Z, Malanoski AP, Onderko EL, Johnson BJ, Moore MH, Phillips DA, Chu BJ, Doyle JF, Eddie BJ, Glaven SM. 2018. Development of a Genetic System for Marinobacter atlanticus CP1 (sp. nov.), a Wax Ester Producing Strain Isolated From an Autotrophic Biocathode. Front Microbiol 9:3176.

327. Onderko EL, Phillips DA, Eddie BJ, Yates MD, Wang Z, Tender LM, Glaven SM. 2019. Electrochemical Characterization of Marinobacter atlanticus Strain CP1 Suggests a Role for Trace Minerals in Electrogenic Activity. Front Energy Res 7:60.

328. Wang Z, Leary DH, Malanoski AP, Li RW, Hervey WJ, Eddie BJ, Tender GS, Yanosky SG, Vora GJ, Tender LM, Lin B, Strycharz-Glaven SM. 2015. A Previously Uncharacterized, Nonphotosynthetic Member of the Chromatiaceae Is the Primary CO_2 -Fixing Constituent in a Self-Regenerating Biocathode. Appl Environ Microbiol 81:699–712.

329. Wang Z, Eddie BJ, Malanoski AP, Hervey WJ, Lin B, Strycharz-Glaven SM. 2015. Complete Genome Sequence of *Marinobacter* sp. CP1, Isolated from a Self-Regenerating Biocathode Biofilm. Genome Announc 3:e01103-15, /ga/3/5/e01103-15.atom.

330. Leary DH, Hervey WJ, Malanoski AP, Wang Z, Eddie BJ, Tender GS, Vora GJ, Tender LM, Lin B, Strycharz-Glaven SM. 2015. Metaproteomic evidence of changes in protein expression following a change in electrode potential in a robust biocathode microbiome. PROTEOMICS 15:3486–3496.

331. Darmon E, Leach DRF. 2014. Bacterial Genome Instability. Microbiol Mol Biol Rev 78:1–39.

332. Marritt SJ, Lowe TG, Bye J, McMillan DGG, Shi L, Fredrickson J, Zachara J, Richardson DJ, Cheesman MR, Jeuken LJC, Butt JN. 2012. A functional description of CymA, an electron-transfer hub supporting anaerobic respiratory flexibility in Shewanella. Biochem J 444:465–474.

333. Myers JM, Myers CR. 2000. Role of the Tetraheme Cytochrome CymA in Anaerobic Electron Transport in Cells of Shewanella putrefaciens MR-1 with Normal Levels of Menaquinone. J Bacteriol 182:67–75.

334. Zhong Y, Shi L. 2018. Genomic Analyses of the Quinol Oxidases and/or Quinone Reductases Involved in Bacterial Extracellular Electron Transfer. Front Microbiol 9:3029.

335. Siguier P, Gourbeyre E, Chandler M. 2014. Bacterial insertion sequences: their genomic impact and diversity. FEMS Microbiol Rev 38:865–891.

336. Yu NY, Wagner JR, Laird MR, Melli G, Rey S, Lo R, Dao P, Sahinalp SC, Ester M, Foster LJ, Brinkman FSL. 2010. PSORTb 3.0: improved protein subcellular localization prediction with refined localization subcategories and predictive capabilities for all prokaryotes. Bioinformatics 26:1608–1615.

337. Fonseca BM, Paquete CM, Neto SE, Pacheco I, Soares CM, Louro RO. 2013. Mind the gap: cytochrome interactions reveal electron pathways across the periplasm of *Shewanella oneidensis* MR-1. Biochem J 449:101–108.

338. Aono E, Baba T, Ara T, Nishi T, Nakamichi T, Inamoto E, Toyonaga H, Hasegawa M, Takai Y, Okumura Y, Baba M, Tomita M, Kato C, Oshima T, Nakasone K, Mori H. 2010. Complete genome sequence and comparative analysis of Shewanella violacea, a psychrophilic and piezophilic bacterium from deep sea floor sediments. Mol Biosyst 6:1216.

339. Brettar I. 2002. Shewanella denitrificans sp. nov., a vigorously denitrifying bacterium isolated from the oxic--anoxic interface of the Gotland Deep in the central Baltic Sea. Int J Syst Evol Microbiol 52:2211–2217.

340. Jin M, Jiang Y, Sun L, Yin J, Fu H, Wu G, Gao H. 2013. Unique Organizational and Functional Features of the Cytochrome c Maturation System in Shewanella oneidensis. PLoS ONE 8:e75610.

341. Bouhenni R, Gehrke A, Saffarini D. 2005. Identification of Genes Involved in Cytochrome c Biogenesis in Shewanella oneidensis, Using a Modified mariner Transposon. Appl Environ Microbiol 71:4935–4937.

342. Cianciotto NP, Cornelis P, Baysse C. 2005. Impact of the bacterial type I cytochrome *c* maturation system on different biological processes: Ccm system and different biological processes. Mol Microbiol 56:1408–1415.

343. Feissner RE, Richard-Fogal CL, Frawley ER, Loughman JA, Earley KW, Kranz RG. 2006. Recombinant cytochromes c biogenesis systems I and II and analysis of haem delivery pathways in Escherichia coli. Mol Microbiol 60:563–577.

344. Frawley ER, Kranz RG. 2009. CcsBA is a cytochrome c synthetase that also functions in heme transport. Proc Natl Acad Sci 106:10201–10206.

345. Richard-Fogal CL, Frawley ER, Feissner RE, Kranz RG. 2007. Heme Concentration Dependence and Metalloporphyrin Inhibition of the System I and II Cytochrome c Assembly Pathways. J Bacteriol 189:455–463.

346. Heinemann IU, Jahn M, Jahn D. 2008. The biochemistry of heme biosynthesis. Arch Biochem Biophys 474:238–251.

347. Dailey HA, Dailey TA, Gerdes S, Jahn D, Jahn M, O'Brian MR, Warren MJ. 2017. Prokaryotic Heme Biosynthesis: Multiple Pathways to a Common Essential Product. Microbiol Mol Biol Rev 81.

348. Sandegren L, Andersson DI. 2009. Bacterial gene amplification: implications for the evolution of antibiotic resistance. Nat Rev Microbiol 7:578–588.

349. Mendonça AG, Alves RJ, Pereira-Leal JB. 2011. Loss of Genetic Redundancy in Reductive Genome Evolution. PLoS Comput Biol 7:e1001082.

350. Banerjee R, Shine O, Rajachandran V, Krishnadas G, Minnick MF, Paul S, Chattopadhyay S. 2020. Gene duplication and deletion, not horizontal transfer, drove intra-species mosaicism of Bartonella henselae. Genomics 112:467–471.

351. Aigle A, Bonin P, Iobbi-Nivol C, Méjean V, Michotey V. 2017. Physiological and transcriptional approaches reveal connection between nitrogen and manganese cycles in Shewanella algae C6G3. Sci Rep 7:44725.

352. Bewley KD, Firer-Sherwood MA, Mock J-Y, Ando N, Drennan CL, Elliott SJ. 2012. Mind the gap: diversity and reactivity relationships among multihaem cytochromes of the MtrA/DmsE family. Biochem Soc Trans 40:1268–1273.

353. Clarke TA, Edwards MJ, Gates AJ, Hall A, White GF, Bradley J, Reardon CL, Shi L, Beliaev AS, Marshall MJ, Wang Z, Watmough NJ, Fredrickson JK, Zachara JM, Butt JN, Richardson DJ. 2011. Structure of a bacterial cell surface decaheme electron conduit. Proc Natl Acad Sci 108:9384–9389.

354. Edwards MJ, Baiden NA, Johs A, Tomanicek SJ, Liang L, Shi L, Fredrickson JK, Zachara JM, Gates AJ, Butt JN, Richardson DJ, Clarke TA. 2014. The X-ray crystal structure of *Shewanella oneidensis* OmcA reveals new insight at the microbe-mineral interface. FEBS Lett 588:1886–1890.

355. Edwards MJ, Hall A, Shi L, Fredrickson JK, Zachara JM, Butt JN, Richardson DJ, Clarke TA. 2012. The Crystal Structure of the Extracellular 11-heme Cytochrome UndA Reveals a Conserved 10-heme Motif and Defined Binding Site for Soluble Iron Chelates. Structure 20:1275–1284.

356. Kasai T, Kouzuma A, Nojiri H, Watanabe K. 2015. Transcriptional mechanisms for differential expression of outer membrane cytochrome genes *omcA* and *mtrC* in *Shewanella oneidensis* MR-1. BMC Microbiol 15:68.

357. Mitchell AC, Peterson L, Reardon CL, Reed SB, Culley DE, Romine MR, Geesey GG. 2012. Role of outer membrane c-type cytochromes MtrC and OmcA in *Shewanella oneidensis* MR-1 cell production, accumulation, and detachment during respiration on hematite. Geobiology 10:355–370.

358. Neto SE, de Melo-Diogo D, Correia IJ, Paquete CM, Louro RO. 2017. Characterization of OmcA Mutants from *Shewanella oneidensis* MR-1 to Investigate the Molecular Mechanisms Underpinning Electron Transfer Across the Microbe-Electrode Interface. Fuel Cells 17:601–611.

359. Ross DE, Brantley SL, Tien M. 2009. Kinetic Characterization of OmcA and MtrC, Terminal Reductases Involved in Respiratory Electron Transfer for Dissimilatory Iron Reduction in *Shewanella oneidensis* MR-1. Appl Environ Microbiol 75:5218–5226.

360. Firer-Sherwood M, Pulcu GS, Elliott SJ. 2008. Electrochemical interrogations of the Mtr cytochromes from Shewanella: opening a potential window. JBIC J Biol Inorg Chem 13:849–854.

361. Yang Y, Chen J, Qiu D, Zhou J. 2013. Roles of UndA and MtrC of Shewanella putrefaciens W3-18-1 in iron reduction. BMC Microbiol 13:267.

362. Ross DE, Ruebush SS, Brantley SL, Hartshorne RS, Clarke TA, Richardson DJ, Tien M. 2007. Characterization of Protein-Protein Interactions Involved in Iron Reduction by Shewanella oneidensis MR-1. Appl Environ Microbiol 73:5797–5808.

363. Lawrence JG, Roth JR. 1996. Selfish Operons: Horizontal Transfer May Drive the Evolution of Gene Clusters. Genetics 143:1843–1860.

364. Pál C, Hurst LD. 2004. Evidence against the selfish operon theory. Trends Genet 20:232–234.

365. Grein F, Ramos AR, Venceslau SS, Pereira IAC. 2013. Unifying concepts in anaerobic respiration: Insights from dissimilatory sulfur metabolism. Biochim Biophys Acta BBA - Bioenerg 1827:145–160.

366. McCrindle SL, Kappler U, McEwan AG. 2005. Microbial Dimethylsulfoxide and Trimethylamine-N-Oxide Respiration, p. 147–201e. *In* Advances in Microbial Physiology. Elsevier.

367. Simon J. 2002. Enzymology and bioenergetics of respiratory nitrite ammonification. FEMS Microbiol Rev 26:285–309.

368. Kanhere A, Vingron M. 2009. Horizontal Gene Transfers in prokaryotes show differential preferences for metabolic and translational genes. BMC Evol Biol 9:9.

369. Caro-Quintero A, Konstantinidis KT. 2015. Inter-phylum HGT has shaped the metabolism of many mesophilic and anaerobic bacteria. ISME J 9:958–967.

370. Wiedenbeck J, Cohan FM. 2011. Origins of bacterial diversity through horizontal genetic transfer and adaptation to new ecological niches. FEMS Microbiol Rev 35:957–976.

371. Smillie CS, Smith MB, Friedman J, Cordero OX, David LA, Alm EJ. 2011. Ecology drives a global network of gene exchange connecting the human microbiome. Nature 480:241–244.

372. Sorek R, Zhu Y, Creevey CJ, Francino MP, Bork P, Rubin EM. 2007. Genome-Wide Experimental Determination of Barriers to Horizontal Gene Transfer. Science 318:1449–1452.

373. Bengtsson-Palme J, Kristiansson E, Larsson DGJ. 2018. Environmental factors influencing the development and spread of antibiotic resistance. FEMS Microbiol Rev 42.

374. Szamecz B, Boross G, Kalapis D, Kovács K, Fekete G, Farkas Z, Lázár V, Hrtyan M, Kemmeren P, Groot Koerkamp MJA, Rutkai E, Holstege FCP, Papp B, Pál C. 2014. The Genomic Landscape of Compensatory Evolution. PLoS Biol 12:e1001935.

375. Brito IL. 2021. Examining horizontal gene transfer in microbial communities. Nat Rev Microbiol 19:442–453.

376. Lower BH, Lins RD, Oestreicher Z, Straatsma TP, Hochella MF, Shi L, Lower SK. 2008. In Vitro Evolution of a Peptide with a Hematite Binding Motif That May Constitute a Natural Metal-Oxide Binding Archetype. Environ Sci Technol 42:3821–3827.

377. Lower BH, Shi L, Yongsunthon R, Droubay TC, McCready DE, Lower SK. 2007. Specific Bonds between an Iron Oxide Surface and Outer Membrane Cytochromes MtrC and OmcA from *Shewanella oneidensis* MR-1. J Bacteriol 189:4944–4952.

378. Jing X, Wu Y, Shi L, Peacock CL, Ashry NM, Gao C, Huang Q, Cai P. 2020. Outer Membrane *c* -Type Cytochromes OmcA and MtrC Play Distinct Roles in Enhancing the Attachment of *Shewanella oneidensis* MR-1 Cells to Goethite. Appl Environ Microbiol 86.

379. Barchinger SE, Pirbadian S, Sambles C, Baker CS, Leung KM, Burroughs NJ, El-Naggar MY, Golbeck JH. 2016. Regulation of Gene Expression in Shewanella oneidensis MR-1 during Electron Acceptor Limitation and Bacterial Nanowire Formation. Appl Environ Microbiol 82:5428–5443.

380. McLean JS, Pinchuk GE, Geydebrekht OV, Bilskis CL, Zakrajsek BA, Hill EA, Saffarini DA, Romine MF, Gorby YA, Fredrickson JK, Beliaev AS. 2008. Oxygen-dependent autoaggregation in Shewanella oneidensis MR-1. Environ Microbiol 10:1861–1876.

381. Wang Q, Jones A-AD, Gralnick JA, Lin L, Buie CR. 2019. Microfluidic dielectrophoresis illuminates the relationship between microbial cell envelope polarizability and electrochemical activity. Sci Adv 5:eaat5664.

382. He S, Tominski C, Kappler A, Behrens S, Roden EE. 2016. Metagenomic Analyses of the Autotrophic Fe(II)-Oxidizing, Nitrate-Reducing Enrichment Culture KS. Appl Environ Microbiol 82:2656–2668.

383. Rowe AR, Rajeev P, Jain A, Pirbadian S, Okamoto A, Gralnick JA, El-Naggar MY, Nealson KH. 2018. Tracking Electron Uptake from a Cathode into *Shewanella* Cells: Implications for Energy Acquisition from Solid-Substrate Electron Donors. mBio 9.

384. Bücking C, Piepenbrock A, Kappler A, Gescher J. 2012. Outer-membrane cytochrome-independent reduction of extracellular electron acceptors in *Shewanella oneidensis*. Microbiology 158:2144–2157.

385. Jørgensen BB, Findlay AJ, Pellerin A. 2019. The Biogeochemical Sulfur Cycle of Marine Sediments. Front Microbiol 10:849.

386. Kappler A, Bryce C, Mansor M, Lueder U, Byrne JM, Swanner ED. 2021. An evolving view on biogeochemical cycling of iron. Nat Rev Microbiol 19:360–374.

387. Thompson KJ, Kenward PA, Bauer KW, Warchola T, Gauger T, Martinez R, Simister RL, Michiels CC, Llirós M, Reinhard CT, Kappler A, Konhauser KO, Crowe SA. 2019. Photoferrotrophy, deposition of banded iron formations, and methane production in Archean oceans. Sci Adv 5:eaav2869.

388. Camacho A, Walter XA, Picazo A, Zopfi J. 2017. Photoferrotrophy: Remains of an Ancient Photosynthesis in Modern Environments. Front Microbiol 08.

389. Canfield DE, Rosing MT, Bjerrum C. 2006. Early anaerobic metabolisms 18.

390. McRose DL, Newman DK. 2021. Redox-active antibiotics enhance phosphorus bioavailability. Science 371:1033–1037.

391. Mevers E, Su L, Pishchany G, Baruch M, Cornejo J, Hobert E, Dimise E, Ajo-Franklin CM, Clardy J. 2019. An elusive electron shuttle from a facultative anaerobe. eLife 8:e48054.

392. Newman DK, Kolter R. 2000. A role for excreted quinones in extracellular electron transfer. Nature 405:94–97.

393. Scott DT, McKnight DM, Blunt-Harris EL, Kolesar SE, Lovley DR. Quinone Moieties Act as Electron Acceptors in the Reduction of Humic Substances by Humics-Reducing Microorganisms 6.

394. Piepenbrock A, Kappler A. 2013. Humic Substances and Extracellular Electron Transfer, p. 107–128. *In* Gescher, J, Kappler, A (eds.), Microbial Metal Respiration. Springer Berlin Heidelberg, Berlin, Heidelberg.

395. Shyu JBH, Lies DP, Newman DK. 2002. Protective Role of tolC in Efflux of the Electron Shuttle Anthraquinone-2,6-Disulfonate. J Bacteriol 184:1806–1810.

396. O'Loughlin EJ. 2008. Effects of Electron Transfer Mediators on the Bioreduction of Lepidocrocite (γ-FeOOH) by *Shewanella putrefaciens* CN32. Environ Sci Technol 42:6876–6882.

397. Turick CE, Tisa LS, Caccavo, F. 2002. Melanin Production and Use as a Soluble Electron Shuttle for Fe(III) Oxide Reduction and as a Terminal Electron Acceptor by *Shewanella algae* BrY. Appl Environ Microbiol 68:2436–2444.

398. Mukherjee S, Bassler BL. 2019. Bacterial quorum sensing in complex and dynamically changing environments. Nat Rev Microbiol 17:371–382.

399. Coursolle D, Baron DB, Bond DR, Gralnick JA. 2010. The Mtr Respiratory Pathway Is Essential for Reducing Flavins and Electrodes in Shewanella oneidensis. J Bacteriol 192:467–474.

400. Dependence of the electron transfer capacity on the kinetics of quinone-mediated Fe(III) reduction by two iron & humic reducing bacteria.pdf.

401. Cordova CD, Schicklberger MFR, Yu Y, Spormann AM. 2011. Partial Functional Replacement of CymA by SirCD in *Shewanella oneidensis* MR-1. J Bacteriol 193:2312–2321.

402. Covington ED, Gelbmann CB, Kotloski NJ, Gralnick JA. 2010. An essential role for UshA in processing of extracellular flavin electron shuttles by Shewanella oneidensis: Flavin processing by UshA in S. oneidensis. Mol Microbiol 78:519–532.

403. Regenspurg S, Brand A, Peiffer S. 2004. Formation and stability of schwertmannite in acidic mining lakes. Geochim Cosmochim Acta 68:1185–1197.

404. Lovley DR, Phillips EJP. 1986. Organic Matter Mineralization with Reduction of Ferric Iron in Anaerobic Sediments. Appl Environ Microbiol 51:683–689.

Appendix I: Flavins, redox and fish, oh my!

5.1 Summary

The EET model system *Shewanella oneidensis* MR-1 excretes FMN and utilizes it as an extracellular electron shuttle. *A. hydrophila* and *V. natriegens* have been shown to perform EET, but their ability to directly or indirectly reduce flavin species differed from *S. oneidensis*. Attempts to describe the ability of *A. hydrophila* and *V. natriegens* to reduce flavins is discussed, revealing a complicated connection between potential, mineral solubility, and cytochrome content that remains to be fully elucidated.

5.2 Introduction

Electron shuttling occurs with a variety of endogenous compounds in multiple microorganisms and enhances extracellular electron transfer, reviewed in (20). *Shewanella oneidensis* MR-1 secretes FMN and subsequently reduces it once outside the cell via the outer membrane Mtr complex to aid in anaerobic respiration, reviewed in (41). *Psuedomonas aeruginosa* produces phenazines which has been shown to aid in anaerobic survival and phosphate acquisition (40, 390). Quinones have also been shown to shuttle electrons in *S. oneidensis* MR-1 (391, 392) and serve as electron acceptors for reduction of humic substances (393). These core groups of electron shuttling molecules differ in structure and redox potential. How electron shuttling molecules interact with specific microorganisms and the environment remains to be elucidated.

Humic substances are chemically complex and diverse, present in all environments with have the potential to play a large role in electron transfer in the environment (394). Anthraquinone-2,6-disulphonate (AQDS) has been used as a soluble humic acid analog to study electron shuttling in EET; however work in *S. oneidensis* MR-1 suggests AQDS can enter the periplasm negating the need for electron transfer across the outer membrane (395). Addition of AQDS increases iron oxide reduction in Shewanella putrefaciens CN32 (396).Addition of melanin increased iron oxide reduction in Shewanella algae BrY (397)

The biological and ecological role of electron shuttling molecules in EET capable *Aeromonas* or *Vibrio* spp. has yet to be established. Previous reports demonstrated addition of anthraquinones increases iron oxide reduction rates in *A. hydrophila* HS01; however, no redox-active mediators were identified in the supernatant of *A. jandaei* grown in a microbial fuel cell (23). While Vibrio spp. are known to secrete quorum

sensing compounds for biofilm formation (398), the author has found no evidence in the literature for the production or use of an endogenous electron shuttle in EET capable *Aeromonas* or *Vibrio* spp.

The following study explores FMN reduction in *A. hydrophila* and *V. natriegens*. No evidence was found to support the hypothesis that *A. hydrophila* directly reduces FMN, yet *A. hydrophila* MtrCAB is capable of FMN reduction when expressed in an *S. oneidensis* mutant. FMN can be added to increase the rate of iron oxide reduction in *A. hydrophila* and *V. natriegens*. In *A. hydrophila*, the increased iron oxide reduction only occurred with autoclaved Schwartmannite but not poorly crystalline FeO(OH).

5.3 Results

FMN Reduction

Direct FMN reduction was measured by monitoring relative fluorescence units (RFU) of oxidized FMN diminish in an anaerobic environment as FMN is reduced. This assay has been validated in *S. oneidensis* MR-1 to study FMN reduction (399). Further analysis of the FMN reduction assay shows two distinct rates of reduction. Initial reduction occurs rapidly followed by a secondary gradual reduction, as measured by fluorescence (Figure 36A). The initial rate of reduction is dependent on the inner membrane quinone oxidoreductase, CymA (Figure 36A). Periplasmic electron shuttles, FccA and CctA are also involved in FMN reduction (Figure 36A), but overlapping functionality causes subtle changes in phenotypes has been established for Fe(III) citrate reduction (46). Lack of FccA and CctA slows the initial and secondary rate of FMN reduction with less proportion of FMN being reduced (Figure 36A). Inversion of RFU values graphed over time displayed the two rates in FMN reduction while highlighting slight differences in initial and secondary FMN reduction rates among mutants strains (Figure 36B). Transforming RFU values by the natural log did not

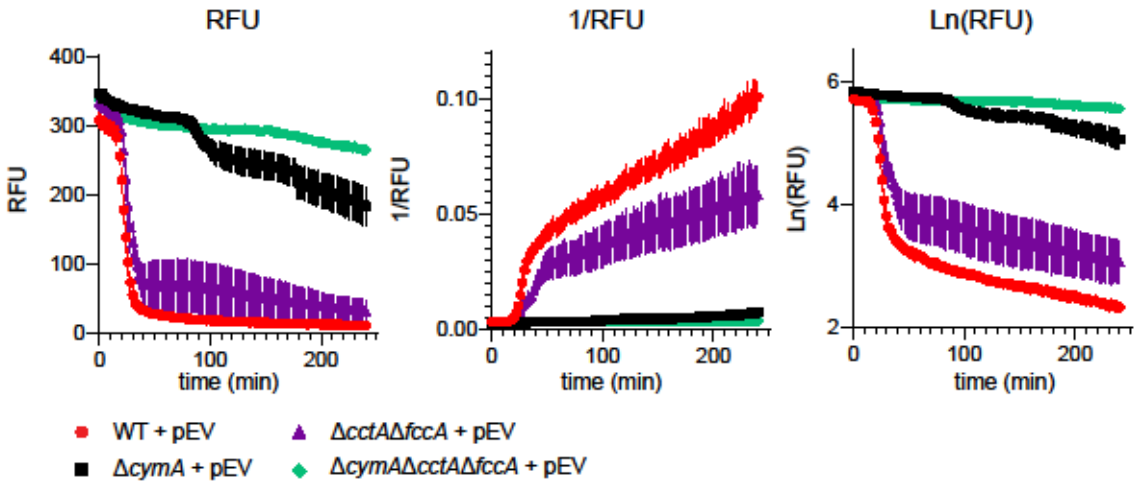

Figure 36. Direct FMN reduction by *S. oneidensis* and EET pathway mutants. *S. oneidensis* WT (●) and mutants lacking inner membrane (Δ*cymA* ■) and/or periplasmic multiheme cytochromes (Δ*fccA* Δ*cctA* ▲) (Δ*cymA* Δ*fccA* Δ*cctA* ♦) carrying an empty vector. A) Y-axis is RFU versus time B) Y-axis is 1/RFU versus time C) Y-axis is Ln(RFU) versus time. Data is representative of at least two independent experiments performed in triplicate, displaying mean ± standard error of the mean (SEM).

Direct reduction of FMN by WT *A. hydrophila* and *V. natriegens* was not observed despite attempts to pre-culture and induce expression of essential EET genes with Fe(III) citrate or Fe(II) SO4 (data not shown). FMN reduction in *A. hydrophila* lacking *mtrA*, a gene essential for reduction of Fe(III) citrate, Fe(III) oxide and Mn(IV) oxide (286), was indistinguishable from a wild-type and complemented strain (Figure 37A). To further investigate the lack of FMN reduction in *A. hydrophila*, live cells were compared to heat-killed cells (Figure 37). No differences were observed across live versus lysed and mutant strains, further suggesting *A. hydrophila* is not capable of directly reducing FMN. Additionally, the Y-axis of FMN reduction in the *S. oneidensis* background is 10x larger than in A. hydrophila strains (Figures 36 and 37).

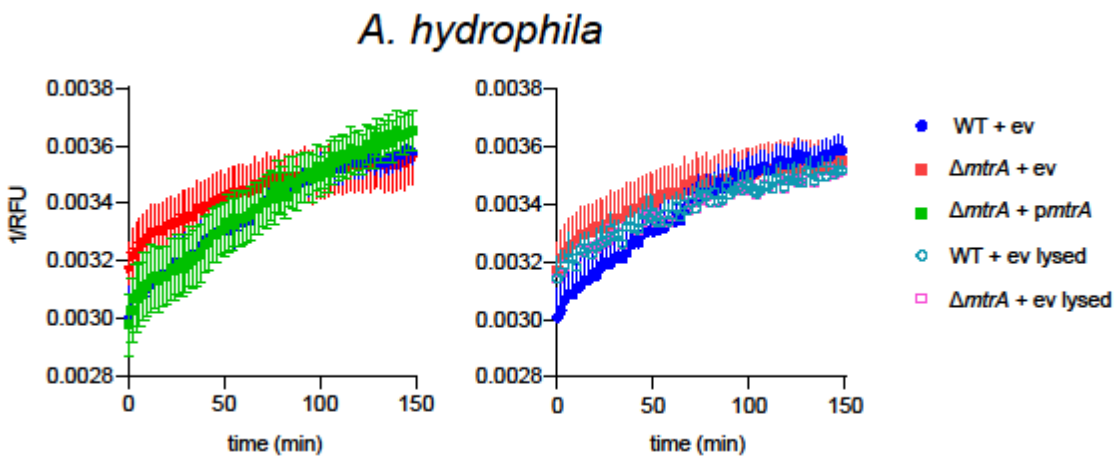

Figure 37. Direct FMN reduction by *A. hydrophila* and mutants. A) FMN reduction of wild-type (●), and mutants lacking mtrA and heterologously complemented with native *mtrA* (■) or an empty vector (■). B) FMN reduction of wild-type and *mtrA* mutant in live (closed symbols) versus heat-killed cells (open symbols).

Genes essential for EET in *A. hydrophila* and *V. natriegens* (90, 286) were heterologously expressed in corresponding *S. oneidensis* mutants and assayed for FMN reduction (Figure 38) in attempts to describe the physiological differences in FMN reduction between these genera. All complementation was performed in trans under the control of the plasmid encoded *lac* promoter. *V. natriegens* PdsA and CymA partially restored FMN reduction in *S. oneidensis* mutants lacking *cymA* to similar levels as native *S. oneidensis* CymA, but total FMN reduction was decreased in both these complemented strains compared to wild-type (Figure 38A). *V. natriegens* PdsA and CymA could also partially restore FMN reduction in *S. oneidensis* Δ*cymA* Δ*fccA* Δ*cctA* strains, lacking periplasmic electron shuttles in addition to CymA (Figure 38B); however the rate and extent decreased compared to the Δ*cymA* mutant (Figure 38A). Expression of *A. hydrophila pdsA/netBCD* did not restore FMN reduction in either *S. oneidensis* Δ*cymA* nor Δ*cymA* Δ*fccA* Δ*cctA* backgrounds (Figure 38 A and B). Complementation with the outer membrane MtrCAB complex from *A. hydrophila* restored FMN reduction at a rate similar to wild-type. Whereas *V. natriegens* MtrCAB yielded a decreased initial rate of reduction and less proportion of flavins reduced compared to wild-type.

One hypothesis to explain differences in rates of reduction is differing amounts of total cytochrome content. *A. hydrophila* HS01 observed less cytochrome production compared to *S. oneidensis* (400). This could explain the decreased FMN reduction observed in the Δ*cymA* strain complemented in trans with So *cymA*::pBBR1MCS-2, a low copy plasmid backbone.

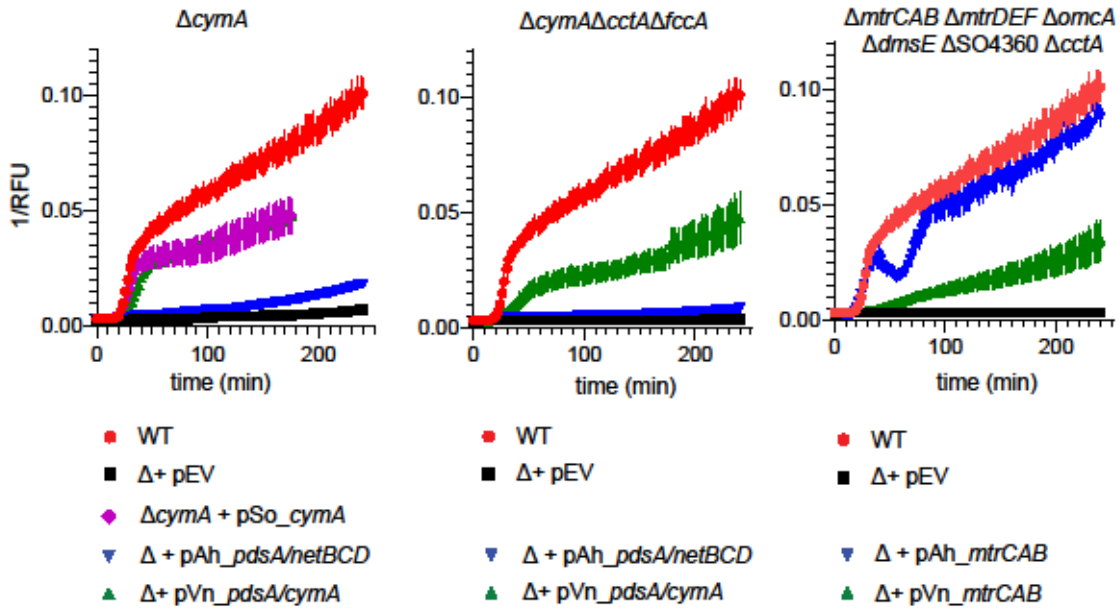

Figure 38. Direct FMN reduction by *S. oneidensis* mutants complemented with homologs from *A. hydrophila* or *V. natriegens*. (A) *S. oneidensis* WT (●) and mutants lacking inner membrane (Δ*cymA*) heterologously complemented with *pdsA-netBCD* from *A. hydrophila* (▼), *pdsA-cymA* from *V. natriegens* (▲) or an empty vector (■). (B) *S. oneidensis* WT (●) and mutants lacking inner membrane and periplasmic multiheme cytochromes (Δ*cymA* Δ*fccA* Δ*cctA*) heterologously complemented with *pdsA-netBCD* from *A. hydrophila* (▼), *pdsA-cymA* from *V. natriegens* (▲) or an empty vector (■). (C) *S. oneidensis* wild-type (WT) (●) and mutants lacking outer membrane multiheme cytochrome complexes (Δ*mtrCAB* Δ*mtrDEF* Δ*omcA* Δ*dmsE* ΔSO4360 Δ*cctA*) heterologously complemented with *mtrCAB* from *A. hydrophila* (▼) or *V. natriegens* (▲) or an empty vector (■). Data is representative of at least two independent experiments performed in triplicate, displaying mean ± standard error of the mean (SEM)

Iron oxide reduction with exogenous FMN

Instead of examining direct FMN reduction as in Figures 36-38, we examined the ability of *A. hydrophila* and *V. natriegens* to use FMN as an electron shuttle for iron oxide reduction. Addition of exogenous FMN increased the rate of Fe (II) production in all strains except for *S. oneidensis* Δ*mtrCAB* Δ*mtrDEF* Δ*omcA* Δ*dmsE* ΔSO4360 Δ*cctA* Δ*fccA* Δ*cymA* (Figure 39). In deletions strains of *A. hydrophila* and *V. natriegens* carrying an empty vector, modest enhancement of iron reduction was observed with the addition of FMN. Inner membrane quinone oxidoreductase mutants retain some iron reduction activity (90, 286, 401) which may account for the small amount of Fe(II) produced and subsequent shuttling observed in these strains.

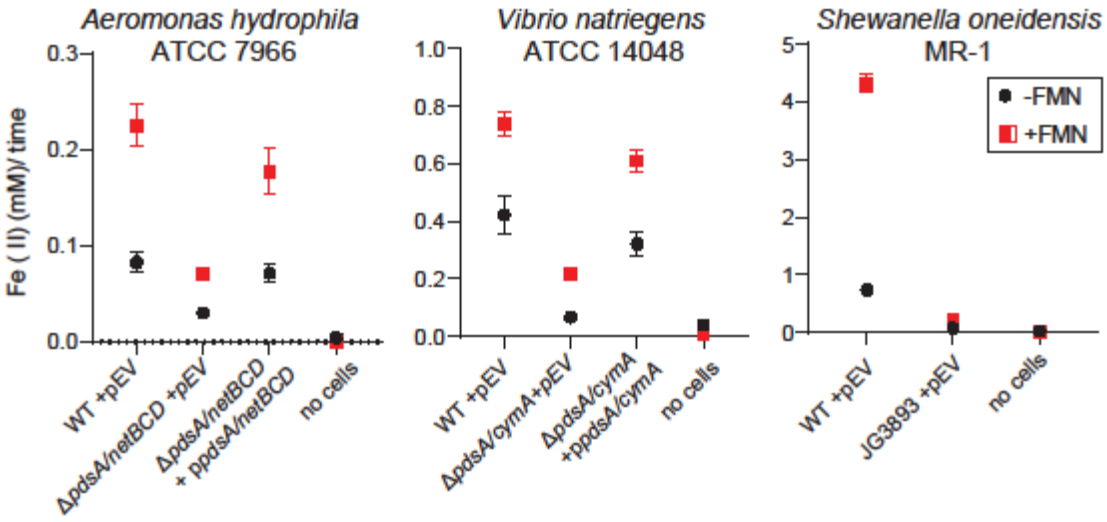

Figure 39. Exogenous FMN increases the rate of autoclaved Schwertmannite reduction in *Aeromonas hydrophila* ATCC7966, *Vibrio natriegens* ATCC 14048 and *S. oneidensis* MR-1 and is dependent on described EET pathways. Rate of FeOOH reduction (●) compared to conditions with 10 μM exogenous FMN (■). A and B) Wild-type and mutants lacking inner membrane and periplasmic genes complemented or with an empty vector. C) *S. oneidensis* MR-1 mutant lacking essential genes for EET (JG3893 Δ*mtrCAB* Δ*mtrDEF* Δ*omcA* Δ*dmsE* ΔSO4360 Δ*cctA* Δ*fccA* Δ*cymA*). Data is representative of two independent experiments performed in triplicate, displaying mean ± standard error of the mean (SEM).

Interestingly, when a lower potential iron oxide with less surface area was used instead of Schwartmannite, FMN enhancement of iron reduction was not observed in *A. hydrophila* (Figure 40A), but still occurred in *S. oneidensis* (Figure 40B). Endogenous production of FMN by *S. oneidensis* is not responsible for the different reduction rates, as a bfe mutant exhibited a similar phenotype (Figure 40B). *S. oneidensis* mutants lacking outer membrane cytochromes (Δ*mtrCAB* Δ*mtrDEF* Δ*omcA* Δ*dmsE* ΔSO4360 Δ*cctA*) showed increased rates of iron oxide reduction comparable to wild-type levels when expressing *A. hydrophila* MtrCAB (Figure 40B), similar to results in Figure 38C.

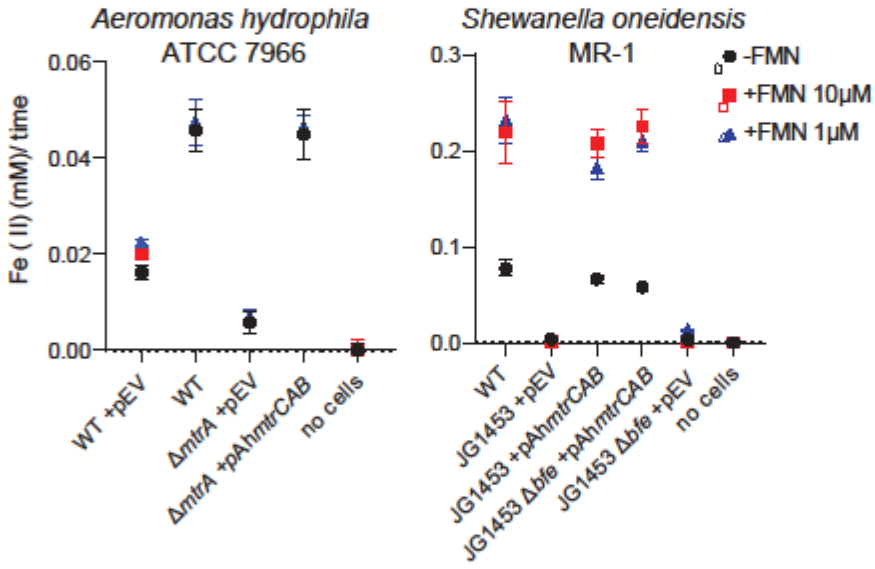

Figure 40. Exogenous FMN increase the rate of autoclaved poorly crystallin FeOOH in *S. oneidensis* but not *A. hydrophila*. Rate of FeOOH reduction (●) compared to conditions with 10 μM (■) or 1 μM (▲) of exogenous FMN in wild-type and mutant strains of A) *A. hydrophila* and B) *S. oneidensis*. (JG1453 Δ*mtrCAB* Δ*mtrDEF* Δ*omcA* Δ*dmsE* ΔSO4360 Δ*cctA*).

The scale of metal reduction in *A. hydrophila* and *V. natriegens* are 10x less compared to *S. oneidensis* MR-1 (Y-axis of Figures 39 and 40). Comparing metal reduction phenotypes across different species can lead to a false negative and should be done with caution and controls. The iron oxide reduction assay supplemented with exogenous FMN does not distinguish if the cell is directly reducing FMN. FMN may interact with the iron oxide to increase solubility, allowing faster rates of iron reduction but not requiring direct FMN reduction. Differences in regulatory regimes, electron donor

(gluconate for *V. natriegens*, and lactate for *A. hydrophila* and *S. oneidensis*) cytochrome content or EET mechanism could contribute to these observed differences.

5.5 Materials and Methods

Bacterial Strains:

FMN reduction was performed similar to FMN reduction assays previously reported (399, 402). Overnight cultures were washed and resuspended to an OD600=1 and inoculated 1:10 into 96 well plates containing minimal medium with 20 mM lactate and 1 μM FMN. Immediately after inoculation, plates were transferred to a dry N_2 atmosphere box where the fluorescence was measured using a Molecular Devices SpectraMax M2 plate reader at 440 nm excitation, 525 nm emission. Controls lacking the electron donor lactate were also performed to control for any abiotic reduction in each assay.

Iron oxide reduction experiments were performed as described previously (286). Briefly, cells were washed and resuspended in minimal medium to equal optical density and inoculated into 96-well plates. Plates were placed into a chamber and degassed with Argon for 15 min, incubating in the dark at room temperature between sampling for Fe(II). Iron oxides were synthesized as, Schwertmannite (403) and poorly crystalline FeO(OH) (404) and added to minimal medium as an electron acceptor. Reduction of iron oxide with and without the addition of FMN were directly compared.